

Fall 11-15-2018

# Use of Sodium Dithionite for Groundwater Restoration Following Uranium In-Situ Recovery Mining at the Smith Ranch-Highalnd Site in Wyoming

Rose J. Harris

*University of New Mexico - Main Campus*

Follow this and additional works at: [https://digitalrepository.unm.edu/eps\\_etds](https://digitalrepository.unm.edu/eps_etds)

Part of the [Geochemistry Commons](#)

---

## Recommended Citation

Harris, Rose J.. "Use of Sodium Dithionite for Groundwater Restoration Following Uranium In-Situ Recovery Mining at the Smith Ranch-Highalnd Site in Wyoming." (2018). [https://digitalrepository.unm.edu/eps\\_etds/248](https://digitalrepository.unm.edu/eps_etds/248)

This Thesis is brought to you for free and open access by the Electronic Theses and Dissertations at UNM Digital Repository. It has been accepted for inclusion in Earth and Planetary Sciences ETDs by an authorized administrator of UNM Digital Repository. For more information, please contact [disc@unm.edu](mailto:disc@unm.edu).

Rose J. Harris

*Candidate*

---

Earth & Planetary Sciences

*Department*

---

This thesis is approved, and it is acceptable in quality and form for publication:

*Approved by the Thesis Committee:*

Dr. Gary Weissmann, Chairperson

---

Dr. Laura Crossey

---

Dr. Jose Cerrato

---

Dr. Paul Reimus

---

---

---

---

---

---

---

---

**USE OF SODIUM DITHIONITE FOR GROUNDWATER  
RESTORATION FOLLOWING URANIUM IN-SITU  
RECOVERY MINING AT THE SMITH RANCH-HIGHLAND  
SITE IN WYOMING**

by

**ROSE J. HARRIS**

**B.A., ENVIRONMENTAL SCIENCE,  
WHEATON COLLEGE (MA), 2014**

THESIS

Submitted in Partial Fulfillment of the  
Requirements for the Degree of

**Master of Science  
Earth & Planetary Sciences**

The University of New Mexico  
Albuquerque, New Mexico

**December, 2018**

## ACKNOWLEDGMENTS

I especially thank Dr. Paul Reimus for giving me the opportunity to earn a Master's degree while continuing my position with the Earth & Environmental Sciences Division at LANL. I thank Dr. Gary Weissmann for his support and for serving as my committee chair, and Dr. Jose Cerrato and Dr. Laura Crossey for serving on my committee. I am really grateful for the assistance, support, and mentorship from many members of the GGRL and Radiological Geochemistry teams at LANL, especially Martin Dangelmayr, Doug Ware, Kat Telfeyan, Emily Kluk, George Perkins, Oana Marina, and Charles Paradis. I thank my parents and family for supporting my decision to stay in New Mexico while I continue my education and career, and I thank Alex Adams and my dear friend Dea Musa for their support during my time earning this degree.



**USE OF SODIUM DITHIONITE FOR GROUNDWATER RESTORATION  
FOLLOWING URANIUM IN-SITU RECOVERY MINING AT THE SMITH  
RANCH-HIGHLAND SITE IN WYOMING**

by

**Rose J. Harris**

**B.A., Environmental Science, Wheaton College (MA), 2014**

**M.S., Earth and Planetary Science, University of New Mexico, 2018**

**ABSTRACT**

Uranium in-situ recovery (ISR) is a subsurface aqueous mining technique used to extract uranium from sandstone roll-front deposits. After ISR mining, groundwater restoration is conducted to decrease concentrations of residual U(VI) and other contaminants leftover in the groundwater. Sodium dithionite, a strong chemical reductant, is being tested for use in groundwater restoration following uranium ISR at the Smith Ranch-Highland site in Wyoming. Sodium dithionite has been used to remediate chromium plumes by creating an in-situ permeable reactive barrier, but there has been no work using sodium dithionite for groundwater restoration following uranium ISR mining.

Laboratory batch and column experiments, and two push-pull field tests were conducted to test the reductive capacity imparted to post-mined sediments from the Smith Ranch-Highland site after treatment with sodium dithionite. In one laboratory column and batch experiment, where sediments had high uranium and organic carbon content, sodium dithionite did not impart a reductive capacity to the post-mined sediments, suggesting dithionite reacts differently with organic carbon which inhibits the reduction of U(VI) to U(IV). In laboratory batch and column experiments with post-mined sediments low in organic carbon content, and in the push-pull field tests, sodium dithionite imparted a

reductive capacity to the sediments that reduced a given amount of aqueous electron acceptors. Thus, the volume of water that can be effectively treated by a dithionite deployment (the metric that mining companies most care about) will depend on the concentration (in equivalents/liter) of electron acceptors that the water contains.

## TABLE OF CONTENTS

<b>LIST OF FIGURES</b> .....	viii
<b>LIST OF TABLES</b> .....	xii
<b>I. INTRODUCTION</b> .....	1
<b>II. LABORATORY COLUMN EXPERIMENTS USED TO EVALUATE THE REDUCTIVE CAPACITY IMPARTED BY SODIUM DITHIONITE ON POST-MINED SEDIMENTS FROM A URANIUM IN-SITU RECOVERY MINE</b> .....	5
2.1 Abstract.....	5
2.2 Introduction.....	6
2.3 Methods .....	9
<i>Site</i> .....	9
<i>Ground waters</i> .....	14
<i>Column Preparation and Operations</i> .....	16
<i>Column Sediment Leaching</i> .....	21
2.4 Results and Discussion .....	22
<i>Reductive capacities: LOC experiments</i> .....	22
<i>Sediment Leaching: Columns LOC-1, LOC-2, and LOC-3</i> .....	29
<i>Effects of dithionite on sediments with high organic carbon</i> .....	34
2.5 Conclusions.....	35
2.6 Supplemental Information .....	37
<b>III. PUSH-PULL FIELD TESTS TO EVALUATE SODIUM DITHIONITE AS A GROUNDWATER RESTORATION OPTION FOLLOWING URANIUM IN-SITU RECOVERY MINING</b> .....	44
3.1 Rationale .....	44
3.2 Methods .....	44
<i>Test site</i> .....	44
<i>Injection and Pump-back</i> .....	46
3.3 Results and Discussion .....	48
<i>Reductive capacity</i> .....	48
<i>Iron</i> .....	51
<i>Uranium Reduction</i> .....	53
3.5 Conclusions.....	54
<b>IV. EFFECTS OF SODIUM DITHIONITE ON POST-MINED SEDIMENTS WITH HIGH ORGANIC CARBON: SEDIMENT REDUCTION BATCH EXPERIMENT</b> .....	55
4.1 Rationale .....	55

4.2 Methods .....	55
4.3 Results and Discussion .....	59
4.4 Conclusions.....	66
<b>V. CONCLUSIONS .....</b>	<b>67</b>
<b>LIST OF APPENDICES .....</b>	<b>72</b>
<b>Appendix A - Aqueous Batch Experiment.....</b>	<b>73</b>
A.1 Rationale .....	73
A.2 Methods.....	73
A.3 Results.....	74
A.4 Conclusions.....	76
<b>Appendix B -X-ray photoelectron spectroscopy .....</b>	<b>77</b>
B.1 Rationale .....	77
B.2 Methods.....	77
B.3 Results .....	77
B.4 Conclusions .....	77
<b>Appendix C - Speciation of Uranium Liberated from Sediments in Dithionite Solution..</b>	<b>78</b>
C.1 Rationale .....	78
C.2 Methods.....	78
C.3 Results .....	78
C.4 Discussion .....	83
<b>Appendix D- Fluvial Deposition in the Paleocene Fort Union Formation at the Smith Ranch-Highland Site in Wyoming.....</b>	<b>84</b>
D.1 Rationale .....	84
D.2 Background.....	84
D.3 Core.....	88
D.4. Well logs .....	91
<b>REFERENCES.....</b>	<b>116</b>

## LIST OF FIGURES

Figure 2.1. Smith Ranch-Highland uranium in-situ recovery site. The sediments used in these experiments were taken from the MOW 4-6 core hole, shown by the star. Waters MS-413, M-402, and MP-423 used in these experiments were collected from Mining Unit 4. Water 15P-314 used in these experiments was collected from Mining Unit 15.....	10
Figure 2.2. Sections of the MOW 4-6 core used in the low organic and high organic carbon content columns.....	12
Figure 2.3. Photograph of Columns LOC-4 and HOC. Schematic represents set-up of all column experiments.....	18
Figure 2.4. Uranium and chloride breakthrough curves for Column LOC-1. The retardation factor between the chloride and uranium breakthrough curves was calculated to be 1.33.....	23
Figure 2.5. Uranium and chloride breakthrough curves for Column LOC-2 with the retardation factor of 1.33 imposed on the chloride breakthrough curve. Gap in data between 3 and 4 pore volumes eluted represents sample loss.....	23
Figure 2.6. Uranium and chloride breakthrough curves for Column LOC-3 with the retardation factor of 1.33 imposed on the chloride breakthrough curve.....	24
Figure 2.7. Uranium and chloride breakthrough curves for Column LOC-4 with the retardation factor of 1.33 imposed on the chloride breakthrough curve. After ~30 pore volumes were eluted, all the uranium that had been initially reduced started oxidizing..	24
Figure 2.8. Sulfate eluted in mg/l plotted against pore volumes eluted in Columns LOC-2, LOC-3, and LOC-4.....	29
Figure 2.9. Iron leached from sediments of Columns LOC-1, LOC-2, and LOC-3.....	30
Figure 2.10. Iron eluted from Columns LOC-1, LOC-2, LOC-3, and LOC-4.....	31
Figure 2.11. Fe, U and Cr (mg/g sediment) leached from column LOC-2, plotted by distance as % of column mass.....	32
Figure 2.12. Fe, U and Cr (mg/g sediment) leached from column LOC-3, plotted by distance as % of column mass.....	33
Figure 2.13. Uranium and chloride breakthrough curves for Column HOC. No retardation factor was imposed on the chloride breakthrough curve because no reductive capacity with respect to uranium was observed.....	35
Figure 2.14. Cations in Column LOC-1 eluent plotted against pore volumes eluted.....	37
Figure 2.15. Anions in Column LOC-1 eluent plotted against pore volumes eluted.....	37
Figure 2.16. Trace metals in Column LOC-1 eluent plotted against pore volumes eluted.....	38

Figure 2.17. Cations in Column LOC-2 eluent plotted against pore volumes eluted.....	38
Figure 2.18. Anions in Column LOC-2 eluent plotted against pore volumes eluted. Gap in data between 3 and 4 pore volumes represents sample loss.....	39
Figure 2.19. Trace metals in Column LOC-2 eluent plotted against pore volumes eluted. Gap in data between 3 and 4 pore volumes represents sample loss. ....	39
Figure 2.20. Anions in Column LOC-3 eluent plotted against pore volumes eluted.....	40
Figure 2.21. Trace metals in Column LOC-3 eluent plotted against pore volumes eluted.....	40
Figure 2.22. Cations in Column LOC-3 eluent plotted against pore volumes eluted.....	41
Figure 2.23. Anions in Column LOC-4 eluent plotted against pore volumes eluted.....	41
Figure 2.24. Anions in Column HOC eluent plotted against pore volumes eluted.....	42
Figure 2.25. Cations in Column LOC-4 eluent plotted against pore volumes eluted. ....	42
Figure 2.26. Cations in Column HOC eluent plotted against pore volumes eluted.....	43
Figure 3.1. Location of wells 15P-308 and 15P-315 relative to the Smith-Ranch Highland uranium in-situ recovery mine.....	45
Figure 3.2. Chloride and uranium breakthrough curves for wells 15P-308 and 15P-315 relative to pre-test concentrations. The retardation factor of 1.33 calculated in the column experiments discussed in Section II was applied to the chloride breakthrough curves to account for any delay in uranium breakthrough that would occur in the absence of dithionite.....	50
Figure 3.3. Concentrations of iron in wells 15P-308 and 15P-315 during pump-back.....	53
Figure 3.4. Ratios of $^{238}\text{U}/^{235}\text{U}$ in wells 15P-308 and 15P-315 on select days during pump-back.....	54
Figure 4.1. Sections of MOW 4-6 core used in sediment reduction batch experiment. Yellow numbers represent sections of the core used in this experiment.....	57
Figure 4.2. Dithionite solutions exposed to sediments after 7 days. Gray precipitate is visible on the surface of the sediments except in reactors #8A and #8B.....	62
Figure 4.3. Concentrations of uranium in MP-423 water on days 1 and 7 after being exposed to dithionite treated sediments.....	63
Figure C.1. Concentrations of uranium in sodium dithionite solutions exposed to sediments from the MOW 4-6 core of the sample splits that were passed through C18 cartridges, and that were not passed through C18 cartridges.....	79

Figure C.2. Concentrations of uranium in dithionite solutions passed through anion exchange resins, and solutions not passed through anion exchange resins. Dithionite solution exposed to sediment 8A and 8B are shown in Figure C.3.....	81
Figure C.3. Concentrations of uranium in dithionite solution passed through anion exchange resins, and not passed through anion exchange resins for dithionite solutions exposed to sediments 8A and 8B.....	81
Figure D.1. Modified from WoldeGabriel et al., 2014. Map of the Smith Ranch-Highland site shown in relation to its location in the Powder River Basin.....	86
Figure D.2. Taken from Ethridge et al. 1981. Inferred depositional system and subsystems upper part of Fort Union, southern Powder River Basin. The Smith Ranch-Highland is just south of Bear Creek Mine.....	87
Figure D.3. MOW 4-6 core.....	89
Figure D.4. Well log showing resistivity (black lines), and gamma counts (red and blue lines) for MOW 4-6 core. Photos of MOW 4-6 core are shown with corresponding depth in the well log.....	90
Figure D.5. Wells that were correlated in Mining Unit 15.....	92
Figure D.6.a. Well 15I-554 to 15I-559 (0 - 280 feet bgs). At about 430 feet bgs, both wells show a resistivity spike of about the same length, suggesting it may be a channel that flowed through both wells.....	93
Figure D.6.b. Well 15I-554 to 15I-559 (280 - 520 feet bgs). At about 430 feet bgs, both wells show a resistivity spike of about the same length, suggesting it may be a channel that flowed through both wells.....	94
Figure D.7.a. (0 - 290 feet bgs). Well 15I-559 to 15I-558.....	95
Figure D.7.b. (290 - 530 feet bgs). Well 15I-559 to 15I-558. ....	96
Figure D.8.a. (0 - 290 feet bgs). Well 15I-558 to 15I-555. ....	97
Figure D.8.b. (290- 530 feet bgs). Well 15I-558 to 15I-555.....	98
Figure D.9.a. Well 15I-555 to 15I-554 (0 - 280 feet bgs). ....	99
Figure D.9.b. Well 15I-555 to 15I-554 (290 - 530 feet bgs). Matching features at ~390 - 430 feet bgs, could be a channel deposit with upward fining then coarsening. Another matching channel deposit from 430 - 450 feet bgs. ....	100
Figure D.10.a. Well 15I-554 to 15P-308 (0 - 280 feet bgs). ....	101
Figure D.10.b. Well 15I-554 to 15P-308 (290 - 530 feet bgs). In both wells, sharp contacts to finer grained deposited at 510 feet bgs and 430 feet bgs. At about 380 feet bgs, similar upward coarsening to upward fining is observed.....	102

Figure D.11.a. Well 15I-566 - 15I-569 (0 - 290 feet bgs). .....	103
Figure D.11.b. Well 15I-566 to 15I-569 (290 - 510 feet bgs). .....	104
Figure D.12.a. Well 15I-569 to 15I-568 (0 - 290 feet bgs). .....	105
Figure D.12.b. Well 15I-569 - 15I-568 (290 - 500 feet bgs). .....	106
Figure D.13.a. Well 15I-568 to 15I-567 (0 - 290 feet bgs). .....	107
Figure D.13.b. Well 15I-568 to 15I-567 (290 - 500 feet bgs).....	108
Figure D.14.a. Well 15I-567 to 15I-566 (0 - 290 feet bgs). .....	109
Figure D.14.b. Well 15I-567 to 15I-566 (290 - 500 feet bgs). .....	110
Figure D.15.a. Well 15I-566 to 15P-315 (0 - 290 feet bgs). .....	111
Figure D.15.b. Well 15I-566 - 15P-315 (290 - 500 feet bgs). Two possible matching channel deposits, about 420 to 450 feet bgs, and 450 to 480 feet bgs. ....	112
Figure D.16.a. Well 15P-308 to 15P-315 (0 - 290 feet bgs). .....	113
Figure D.16.b. Well 15P-308 to 15P-315 (290 - 530 feet bgs). .....	114



**LIST OF TABLES**

Table 2.1. X-ray diffraction data for sediments used in LOC and HOC column experiments. .... 12

Table 2.2. XRF data for sediments used in LOC and HOC column experiments. .... 13

Table 2.3. Concentrations of selected constituents of ground waters used in column experiments. .... 15

Table 2.4. Column parameters. .... 16

Table 2.5. Operational details for each experiment. .... 20

Table 2.6. Moles of dithionite injected into each column, liters of water recovered between chloride and uranium breakthrough, the ratio of water recovered between chloride and uranium breakthrough relative to moles of dithionite injected, the moles of uranium reduced, and the ratio of moles of uranium reduced to moles of dithionite injected in column experiments LOC-2, LOC-3, and LOC-4. .... 27

Table 2.7. Equivalentents per liter of potential electron acceptors for 15P-314 and MP-423 waters. .... 28

Table 2.8. Uranium mass balance for Columns LOC-2, LOC-3, and LOC-4. .... 33

Table 3.1. Concentrations of selected constituents in wells 15P-308 and 15P-315 before the push-pull tests. Data provided by Cameco. .... 46

Table 3.2. Alkalinity, calcium, uranium, and sulfate in the post-mined waters used in the column experiments and in wells 15P-308 and 15P-315 before the push-pull tests. .... 49

Table 3.3. Moles of dithionite injected, liters of water recovered between chloride and uranium breakthrough, the ratio of liters of water recovered between chloride and uranium breakthrough relative to moles of dithionite injected, the moles of uranium reduced, and the moles of uranium reduced relative to dithionite injected in wells 15P-308 and 15P-315. .... 51

Table 4.1. Organic carbon and uranium content for the sediments used in this experiment. Rows in white have low organic carbon content, and rows in gray have high organic carbon content (>1%). .... 56

Table 4.2. Concentrations of selected constituents of M-402 and MP-423 waters. .... 59

Table 4.3. pH and concentrations of selected constituents in dithionite solutions exposed to post-mined sediments. .... 61

Table 4.4. Uranium concentrations (mg/l) in MP-423 water on days 1 and 7 after being exposed to sediments treated with sodium dithionite. .... 64

Table 4.5. Ratios of moles of dithionite per gram of organic carbon for the high organic carbon column experiment and sediment reduction batch experiment, and sediment 8 in the sediment reduction batch experiment. .... 65

Table 5.1. Moles of dithionite injected, liters of water recovered between chloride and uranium breakthrough, the ratio of liters of water recovered between chloride and uranium breakthrough relative to the moles of dithionite injected, moles of uranium reduced, and moles of uranium reduced relative to moles of dithionite injected in the LOC column experiments and push-pull field tests. .... 68

Table A.1. Concentration of selected constituents in MP-423 water used in aqueous batch experiment. .... 74

Table A.2. Uranium concentrations of post-mined untreated MP-423 water after being exposed to sodium dithionite or sodium sulfide for 24 hours. .... 75

Table C.1. Concentrations of uranium in sodium dithionite solutions in the 3 sample splits, passed through the C18 cartridge, and not passed through the C18 cartridge. .... 80

Table C.4. Concentrations of uranium in dithionite solutions passed through anion exchange resins, and solutions not passed through anion exchange resins. Sample 2A-2 was spilled, so there was not enough solution to pass through the anion exchange resin for analysis. .... 82

Table D.1. Well screen intervals for wells in Mining Unit 15. .... 92

## I. INTRODUCTION

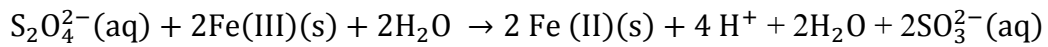
Uranium is mined primarily for use in nuclear energy production (Gallegos et al., 2015; Brown et al., 2016). About half of the uranium produced globally is mined by in-situ recovery (ISR), an aqueous mining technique that can extract uranium from lower grade ores without producing hazardous dust or mine tailings generated by conventional shaft or open pit mining (Saunders et al., 2016). During ISR, a lixiviant, which usually contains an oxidant ( $O_2(g)$ ) and a complexing agent ( $CO_2(g)$ ) is injected into a uranium ore-bearing sandstone to oxidize and solubilize the uranium (Davis & Curtis, 2007, Saunders et al., 2016, Gallegos et al., 2015). The solubilized uranium forms uranyl carbonate complexes ( $UO_2(CO_3)_2^{2-}$ ), or ternary uranyl carbonate complexes, such as  $Ca_2UO_2(CO_3)_3^0$  and  $Mg_2UO_2(CO_3)_3^0$ . The uranium-rich water is pumped to the surface by a production well and is extracted by ion exchange (Gallegos et al., 2015).

Once uranium production is complete, the Nuclear Regulatory Commission requires that uranium and other contaminants such as arsenic, selenium, vanadium, and molybdenum that were liberated during ISR be restored to pre-mining levels (Saunders et al. 2016). Groundwater sweep, reverse osmosis, injection of chemical reductants, and biostimulation are common groundwater restoration techniques used after ISR mining (Davis & Curtis, 2007; Gallegos et al., 2015, Saunders et al., 2016). One of the challenges in post-mining groundwater restoration is to ensure concentrations of all contaminants stay reduced over the long term (Davis & Curtis, 2007, Gallegos et al., 2015).

Sodium dithionite is a strong chemical reductant being tested for use in post-mining groundwater restoration at the Smith Ranch-Highland uranium ISR site. The Smith Ranch-Highland site, located in Converse County, Wyoming, was at one time the largest domestic

producer of uranium (WoldeGabriel et al., 2015), but the site is currently in restoration mode. Sodium dithionite has never been used for groundwater restoration following uranium ISR, but it has been used to create an in-situ permeable reactive barrier to reduce Cr(VI) (Ludwig et al., 2007).

Previous work indicates that sodium dithionite manipulates the reduction-oxidation status of the aquifer by reducing existing ferric oxide aquifer solid phases to reactive ferrous iron through the following reaction:



(Amonette et al., 1994). Ferrous iron generated by the injection of dithionite was thought to have generated abiotic reduction of Cr (VI) to Cr (III), and may do the same for reduction of U(VI) to U(IV).

The goal of this Master's thesis is to evaluate the use of sodium dithionite in groundwater restoration following uranium ISR mining at the Smith Ranch-Highland site using laboratory batch and column experiments and two push-pull field tests. While other contaminants besides uranium are also targeted during post-mining groundwater restoration, the primary focus of this study is uranium fate and transport, because concentrations of uranium are often significantly higher than other contaminants that may have been liberated during ISR. This thesis is organized into the following five sections and Appendices.

- Section I: Introduction
- Section II: Laboratory Column experiments used to evaluate the reductive capacity imparted by sodium dithionite on post-mined sediments from a uranium in-situ

recovery mine. The goal of these column experiments was to compare reductive capacities imparted by sodium dithionite on post-mined sediments with low organic carbon content from the same section of core that were treated with different amounts of sodium dithionite, and to compare the reductive capacities imparted by sodium dithionite on post-mined sediments with high organic carbon content. This section is structured as a manuscript.

- Section III: Push-pull field tests used to evaluate sodium dithionite as a groundwater restoration option following uranium in-situ recovery mining. The results of two push-pull field tests conducted at the Smith Ranch are discussed in this section.
- Section IV: Effects of sodium dithionite on post-mined sediments containing high organic carbon: Sediment Reduction Batch Experiment. The results of a sediment reduction batch experiment that was conducted to gain more insight on the responses of post-mined sediments with high organic carbon content to treatment with sodium dithionite are discussed in this section.
- Section V: Conclusions
- Appendices
  - Appendix A: Aqueous Batch Experiment. The results of an aqueous batch experiment that was conducted to see if dithionite could reduce uranium directly in post-mined untreated water are discussed in this section.
  - Appendix B: X-ray photoelectron spectroscopy. This section documents an attempt to use x-ray photoelectron spectroscopy to look for reduction of

U(VI) to U(IV) on post-mined sediments treated with sodium dithionite and then exposed to post-mined water with uranium.

- Appendix C: Speciation of Uranium in Dithionite Solution. The results of an experiment conducted to gain insight on the speciation of uranium in dithionite solution are discussed in this section.
- Appendix D: Fluvial Deposition in the Paleocene Fort Union Formation at the Smith Ranch-Highland site in Wyoming. Details on the deposition of the Paleocene Fort Union formation at SRH are provided in this section. Well logs and the MOW 4-6 core taken from SRH and core were studied to match observations from the literature about deposition of the Paleocene Fort Union formation.

## **II. LABORATORY COLUMN EXPERIMENTS USED TO EVALUATE THE REDUCTIVE CAPACITY IMPARTED BY SODIUM DITHIONITE ON POST-MINED SEDIMENTS FROM A URANIUM IN-SITU RECOVERY MINE**

### 2.1 Abstract

A series of column experiments were conducted to compare the reduction capacities imparted to post-mined sediments from the Smith Ranch-Highland (SRH) uranium in-situ recovery (ISR) site after treatment with sodium dithionite. The first goal of this study was to compare the reductive capacities (with respect to U(VI) reduction) imparted by varying amounts of dithionite to post-mined sediments with low organic carbon content (LOC) from the same section of core. The sediments from three of the LOC columns were leached with 2 M nitric acid after uranium breakthrough to determine the spatial distribution and mass balance of various elements on the sediments. A fourth LOC column experiment was run using the same sediments as the other three LOC columns, but with different ground waters. It was found that regardless of the concentration of U(VI) in the water, every mole of dithionite used in a given experiment resulted in the removal/reduction of U(VI) from a similar volume of water. This suggests other electron acceptors besides U(VI) in the water consume most of the reductive capacity imparted by the dithionite. The second goal of this study was to compare the response of post-mined sediments with high organic carbon content (HOC) to the response of the sediments with low organic carbon content to treatment with sodium dithionite. A fifth column experiment was run essentially in duplicate to the fourth LOC column experiment, but was packed with sediments with high organic carbon content. In the HOC column experiment, the dithionite appeared to liberate uranium from the organic carbon without imparting any measurable reduction capacity to the sediments. It is concluded that a higher percentage of organic carbon content in

sediments results in a different set of dithionite reactions and reaction products than sediments with a low percentage of uranium and organic carbon content.

## 2.2 Introduction

About half of the uranium produced globally is mined by ISR, an aqueous mining technique that can extract uranium from lower grade ores without producing hazardous dust or mine tailings generated by conventional open pit mining (Saunders et al., 2016). During ISR, a lixiviant, which usually contains an oxidant ( $O_2(g)$ ) and a complexing agent ( $CO_2(g)$ ) is injected into a uranium ore-bearing sandstone to oxidize the uranium from its insoluble form of U(IV) to its soluble form of U(VI) (Davis & Curtis, 2007, Saunders et al., 2016, Gallegos et al., 2015). The solubilized U(VI) then forms uranyl carbonate complexes ( $UO_2(CO_3)_2^{2-}$ ), or ternary uranyl carbonate complexes ( $Ca_2UO_2(CO_3)_3^0$  and  $Mg_2UO_2(CO_3)_3^0$ ) with ions in the ground water. The uranium-rich water is pumped to the surface by a production well and is extracted by ion exchange. (Gallegos et al., 2015)

Once uranium production is complete, the Nuclear Regulatory Commission requires that uranium and other redox sensitive heavy metals (such as arsenic, selenium, and molybdenum) that were liberated during ISR must be restored to pre-mining levels. Pre-mining levels of uranium are often higher than the EPA maximum contaminant level of 30 ppb for uranium (EPA, 2001). Groundwater sweep and reverse osmosis are common first steps in post-mining groundwater restoration. During groundwater sweep, post-mined groundwater is pumped out of the ore zone and replaced with native groundwater that is drawn in from outside the ore zone. Next, groundwater may be pumped to the surface,



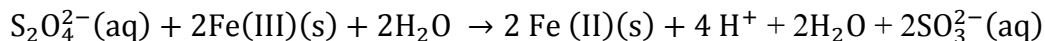
treated with reverse osmosis to reduce concentrations of contaminants, and reinjected into the aquifer (Saunders et al., 2016).

After groundwater sweep and reverse osmosis, chemical reductants or biostimulants may be injected to reduce any remaining U(VI) back to U(IV) (Davis & Curtis, 2007; Gallegos et al., 2015, Saunders et al., 2016). The injection of chemical reductants and biostimulants can also reduce other redox-sensitive elements in ore-zone sediments that were oxidized during mining, which restores the sediments to their pre-mining reducing conditions that were conducive to the formation of the roll-front deposit in the first place. At Smith Ranch-Highland, H<sub>2</sub>S has been injected as a chemical reductant after ISR mining, but no significant changes in uranium concentrations were reported (Borch & Roche & Johnson, 2012).

Reduction of U(VI) to U(IV) with simultaneous reduction of other sediments is a preferred mechanism for groundwater restoration because U(IV) should not oxidize to soluble U(VI) as long as the sediments retain reductive capacity (Ray et al., 2011; Singh et al., 2013). The Smith Ranch-Highland site is an ideal location for maintaining reducing conditions after groundwater restoration because the aquifer is anoxic, with few electron acceptors available to oxidize the sediments. This situation contrasts shallow uranium-contaminated environments (such as mill tailings sites), which have been the focus of most previous groundwater restoration research, as these environments receive a steady supply of electron acceptors via percolation of oxygenated meteoric water (Dreesen et al., 1982; Elias et al., 2003).

Amonette et al. (1994) was the first to suggest the use of sodium dithionite to create an in-situ permeable redox barrier. Amonette et al. (1994) suggested that sodium dithionite

manipulates the reduction-oxidation status of the aquifer by reducing existing ferric oxide aquifer solid phases to reactive ferrous iron through the following reaction:



Since this technique was introduced, many lab and field studies have shown that the reactive ferrous iron generated by the dithionite reduces soluble Cr (VI) to insoluble Cr (III) (Amonette et al., 1994; Istok et al., 1999; Ludwig et al., 2007; Cheng et al., 2009; Li et al., 2017). To date, there has been no work using sodium dithionite to reduce U(VI) at uranium ISR mines or any other uranium-contaminated sites.

Similar to chromium (VI), the reduction of U(VI) initiated by reduced iron has been observed on many occasions. Lee et al. (2013) used biostimulation to generate iron sulfides, which reduced U(VI) to U(IV). Liger et al. (1999) reported that at a near-neutral pH range, ferrous iron reduced U(VI) as long as soluble iron and mineral surfaces were present to catalyze the electron transfer process. Scott et al. (2005) showed that magnetite reduced U(VI) to U(IV) by electron transfer between Fe and U.

In this study, laboratory column experiments were conducted to compare the reductive capacities imparted to post-mined sediments from a uranium ISR mine after treatment with sodium dithionite. The first goal of this study was to compare the reductive capacities imparted to post-mined sediments with low organic carbon content (LOC) from the same section of post-mined core after treatment with varying amounts of sodium dithionite. The second goal of this study was to compare the effects of sodium dithionite on post-mined sediments with high organic carbon content to post-mined sediments with low organic carbon content. More emphasis is placed on the LOC experiments. The LOC

sediments appeared to be more permeable than the HOC sediments and appeared to have been better leached during the ISR process, indicated by a yellowish color after being oxidized (WoldeGabriel et al., 2014). If the more permeable LOC sediments were more accessible to leaching fluids during ISR mining, they will likely be more accessible during groundwater restoration.

## 2.3 Methods

### *Site*

Water and sediments used in these experiments were taken from the Smith Ranch-Highland uranium ISR site, located near Douglas, Wyoming (Figure 2.1). Uranium at SRH exists in sandstone roll-front deposits in the Paleocene Fort Union formation at depths of 61 - 366 m below ground surface (Brown et al., 2016). SRH, operated by Cameco Resources, was the largest domestic producer of uranium between 2003 and 2016, but the site is no longer producing uranium and is focusing on restoration.

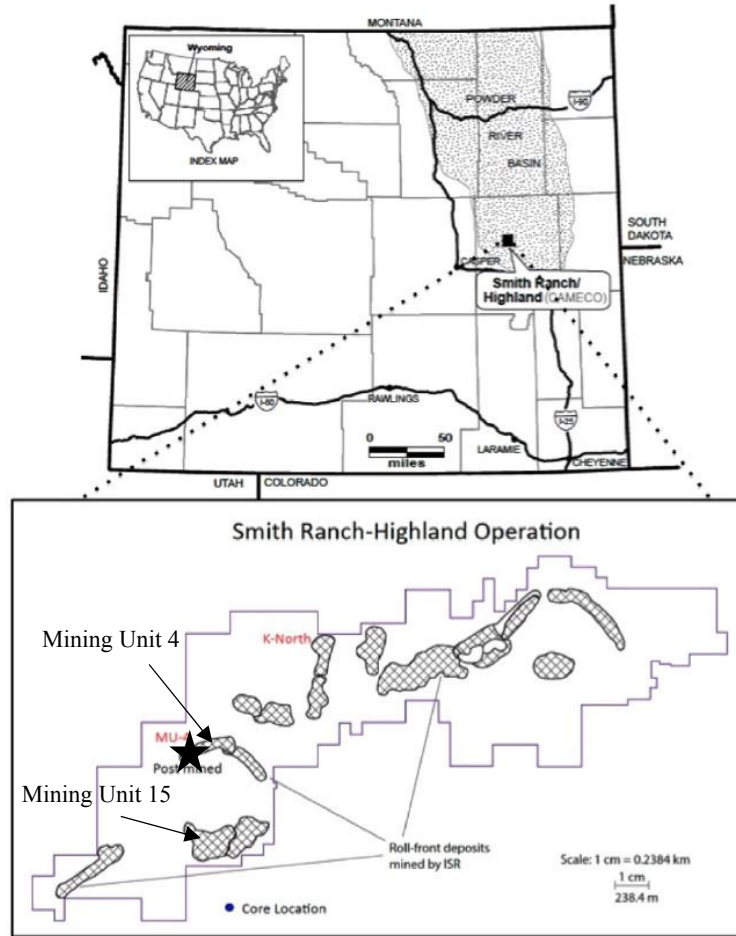


Figure 2.1. Smith Ranch-Highland uranium in-situ recovery site. The sediments used in these experiments were taken from the MOW 4-6 core hole, shown by the star. Waters MS-413, M-402, and MP-423 used in these experiments were collected from Mining Unit 4. Water 15P-314 used in these experiments was collected from Mining Unit 15.

## *Core*

The sediments used in the column experiments came from the MOW 4-6 core, whose location is shown in Figure 2.1. The MOW 4-6 core was collected from Mining Unit 4 after mining activities were completed. Sediments used in column experiments LOC-1, LOC-2, LOC-3, and LOC-4 came from the 782 feet bgs section of core. This section of core is a sandstone with low uranium (0.02 mg uranium/g sample) and organic carbon content (0.38%) (WoldeGabriel et al., 2014). Organic carbon content was measured using a Costech elemental analyzer coupled to a Thermo MAT-253 isotope ratio mass spectrometer. Yellowish-orange stains and alteration colors suggest it was oxidized during ISR (WoldeGabriel et al., 2014).

Sediments used in the high organic carbon (HOC) column experiment came from the 769 feet bgs section of the MOW 4-6 core. This section of core is a massive sandstone with carbonaceous shale. This section of core has a grayish color, which suggests it was not well leached during the ISR process, or it would have taken on a yellowish color after being oxidized, like the 782 feet bgs section of core (WoldeGabriel et al., 2014). It has high uranium (2.57 mg uranium/g sample) and organic carbon content (7.73%). Photographs of the sections of core, x-ray diffraction data, and x-ray fluorescence data of the sediments used to pack the columns are shown in Figure 2.2 and Tables 2.1 and 2.2, respectively.

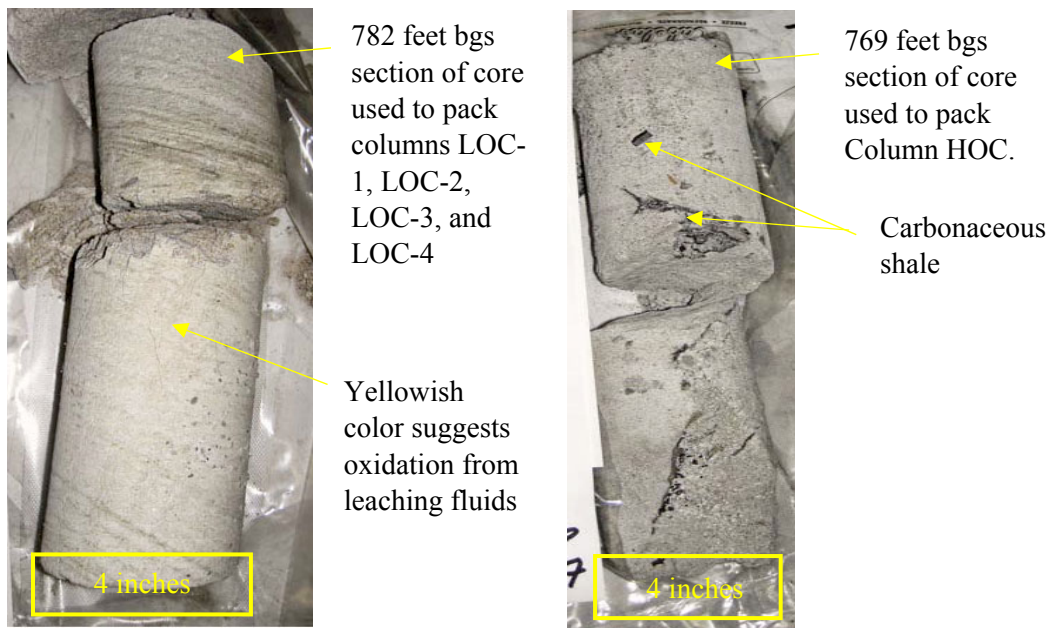


Figure 2.2. Sections of the MOW 4-6 core used in the low organic and high organic carbon content columns.

Core hole	MOW 4-6	MOW 4-6
Depth (ft)	769	782
quartz	58.6	72.7
albite	3.6	4.7
K-feldspar	24.0	11.3
muscovite	3.6	3.1
kaolinite	1.2	1.9
calcite	0.6	+
smectite	6.0	6.0
pyrite	2.4	b.d.
coffinite	++	b.d.
<b>Total</b>	<b>100</b>	<b>100</b>

+ Concentration less than 0.5 wt%

++ Present but not quantifiable due to lack of standard.

b.d. Below detection limit

Table 2.1. X-ray diffraction data for sediments used in LOC and HOC column experiments.

<b>Element/oxide</b>	<b>782</b>	<b>769</b>
Na <sub>2</sub> O %	0.36	0.31
MgO %	0.46	0.47
Al <sub>2</sub> O <sub>3</sub> %	5.62	5.24
SiO <sub>2</sub> %	87.88	73.05
P <sub>2</sub> O <sub>5</sub> %	0.045	0.055
K <sub>2</sub> O %	2.03	1.98
CaO %	0.31	0.55
TiO <sub>2</sub> %	0.16	0.15
MnO %	0.008	0.007
Fe <sub>2</sub> O <sub>3</sub> %	0.953	2.185
V ppm	67	120
Cr ppm	17	30
Ni ppm	13	23
Cu ppm	7	16
Zn ppm	15	19
Ga ppm	<7.5	7.4
Ge ppm	15.3	79.1
As ppm	<18	41.7
Rb ppm	64	119.8
Sr ppm	56	54
Y ppm	8	18.1
Zr ppm	144	167
Nb ppm	16	67.1
Ba ppm	457	385
La ppm	<22.8	25.6
Ce ppm	34.2	39.1
Nd ppm	<19.8	<19.8
Sm ppm	<15.6	<15.6
Gd ppm	<14.4	<14.4
Tb ppm	<20.7	<20.7
Hf ppm	<9.3	<9.3
Pb ppm	15	22
Th ppm	<5.4	6.2
U ppm	23.7	2569.7
Mo ppm	NR	NR
Pd ppm	NR	NR
Co ppm	NR	NR
Se ppm	NR	NR
Bi ppm	NR	NR
LOI** %	2.09	15.68
Total %	100.03	100.14

Table 2.2. XRF data for sediments used in LOC and HOC column experiments.

### *Ground waters*

Four different ground waters from SRH were used in these experiments. Two “background” waters were used to represent pre-mining conditions with low uranium and alkalinity, and two “post-mined” waters were used to represent post-mined conditions with high uranium and alkalinity. Background waters MS-413 and M-402 were collected from monitoring wells in Mining Unit 4 (shown in Figure 2.1). The first post-mined water, 15P-314, was collected from Mining Unit 15 (shown in Figure 2.1) after mining and before any groundwater restoration was conducted. The second post-mined water, MP-423, was collected from Mining Unit 4 after mining and after the well was treated with reverse osmosis, which explains the lower uranium concentration of post-mined water MP-423 relative to 15P-314 (3.8 mg/l compared to 26.1 mg/l).

Concentrations of selected constituents for these ground waters are found in Table 2.3. Cations were analyzed by inductively coupled plasma optical emission spectrometry (ICP-OES), trace metals were measured by inductively couple plasma mass spectroscopy (ICP-MS), anions were measured using ion chromatography (IC), and alkalinity and pH were measured using an autotitrator. All concentrations shown in Table 2.3 are representative of the samples after they were collected in the field and shipped to LANL, and not representative of column eluent.



<b>Constituent</b>	<b>MS-413</b>	<b>15P-314</b>	<b>M-402</b>	<b>MP-423</b>
Ca <sup>2+</sup> (mg/l)	111	383	51.1	409
Na <sup>+</sup> (mg/l)	20.6	33.7	18.8	40.7
Mg <sup>2+</sup> (mg/l)	31.1	86.8	13.0	95.5
K <sup>+</sup> (mg/l)	7.79	15.1	5.94	17.7
Fe <sup>2+</sup> (mg/l)	0.11	0.31	0	0
U(VI) (mg/l)	0.06	26.1	0.03	3.79
Cl <sup>-</sup> (mg/l)	7.02	98.2	4.20	128
SO <sub>4</sub> <sup>2-</sup> (mg/l)	235	608	75.6	646
NO <sub>2</sub> <sup>-</sup> (mg/l)	<0.01	<0.01	<0.01	<0.01
NO <sub>3</sub> <sup>-</sup> (mg/l)	0.00	0.02	<0.01	<0.01
pH	7.94	6.78	8.20	6.99
Alkalinity (mg/l as HCO <sub>3</sub> <sup>-</sup> )	269	794	198	746

Table 2.3. Concentrations of selected constituents of ground waters used in column experiments.

### *Column Preparation and Operations*

The MOW 4-6 core is relatively unconsolidated, so the sediments were scraped from the interior of the core with a metal spatula. The sediments used to pack the columns were taken from the inside of the core to avoid using areas on the outside of the core that could have been contaminated by polymer additives that were used to improve core recovery during drilling. Sediments were dry-packed into the glass columns. Columns LOC-1, LOC-2, and LOC-3 were 0.5 inches in diameter and 12 inches in length. Columns LOC-4 and HOC were 1 inch in diameter and 12 inches in length. Table 2.4 shows the sediment in grams packed in the columns, porosity (calculated by dividing the volume of the sediments by the volume of the glass column in which the sediments were packed), and pore volumes of each column experiment.

Column	Sediment (g)	Porosity	Pore Volume (ml)
LOC-1	85.7	0.46	24.5
LOC-2	85.6	0.47	24.8
LOC-3	85.8	0.46	24.5
LOC-4	232	0.52	60
HOC	210	0.58	60

Table 2.4. Column parameters.

A KD Scientific syringe pump was used to inject the influent solutions at a rate of 0.4 ml/hour through Columns LOC-1, LOC-2, and LOC-3 and at a rate of 1.2 ml/hour through Columns LOC-4 and HOC. The residence times calculated for each column experiment were 61.3, 62, 61.3 hours, for Columns LOC-1, LOC-2, LOC-3, and 100 hours for Columns LOC-4 and HOC, respectively. Effluent samples were collected with an ISCO Foxy Jr Fraction collector every 7.5 hours for Columns LOC-1, LOC-2, and LOC-3, and every 3 hours for Columns LOC-4 and HOC. Effluent samples were analyzed for major cations by ICP-OES, anions by IC, and trace metals by ICP-MS. The set-up of the HOC

and LOC-4 column experiment and a schematic representing the set up all column experiments are shown in Figure 2.3.

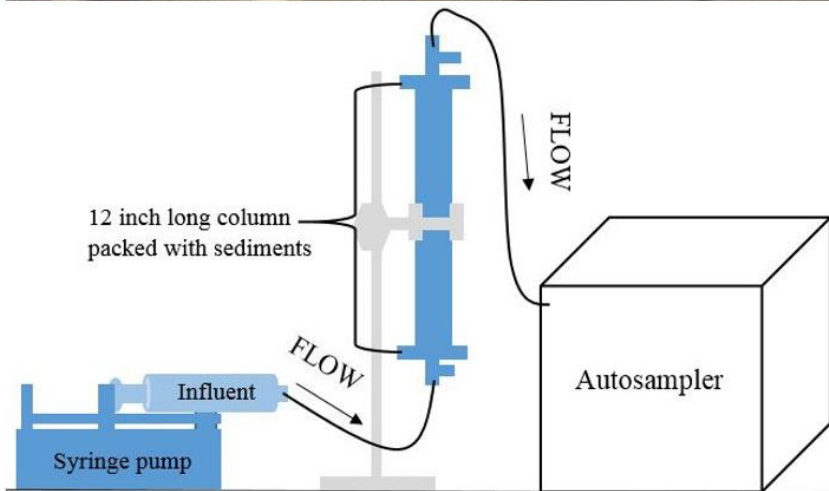


Figure 2.3. Photograph of Columns LOC-4 and HOC. Schematic represents set-up of all column experiments.

Table 2.5 shows the pore volumes of each influent solution injected into each column. The columns were first pre-flushed with degassed background water to ensure that uranium concentrations eluting from the column were stable before the dithionite was injected. Once uranium concentrations were stable, the dithionite solutions were injected into each column, and were immediately followed by the injection of post-mined waters. The injection of post-mined water after a dithionite injection was done to simulate a field treatment, in which dithionite would be injected into the post-mined aquifer, and post-mined water with soluble U(VI) would flow through the dithionite treated area and be reduced.

Column Experiment	Solution Injected (ml)	Pore Volumes Injected	Influent solution
LOC-1	9.8	0.4	Degassed MS-413 plus 120 mg/l KBr tracer
	10.3	0.42	Degassed MS-413
	61.2	2.50	15P-314 spiked with 0.5 mg/l Cr(VI) (injected as $\text{CrO}_4^-$ )
LOC-2	9.8	0.39	Degassed MS-413 plus 120 mg/l KBr tracer
	9.6	0.39	Degassed 0.05 M $\text{Na}_2\text{S}_2\text{O}_4$ buffered with 0.05 M $\text{Na}_2\text{SO}_3$ in MS-413 water
	176	7.08	15P-314 spiked with 0.5 mg/l Cr(VI) (injected as $\text{CrO}_4^-$ )
LOC-3	10.2	0.42	Degassed 0.05 M $\text{Na}_2\text{S}_2\text{O}_4$ buffered with 0.05 M $\text{Na}_2\text{SO}_3$ in MS-413 water plus 120 mg/l KBr tracer
	10.4	0.43	Degassed 0.05 M $\text{Na}_2\text{S}_2\text{O}_4$ buffered with 0.05 M $\text{Na}_2\text{SO}_3$ in MS-413 water
	363	14.8	15P-314 spiked with 0.5 mg/l Cr(VI) (injected as $\text{CrO}_4^-$ )
LOC-4	120	2	Degassed M-402 water
	112	1.93	Degassed 0.05 M $\text{Na}_2\text{S}_2\text{O}_4$ buffered with 0.05 M $\text{Na}_2\text{SO}_3$ in degassed M-402 water plus 400 mg/l LiBr tracer
	4,200	69.7	MP-423
HOC	120	2	Degassed M-402 water
	113	1.94	Degassed 0.05 M $\text{Na}_2\text{S}_2\text{O}_4$ buffered with 0.05 M $\text{Na}_2\text{SO}_3$ in degassed M-402 water plus 400 mg/l LiBr tracer
	2,220	36.6	MP-423

Table 2.5. Operational details for each experiment.

Because dithionite is unstable in solution and degrades faster in the presence of oxygen, the background waters MS-413 and M-402 were vacuum degassed to remove oxygen prior to the addition of dithionite (Lister & Garvie, 1959; Rinker et al., 1965; Lem & Wayman, 1970). The 0.05 M sodium dithionite solutions were buffered with 0.05 M sodium sulfite. Because dithionite is unstable in solution and degrades faster at a lower pH, adding a buffer to a dithionite solution can help slow its degradation (Rinker et al., 1960; Wayman & Lem, 1970). Sodium sulfite was selected as a suitable buffer for water from the Smith-Ranch. The ground water at Smith-Ranch is very hard and contains significant calcium (as shown in Table 2.3). Due to the high calcium concentrations, other buffers such as bicarbonate could result in calcite precipitation (Appendix A). Also, introducing carbonate or bicarbonate would provide opportunities for the formation of calcium-uranyl-carbonate complexes (Dong & Brooks, 2006).

Post-mined waters 15P-314 and MP-423 were not degassed prior to injection into the columns. The post-mined waters were stored at room temperature while the experiments were running. Every time the containers were opened, they were exposed to oxygen. In a field deployment, post-mined waters flowing through the aquifer are anoxic. Therefore, any reductive capacities observed in column experiments could be higher in the field because the waters will not be oxygenated.

#### *Column Sediment Leaching*

Columns LOC-1, LOC-2, and LOC-3 were stopped and frozen when uranium broke through to concentrations approaching that of the 15P-314 water. The frozen sediments from columns LOC-1, LOC-2, and LOC-3 were then cut into ~ 1 cm sections and each section was leached with 20 ml of 2 M nitric acid for two days. Sediments were placed on

a shaker table at room temperature during the leaching. After two days, the acidic supernatant was centrifuged, filtered, and analyzed for cations using ICP-OES and for trace metals using ICP-MS. Because no dithionite was injected into column LOC-1, the sediment samples from LOC-1 provided “background” levels of leachable constituents on the sediments.

Any species consistently determined to be above or below background levels was considered to be of potential interest in providing clues as to the geochemical processes occurring during the column experiments. However it is important to note that the sediments are heterogeneous, so subtracting the background does not provide an exact concentration of what was leached off the sediments. The sediments from Columns LOC-4 and HOC were not leached.

## 2.4 Results and Discussion

### *Reductive capacities: LOC experiments*

Figures 2.4 through 2.7 show uranium and chloride breakthrough curves plotted relative to their injection concentrations ( $c/c_0$ ) for Columns LOC-1 through LOC-4. Because it is conservative, chloride breakthrough represents the breakthrough of 15P-314 water in Columns LOC-1, LOC-2, and LOC-3, and the breakthrough of MP-423 water in Column LOC-4. Uranium breakthrough indicates that the reductive capacity imparted by the dithionite is depleted. Plots for all cations, anions, and trace metals in the column eluent for each experiment can be found in Section 2.6, Supplemental Information.



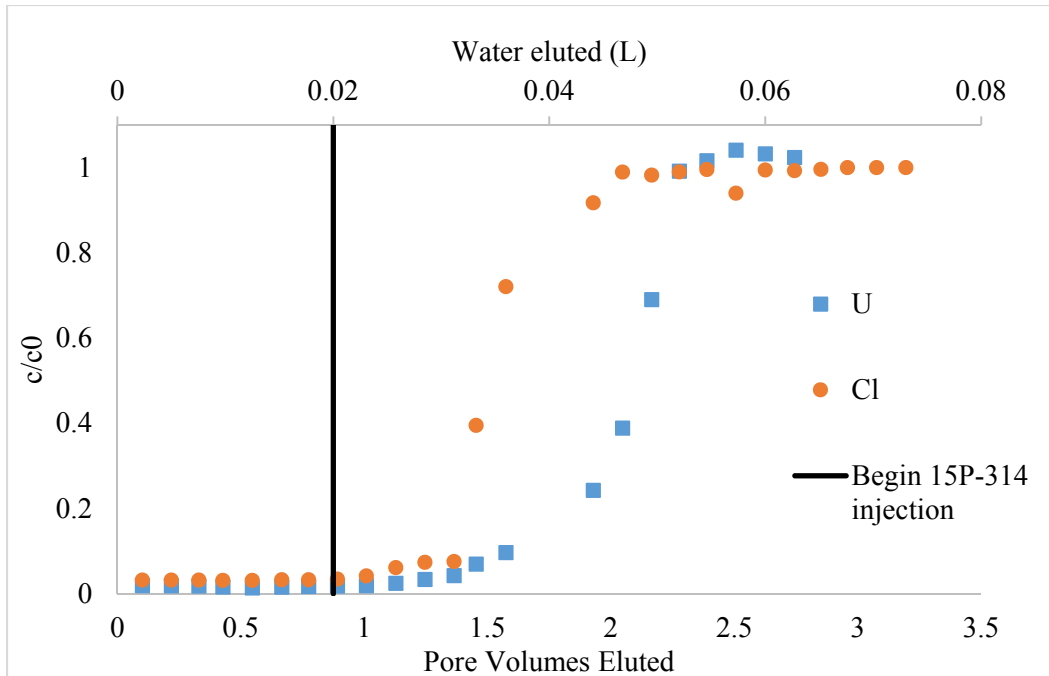


Figure 2.4. Uranium and chloride breakthrough curves for Column LOC-1. The retardation factor between the chloride and uranium breakthrough curves was calculated to be 1.33.

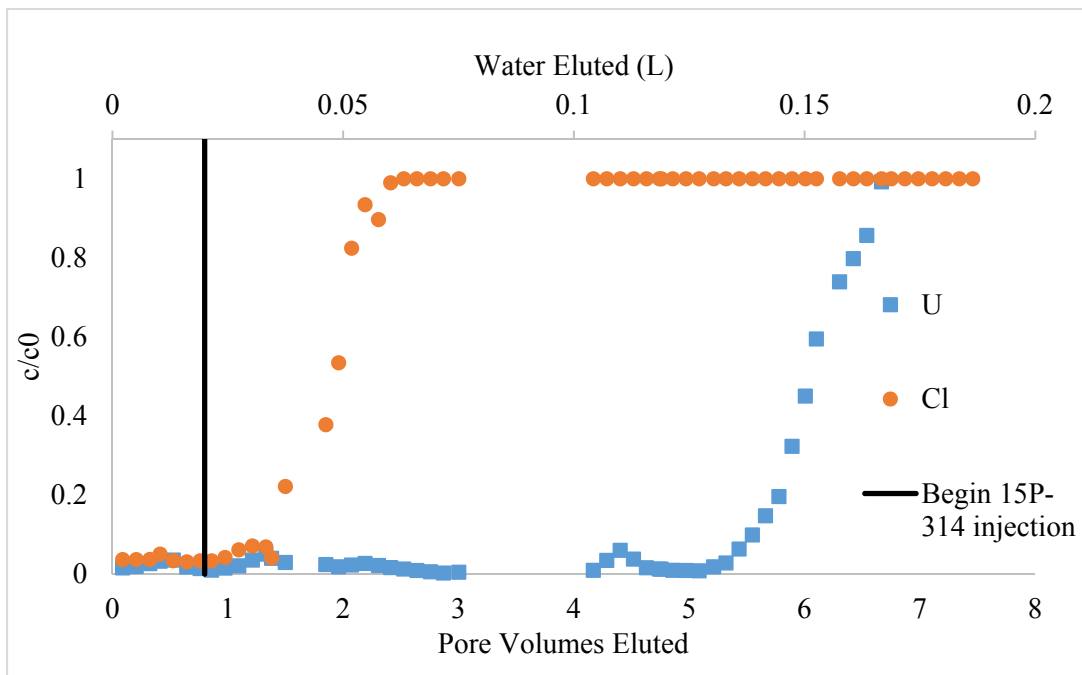


Figure 2.5. Uranium and chloride breakthrough curves for Column LOC-2 with the retardation factor of 1.33 imposed on the chloride breakthrough curve. Gap in data between 3 and 4 pore volumes eluted represents sample loss.

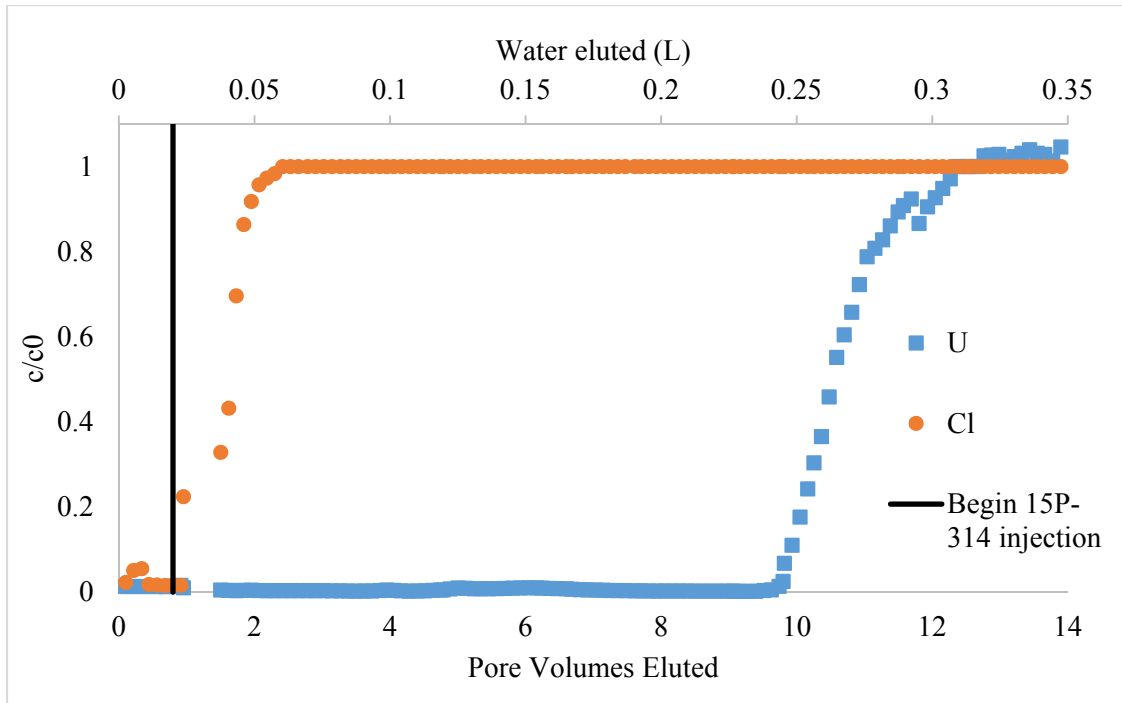


Figure 2.6. Uranium and chloride breakthrough curves for Column LOC-3 with the retardation factor of 1.33 imposed on the chloride breakthrough curve.

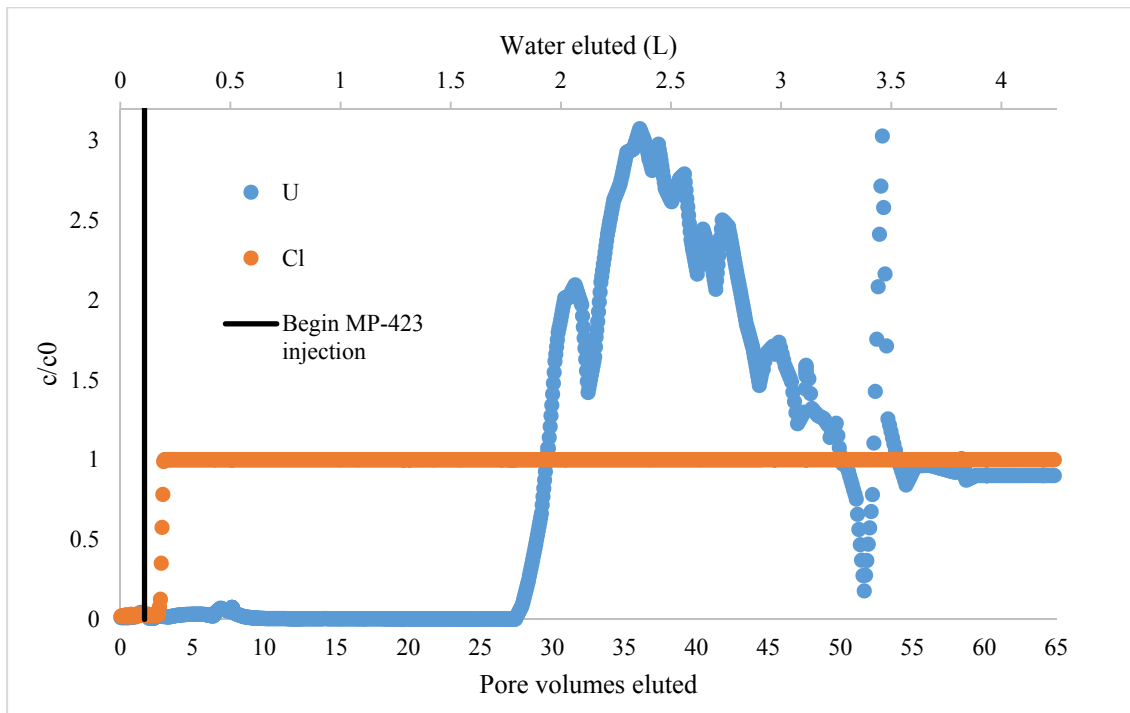


Figure 2.7. Uranium and chloride breakthrough curves for Column LOC-4 with the retardation factor of 1.33 imposed on the chloride breakthrough curve. After ~30 pore volumes were eluted, all the uranium that had been initially reduced started oxidizing.

Figure 2.4 shows that even though there was no dithionite injected into Column LOC-1, the uranium breakthrough was slightly delayed relative to the chloride. A delay in uranium breakthrough relative to a conservative tracer has been observed in other column experiments using sediments and waters from SRH, likely due to uranium sorption onto mineral surfaces such as clays or iron oxides (Dangelmayr et. al., 2017). The retardation factor between the breakthrough of uranium and chloride for Column LOC-1 was calculated to be 1.33. This retardation factor of 1.33 was imposed on the chloride breakthrough curves for Columns LOC-2, LOC-3, and LOC-4 when calculating the reductive capacities imparted by the dithionite to subtract a delay in breakthrough that would occur in the absence of dithionite.

Even though Column LOC-4 had different post-mined water injected through it than Columns LOC-1, LOC-2, and LOC-3, the same retardation factor was used because the alkalinity and calcium concentrations of the post-mined waters used were very similar. Due to the formation of calcium-uranyl-carbonate complexes ( $\text{Ca}_2\text{UO}_2(\text{CO}_3)_3^0$  and  $\text{CaUO}_2(\text{CO}_3)_3^{2-}$ ), alkalinity and calcium are considered to be the most important groundwater chemistry parameters that influence uranium solubility and mobility (Dong & Brooks, 2006; Saunders et al., 2016). The alkalinity and calcium concentrations of the post-mined water injected into Columns LOC-1, LOC-2, and LOC-3 was 794 mg/l and 384 mg/l, respectively. The alkalinity and calcium of the post-mined water injected into Column LOC-4 was 747 mg/l and 409 mg/l, respectively.

Figures 2.5 and 2.6 show that the uranium breakthrough was significantly delayed relative to the chloride. The delay in uranium breakthrough represents the period during which uranium was reduced as a result of the dithionite injection. Columns LOC-2 and

LOC-3 were stopped when concentrations of uranium broke through to that of the 15P-314 water.

Column LOC-4 was kept running after uranium broke through to concentrations of the MP-423 water. Figure 2.7 shows that the uranium initially reduced by the dithionite was oxidized between 30 and 50 pore volumes eluted from the column. This is likely due to the oxygen in the post-mined water that was injected into the column. Assuming the post-mined waters were saturated with respect to oxygen, 2.7 milliequivalents of oxygen were injected into the column until uranium stopped being oxidized at 50 pore volumes. If 0.06 milliequivalents of uranium were reduced, the oxygen injected into the column during the period that uranium was being oxidized was more than enough to oxidize the uranium that had been reduced.

It is reasonable to expect, for similar sediments, that every mole of dithionite deployed should impart a reduction capacity to the sediments that is capable of reducing a given number of equivalents of aqueous electron acceptors (e.g.,  $O_2$ ,  $NO_3^-$ , U(VI)) as they flow through the dithionite-treated zone. These column experiments revealed that in post-mined waters from the Smith-Ranch, uranium does not appear to be the major electron acceptor. The volume of water recovered between the chloride and uranium breakthrough curves was calculated by integrating the area between the two curves. Table 2.6 shows the moles of dithionite injected into each column, liters of water recovered between chloride and uranium breakthrough, the ratio of water recovered between chloride and uranium breakthrough relative to moles of dithionite injected, the moles of uranium reduced, and the moles of uranium reduced relative to dithionite injected in Columns LOC-2, LOC-3, and LOC-4. The ratios of water recovered between chloride and uranium breakthrough

relative to moles of dithionite injected are in closer agreement than the ratios of the moles of uranium reduced relative to the moles of dithionite injected. The fact that the dithionite treated a fixed volume of water rather than a fixed amount of U(VI) is a strong indication that there are additional electron acceptors in the water besides U(VI) that are likely consuming reduction capacity (and likely to a greater degree than U(VI)).

Column	Moles of dithionite injected	Liters of water recovered between chloride and uranium breakthrough	Ratio of water recovered between chloride and uranium breakthrough relative to moles of dithionite injected	Moles of uranium reduced	Moles of uranium reduced relative to moles of dithionite injected
LOC-2	4.8E-04	0.09	179	1.06E-05	2.2E-02
LOC-3	1.0E-03	0.24	238	2.30E-05	2.2E-02
LOC-4	5.6E-03	1.80	321	2.96E-05	5.3E-03

Table 2.6. Moles of dithionite injected into each column, liters of water recovered between chloride and uranium breakthrough, the ratio of water recovered between chloride and uranium breakthrough relative to moles of dithionite injected, the moles of uranium reduced, and the ratio of moles of uranium reduced to moles of dithionite injected in column experiments LOC-2, LOC-3, and LOC-4.

Another major electron acceptor that could be consuming reductive capacity imparted by dithionite is sulfate. The 15P-314 and MP-423 waters injected into the columns had 609 mg/l and 647 mg/l of sulfate, respectively. Sulfate, whose oxidation state is +6, has the potential to be reduced to several different oxidation states, ranging from +4 ( $\text{SO}_3^-$ ) to -2 ( $\text{S}^-$ ). Table 2.7 shows the equivalents per liter of potential electron acceptors in the 15P-314 and MP-423 waters. The equivalents per liter of sulfate are greater than uranium, nitrate, or oxygen, the other potential electron acceptors in the two-post mined

waters. In Columns LOC-2, LOC-3, and LOC-4, 69 %, 77 %, and 57% of sulfur was recovered from the columns relative to what was injected. Some of the unrecovered sulfur could have been sulfate in the influent that was reduced. Reduced sulfur could have reacted with Fe(II) and precipitated as iron sulfides (Liu et al., 2017).

<b>Constituent</b>	<b>15P-314 (eq/L)</b>	<b>MP-423 (eq/L)</b>
U(VI)	2.2E-04	3.2E-05
SO <sub>4</sub> <sup>2-</sup>	1.2E-02	1.3E-02
NO <sub>3</sub> <sup>-</sup>	6.5E-07	0
O <sub>2</sub>	9.0E-04	9.0E-04

Table 7.7. Equivalents per liter of potential electron acceptors for 15P-314 and MP-423 waters.

Figure 2.8 shows sulfate eluted from Columns LOC-2, LOC-3, and LOC-4. The large amount of sulfate eluted at the beginning of the experiments appears to contradict the statement that sulfate is being reduced by the dithionite. However, sodium dithionite is highly reactive with sediments and unstable in solution. This results in disproportionation reactions yielding sulfite, bisulfite, and thiosulfate (Amonette et al., 1994, Istok et al., 1999; Ludwig et al., 2007). When these reduced sulfur species in the column eluent were exposed to the atmosphere in the autosampler, they could have oxidized to sulfate. In addition, sulfate is a direct degradation product of dithionite (LANL, 2018). The oxidation of intermediate sulfur species formed by dithionite degradation in the autosampler and the degradation of dithionite into sulfate account for the large amount of sulfate eluted at the beginning of the experiment. The incomplete sulfur recovery from the columns and the

greater equivalents per liter of sulfate compared to uranium supports the idea that sulfate could have been consuming the reduction capacity of dithionite. Future research should assess the sulfate reactions in more detail.

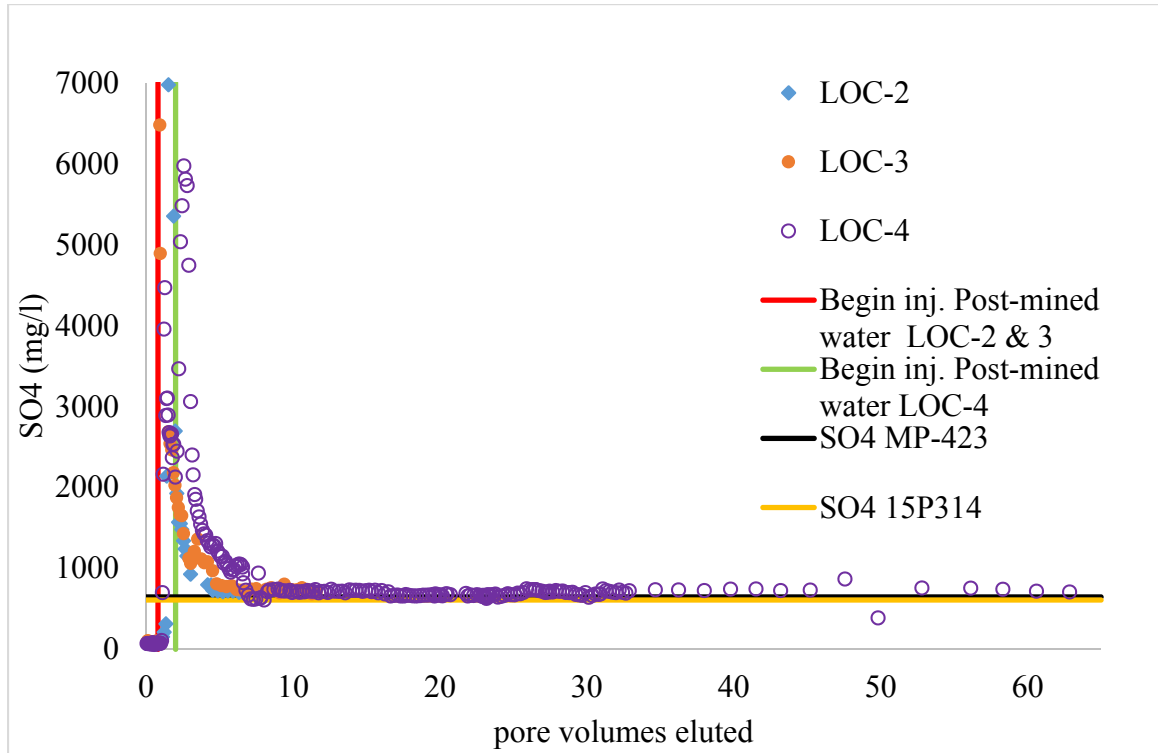


Figure 2.8. Sulfate eluted in mg/l plotted against pore volumes eluted in Columns LOC-2, LOC-3, and LOC-4.

*Sediment Leaching: Columns LOC-1, LOC-2, and LOC-3*

Figure 2.9 shows the iron leached from the sediments of Columns LOC-1, LOC-2, and LOC-3. Iron (in mg per 1 g sediment) is plotted against “distance as % of column mass.” 0% represents the sediment at the column inlet, while 100% represents sediments at the column outlet. 53, 42, and 46 mg of iron were leached off the sediments in Columns LOC-1, LOC-2, and LOC-3, respectively. The decreased amounts of iron leached from the sediments in Columns LOC-2 and LOC-3 relative to Column LOC-1 could be due to reduction of Fe (III) to Fe (II) with corresponding dissolution of the Fe(II) resulting from the dithionite injection (Amonette et al., 1994). Figure 2.10 shows Fe(II) eluted from

Columns LOC-1, LOC-2, LOC-3, and LOC-4. No iron was recovered in the Column LOC-1 eluent (which had no dithionite injected into it). 2.91E-03 mg of iron were recovered from Column LOC-2, 3.25E-03 mg of iron were recovered from Column LOC-3, and 3.7E-02 mg of iron were recovered from Column LOC-4. The Fe(II) recovered from Columns LOC-2, LOC-3, and LOC-4 was likely Fe(II) which dissolved after Fe(III) in the sediments was reduced to Fe(II) as a result of the dithionite injection.

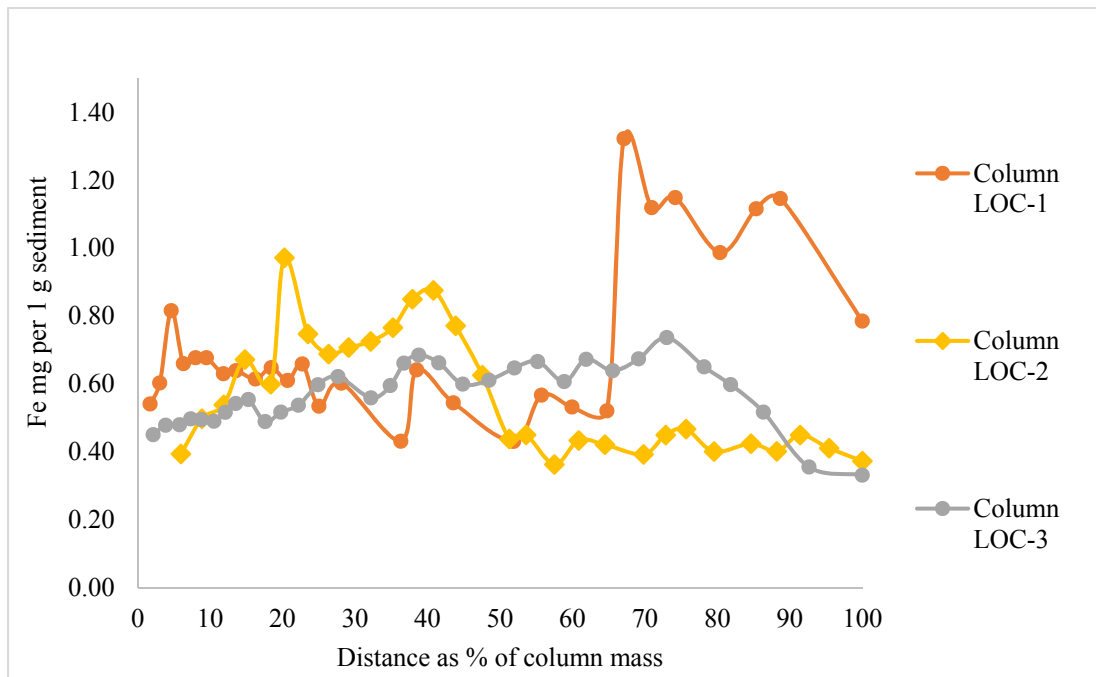


Figure 2.9. Iron leached from sediments of Columns LOC-1, LOC-2, and LOC-3.



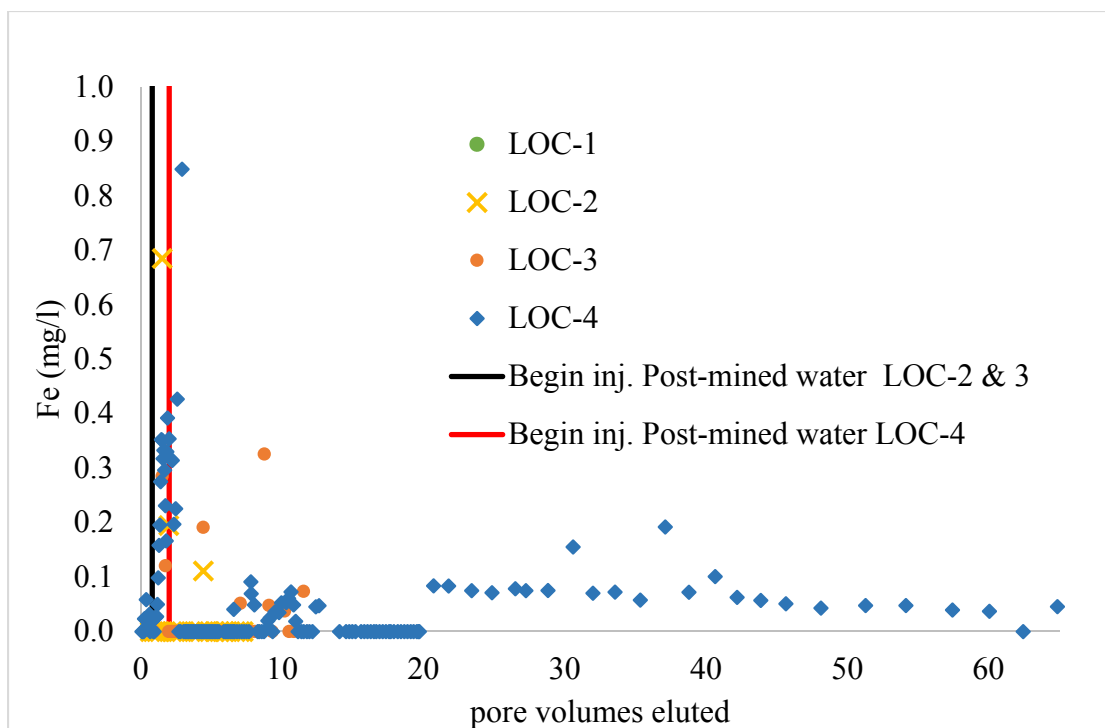


Figure 2.10. Iron eluted from Columns LOC-1, LOC-2, LOC-3, and LOC-4.

Figures 2.11 and 2.12 show chromium, uranium, and iron leached from the sediments of Columns LOC-2 and LOC-3. Chromium (injected as  $\text{CrO}_4^-$ ) was leached from the column inlet to about 10 % of column LOC-2, and from the column inlet to 20 % of column LOC-3. Chromium never broke through in the column eluent which suggests it was still being reduced, even after the reduction capacity for uranium was exhausted.

Uranium was leached from 10% to 40% of column LOC-2, and from 20% to 70% of Column LOC-3. Uranium was leached about twice as far in Column LOC-3 as Column LOC-2. There are two possibilities for this. The first is that Column LOC-3 had two times the amount of dithionite injected into it compared to Column LOC-2. Perhaps the dithionite injection reached twice as far into Column LOC-3, and reduced uranium onto the sediments for twice the distance. Or, Column LOC-3 was run about twice as long as Column LOC-2 (~12 pore volumes versus ~7 pore volumes). The distribution of uranium

further into Column LOC-3 could represent a pulse of uranium reduced by the dithionite oxidizing and travelling through the column. Column LOC-4 showed that the reduction imparted by the dithionite is reversible. If Column LOC-2 had been kept running as long as LOC-3, we expect that the uranium pulse would have shifted further in the column and appear more similar to LOC-3.

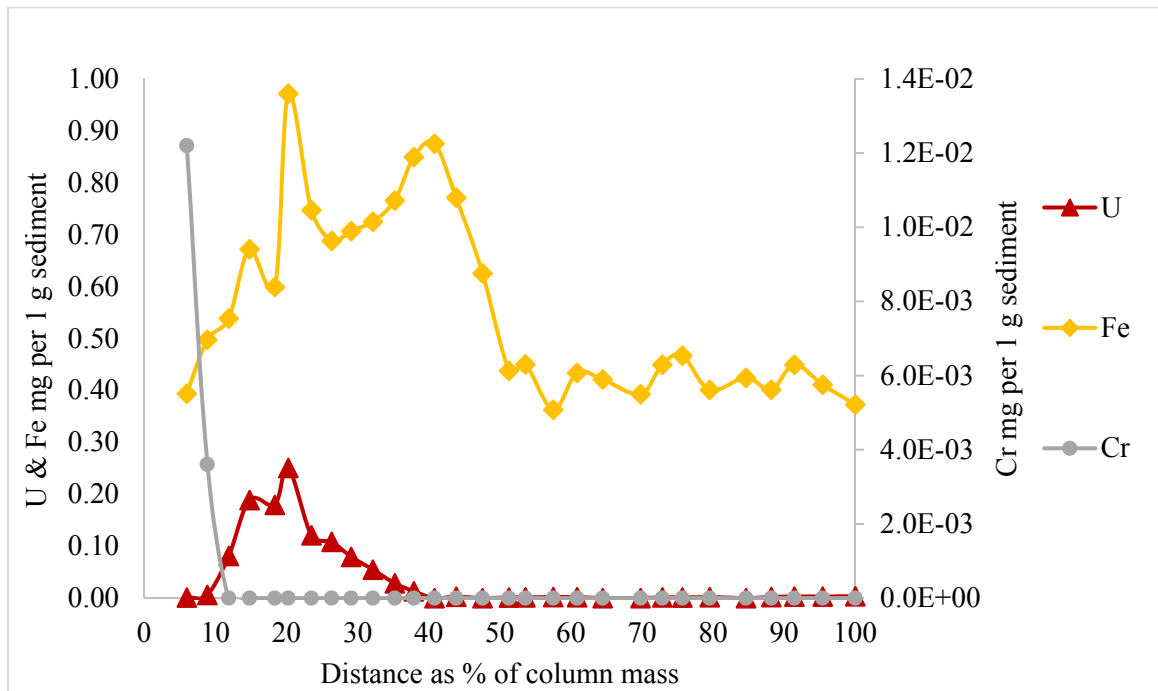


Figure 2.11. Fe, U and Cr (mg/g sediment) leached from column LOC-2, plotted by distance as % of column mass.

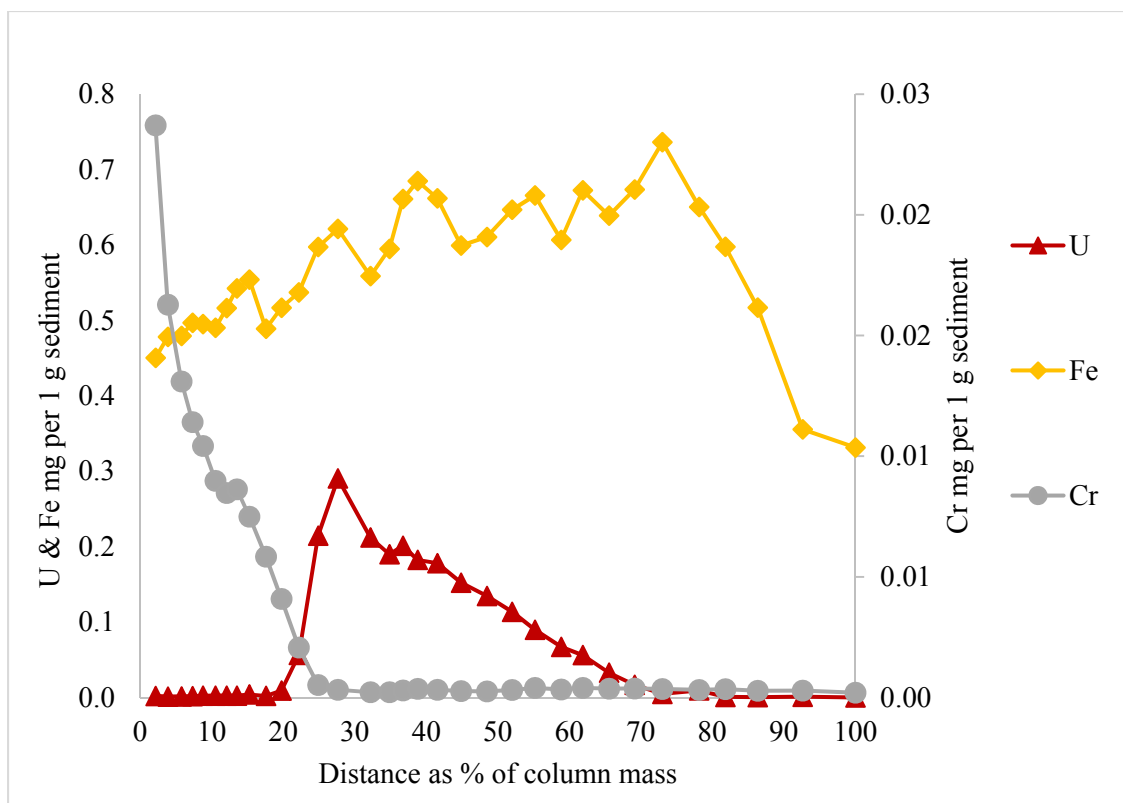


Figure 2.12. Fe, U and Cr (mg/g sediment) leached from column LOC-3, plotted by distance as % of column mass.

The uranium leached from the column sediments was included in the total uranium recoveries for Columns LOC-2 and LOC-3. Table 2.7 shows the uranium recoveries for Columns LOC-2, LOC-3, and LOC-4, including what was recovered from the sediments and the eluent.

Column Experiment	U(VI) recovered in eluent (moles)	U(VI) recovered from sediments (moles)	U(VI) injected (moles)	Total U(VI) recovery (%)
LOC-1	6.5E-06	NA	0	90
LOC-2	4.54E-06	1.06E-05	2.08E-05	73
LOC-3	9.8E-06	2.3E-05	4.3E-05	77
LOC-4	5.8E-05	NA	6.4E-05	90

Table 2.8. Uranium mass balance for Columns LOC-2, LOC-3, and LOC-4.

*Effects of dithionite on sediments with high organic carbon*

The second goal of this study was to compare the effects of sodium dithionite between sediments that contained high and low organic carbon content. The sediments with low organic carbon content all had reductive capacities imparted to them with respect to U(VI) after treatment with dithionite. A high organic carbon content column (HOC) was run in essentially the same manner as Column LOC-4, except we used sediments with high organic carbon content. Figure 2.12 shows uranium and chloride breakthrough curves for Column HOC. Concentrations of uranium eluting from the column stayed at or above injection concentrations for the entire duration of the experiment. 35.4  $\mu\text{mol}$  of uranium were injected into the column, and 56.9  $\mu\text{mol}$  of uranium were recovered. Clearly, the sodium dithionite did not impart any reductive capacity (at least with respect to U(VI) reduction) to the high organic carbon sediments, and instead liberated uranium from the sediments. The excess uranium recovered from the column was likely liberated from the organic carbon in the sediments, which tends to be rich in uranium (Idiz et al., 1986; Zielinski & Meier, 1988). The HOC column had approximately 7.73% organic carbon while the LOC columns had approximately 0.38% organic carbon.

The difference in organic carbon and uranium content of the sediments is likely responsible for the difference in behaviors between the LOC and HOC columns. The HOC column sediments contained approximately 0.54 grams of uranium, while the LOC column sediments had only approximately 0.0046 g of uranium. The HOC column sediments did not appear to have been leached during the ISR process because they appeared less permeable, contained more uranium, and did not take on a yellowish color after being oxidized (WoldeGabriel et al., 2014). The higher uranium content and more reduced state of the HOC column sediments must have interfered with the dithionite degradation.

Even though the HOC column yielded net uranium production, a calculation revealed that only 1.1 % of uranium that was in the column sediments was liberated as a result of the dithionite injection. 0.008 grams of uranium were injected into the HOC column, and 0.014 grams were recovered. The extra 0.006 grams of uranium that were recovered from the column experiment are only 1.1 % of the uranium that was in the column sediments. This suggests that if dithionite was deployed in a field setting with uranium rich organic carbon content, it would not impart a reducing capacity to the sediments, and it could liberate a small amount of uranium in the sediments.

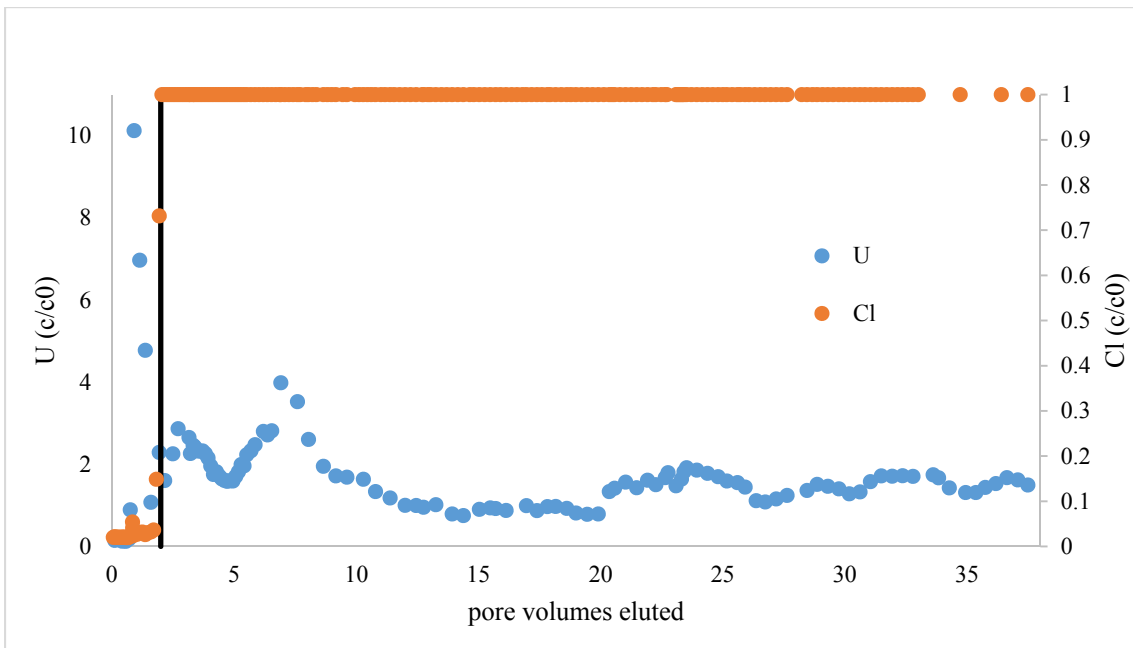


Figure 2.13. Uranium and chloride breakthrough curves for Column HOC. No retardation factor was imposed on the chloride breakthrough curve because no reductive capacity with respect to uranium was observed.

## 2.5 Conclusions

The first goal of this study was to compare the reductive capacities of post-mined sediments with low organic carbon content to treatment with varying amounts of sodium dithionite. Columns LOC-2, LOC-3, and LOC-4 used post-mined sediments from the same section of core with low organic carbon content, but were treated with different amounts

of dithionite. For Columns LOC-2, LOC-3, and LOC-4, it is reasonable to expect, for similar sediments, that every mole of dithionite deployed should impart a reduction capacity to the sediments that is capable of reducing a given number of equivalents of aqueous electron acceptors (e.g., O<sub>2</sub>, NO<sub>3</sub><sup>-</sup>, U(VI)) as they flow through the dithionite-treated zone. The fact that dithionite treated a fixed volume of water in Columns LOC-2, LOC-3, and LOC-4 despite the differences in uranium concentrations in the water, is a strong indication that there are additional electron acceptors in the water besides U(VI) that are likely consuming the reduction capacity (and likely to a greater degree than U(VI)). Sulfate is the most likely electron acceptor in the post-mined water in addition to uranium that consumes the reductive capacity imparted by the dithionite. This implies that the volume of water treated by a dithionite deployment will depend on the amount of electron acceptors in the water.

The second goal of this study was to compare the responses of sediments with high organic carbon content to the response of sediments with low organic carbon content to treatment with sodium dithionite. The sediments with low organic carbon content all had reduction capacities imparted to them after treatment with sodium dithionite. But the sediments with high organic carbon content did not have a reduction capacity imparted to them after treatment with sodium dithionite. The dithionite appeared to liberate uranium from the organic carbon content in the sediments. The higher uranium and organic carbon content, and the more reduced state of the sediments in the HOC column appeared to result in a different set of dithionite reactions and reaction products.

2.6 Supplemental Information

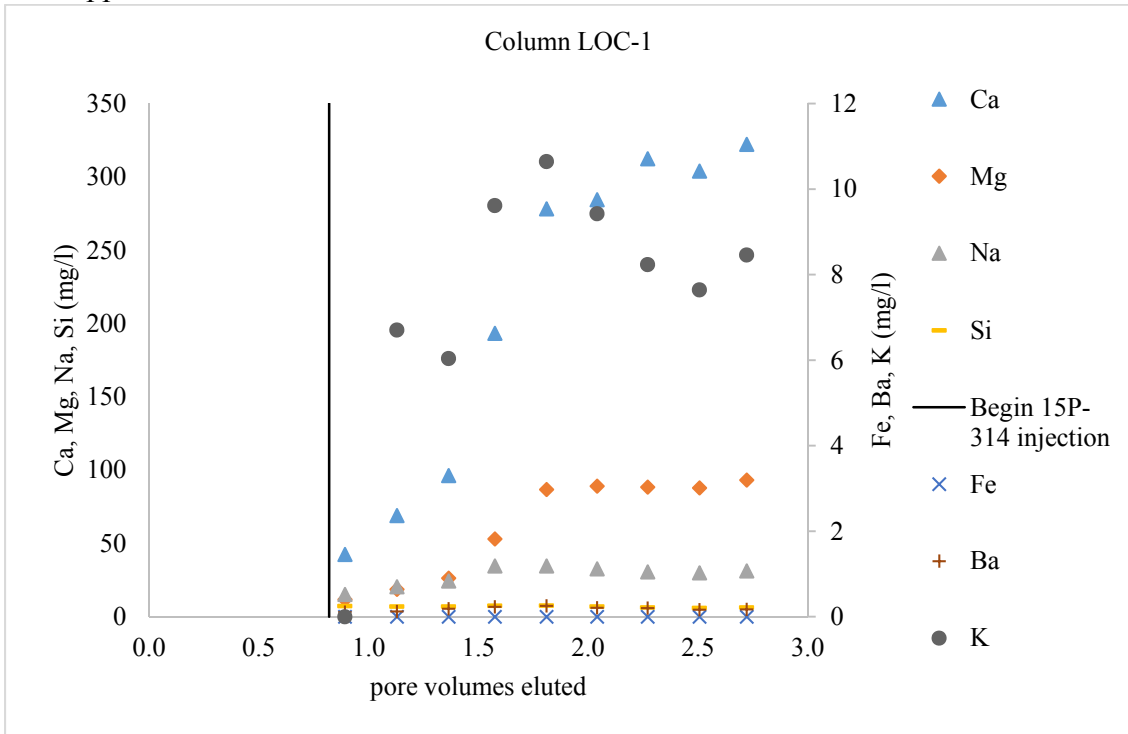


Figure 2.14. Cations in Column LOC-1 eluent plotted against pore volumes eluted.

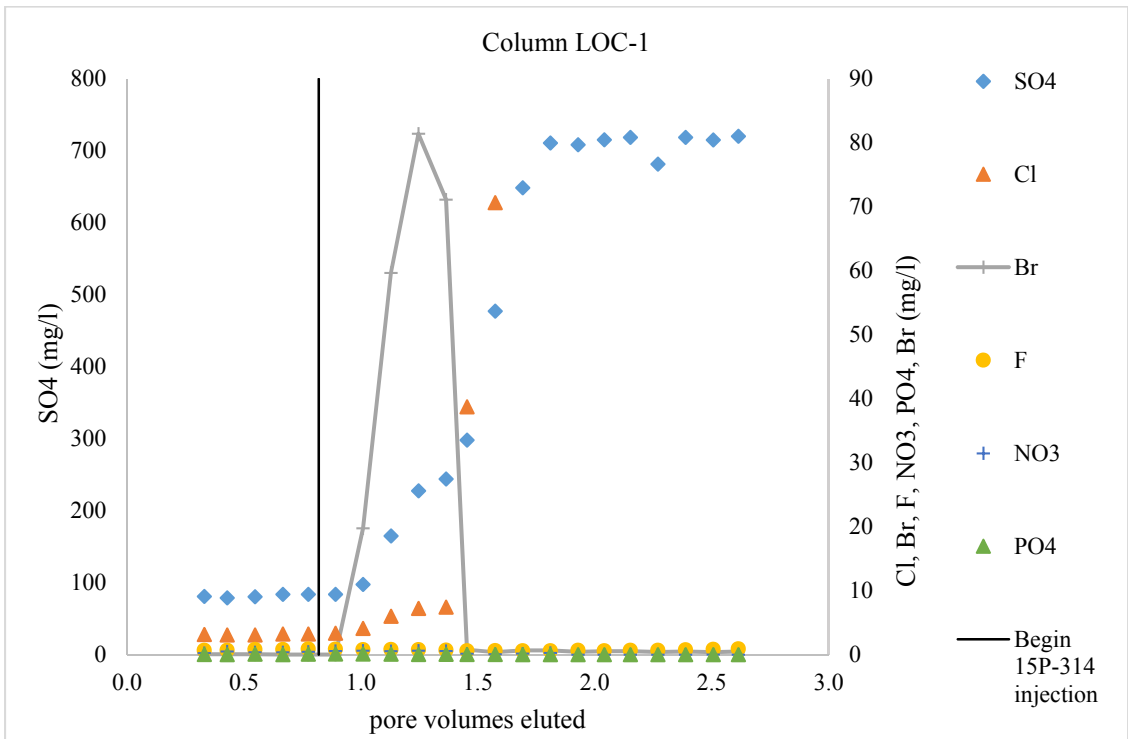


Figure 2.15. Anions in Column LOC-1 eluent plotted against pore volumes eluted.

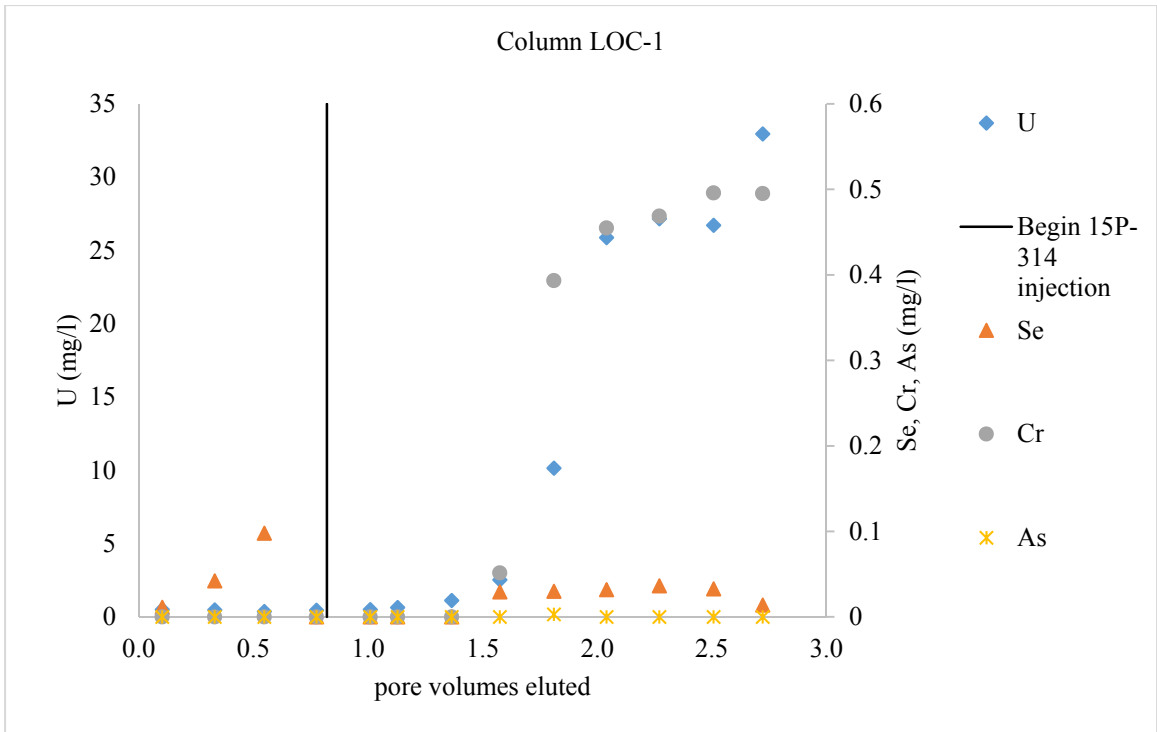


Figure 2.16. Trace metals in Column LOC-1 eluent plotted against pore volumes eluted.

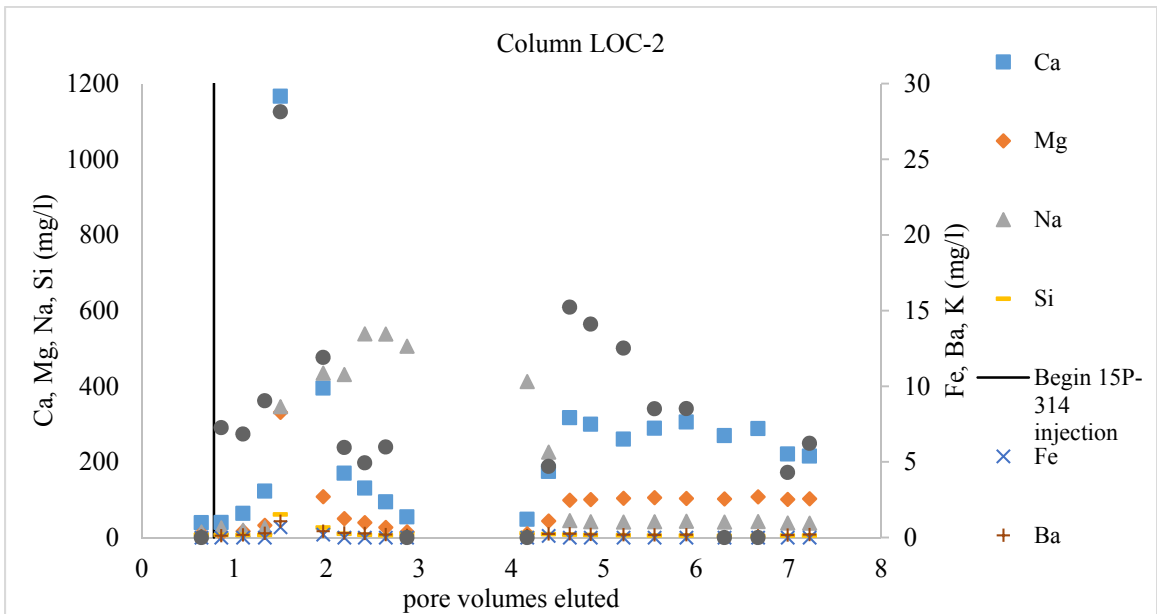


Figure 2.17. Cations in Column LOC-2 eluent plotted against pore volumes eluted.



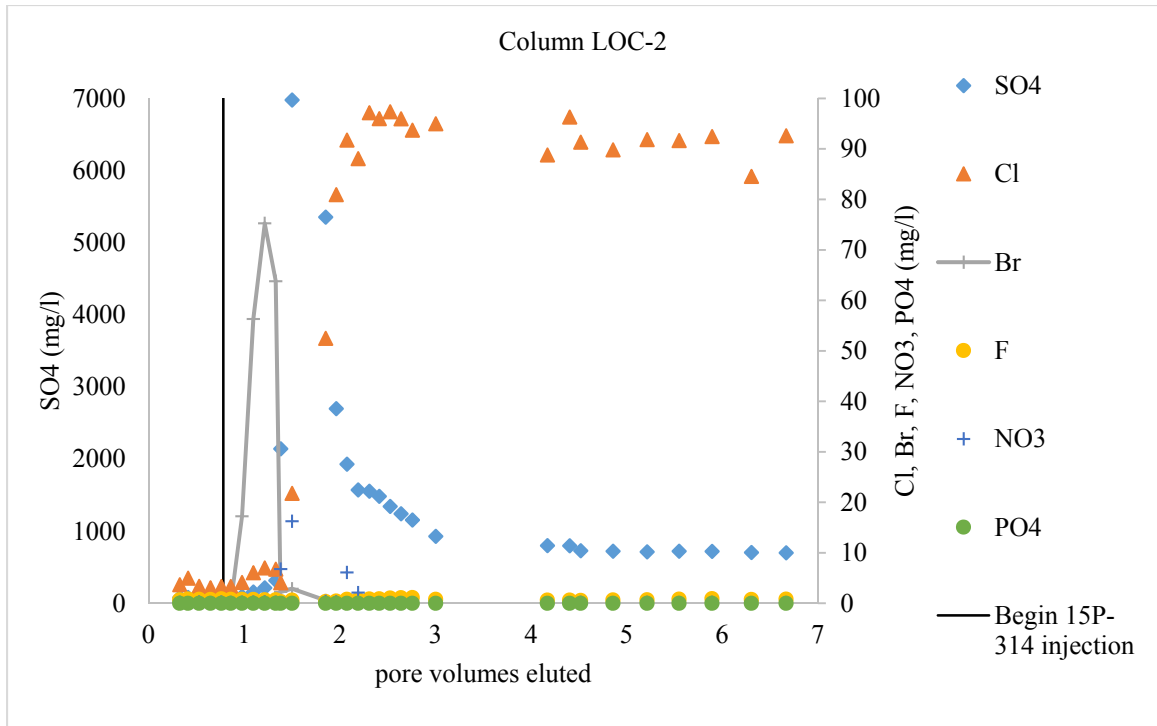


Figure 2.18. Anions in Column LOC-2 eluent plotted against pore volumes eluted. Gap in data between 3 and 4 pore volumes represents sample loss.

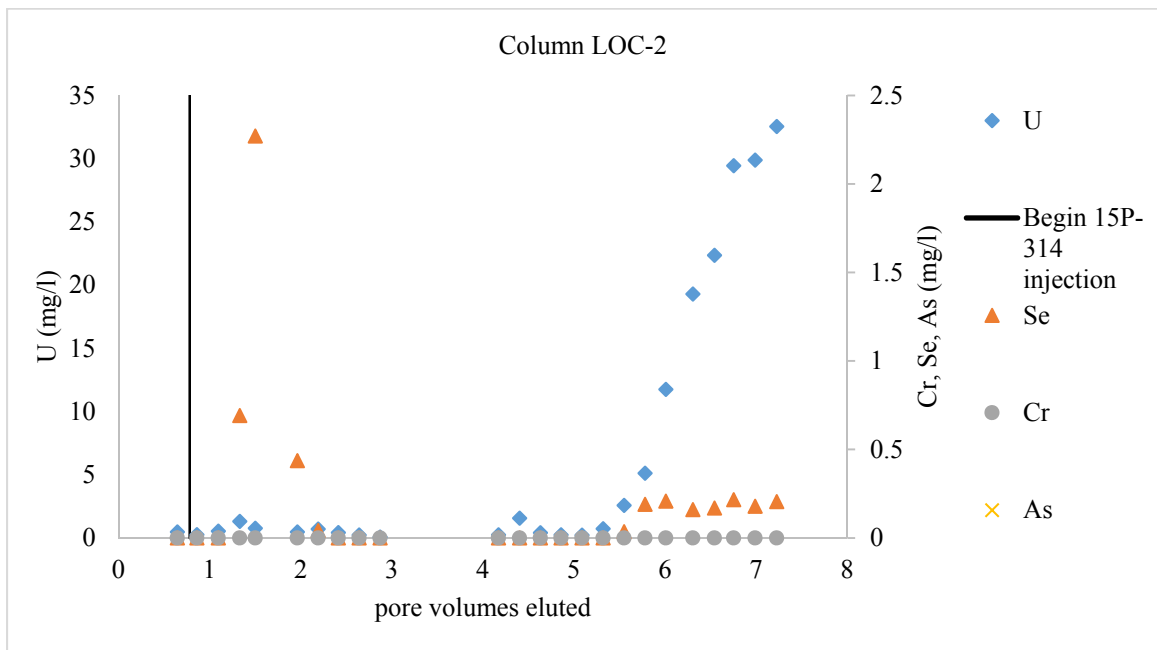


Figure 2.19. Trace metals in Column LOC-2 eluent plotted against pore volumes eluted. Gap in data between 3 and 4 pore volumes represents sample loss.

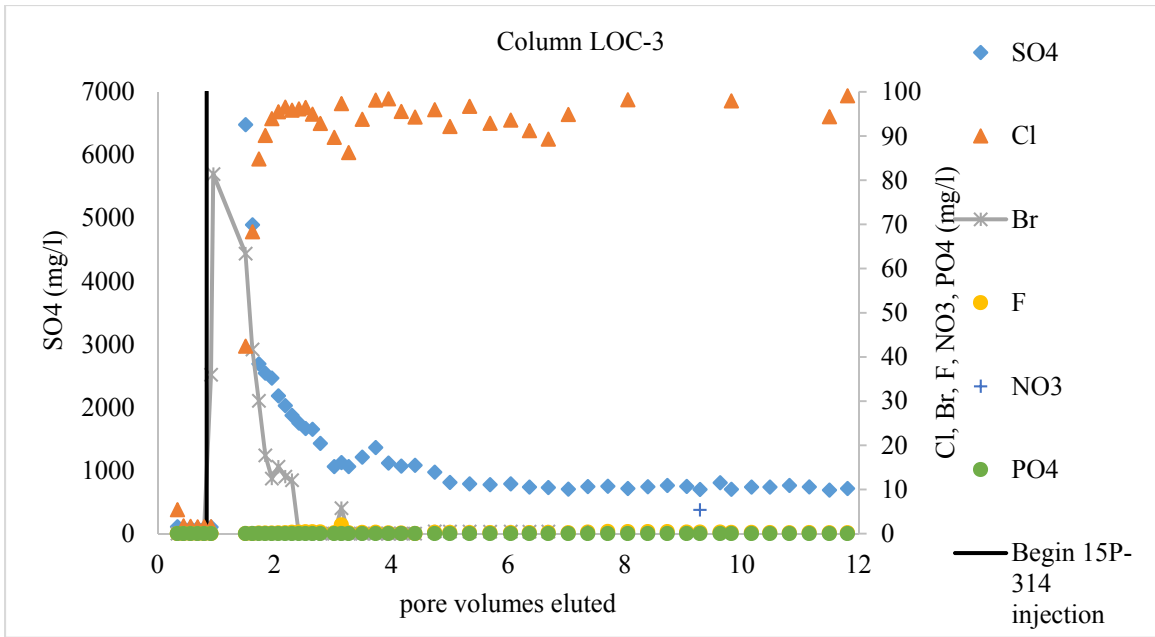


Figure 2.20. Anions in Column LOC-3 eluent plotted against pore volumes eluted.

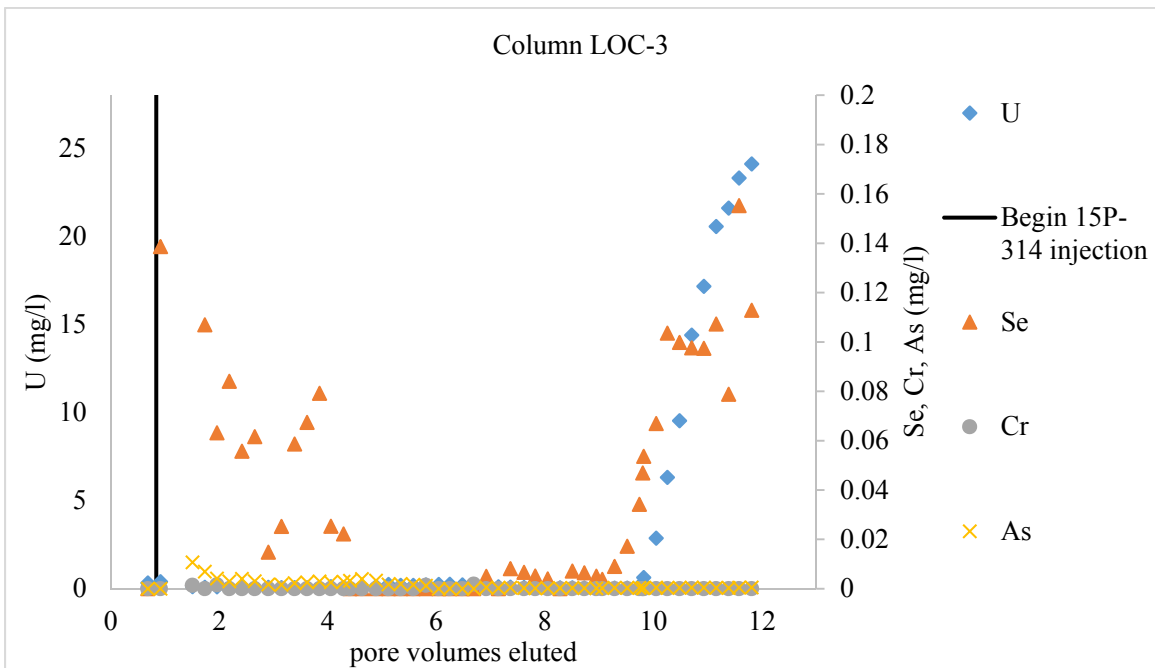


Figure 2.21. Trace metals in Column LOC-3 eluent plotted against pore volumes eluted.

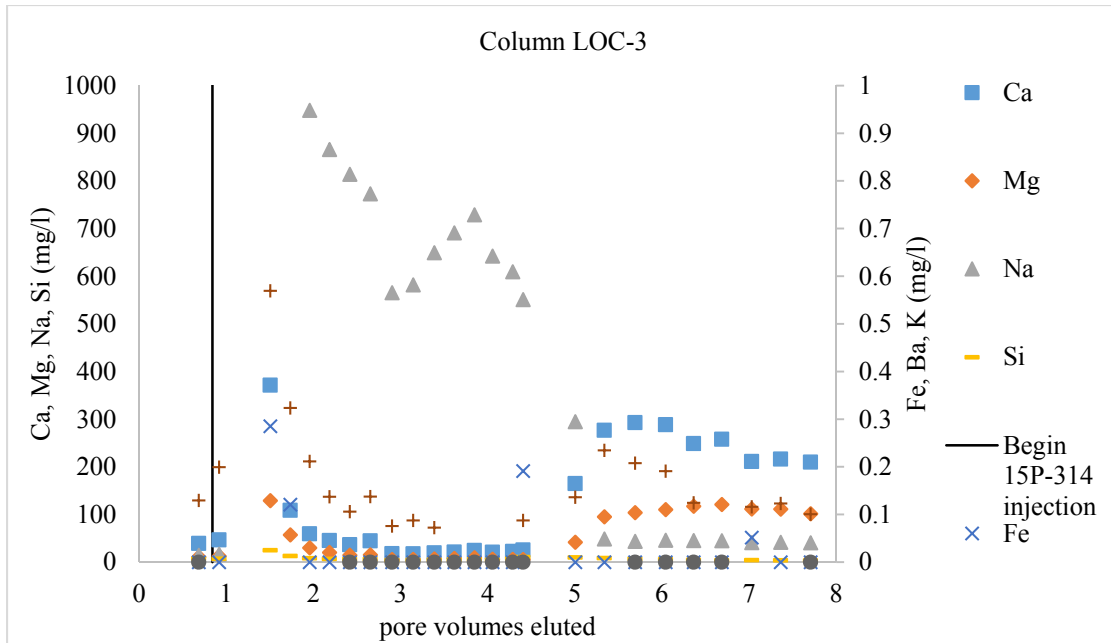


Figure 2.22. Cations in Column LOC-3 eluent plotted against pore volumes eluted.

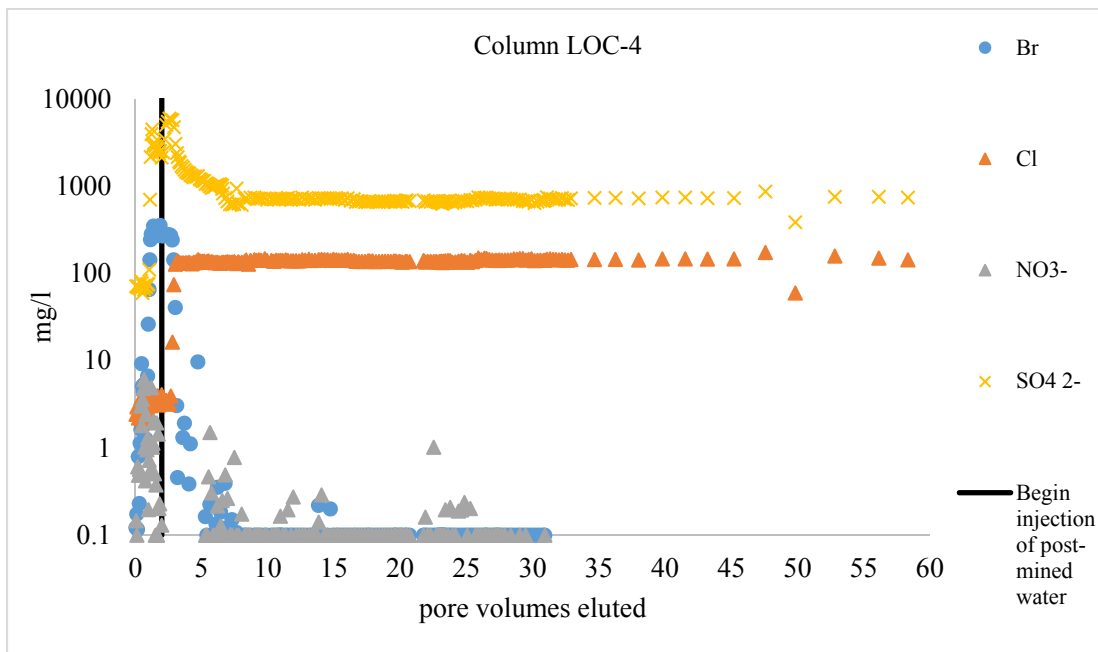


Figure 2.23. Anions in Column LOC-4 eluent plotted against pore volumes eluted.

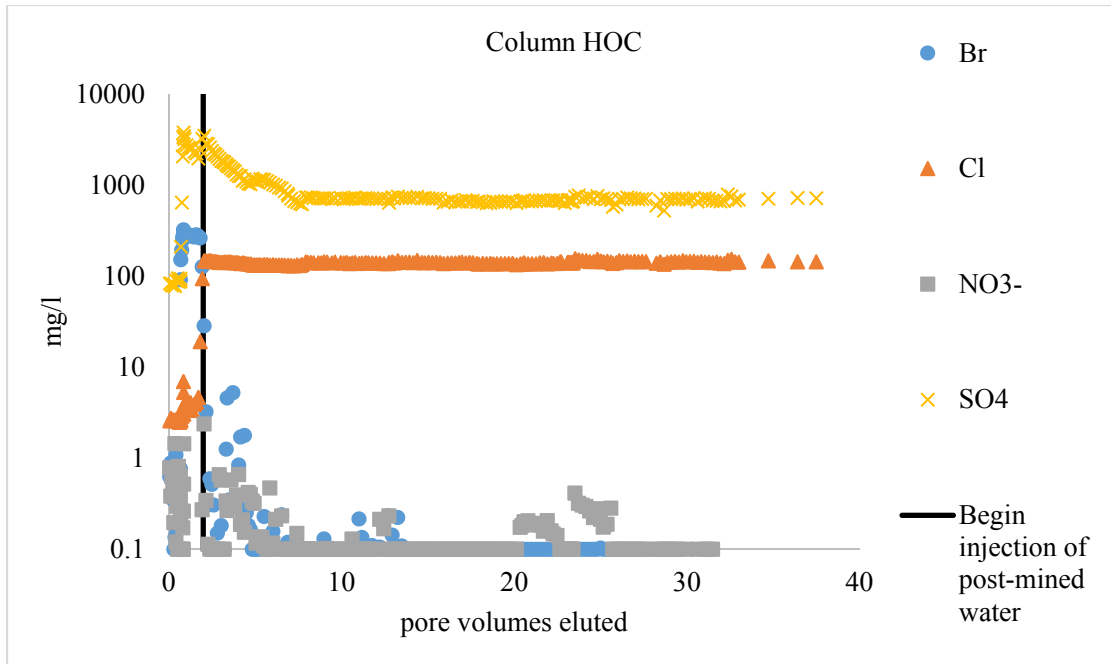


Figure 2.24. Anions in Column HOC eluent plotted against pore volumes eluted.

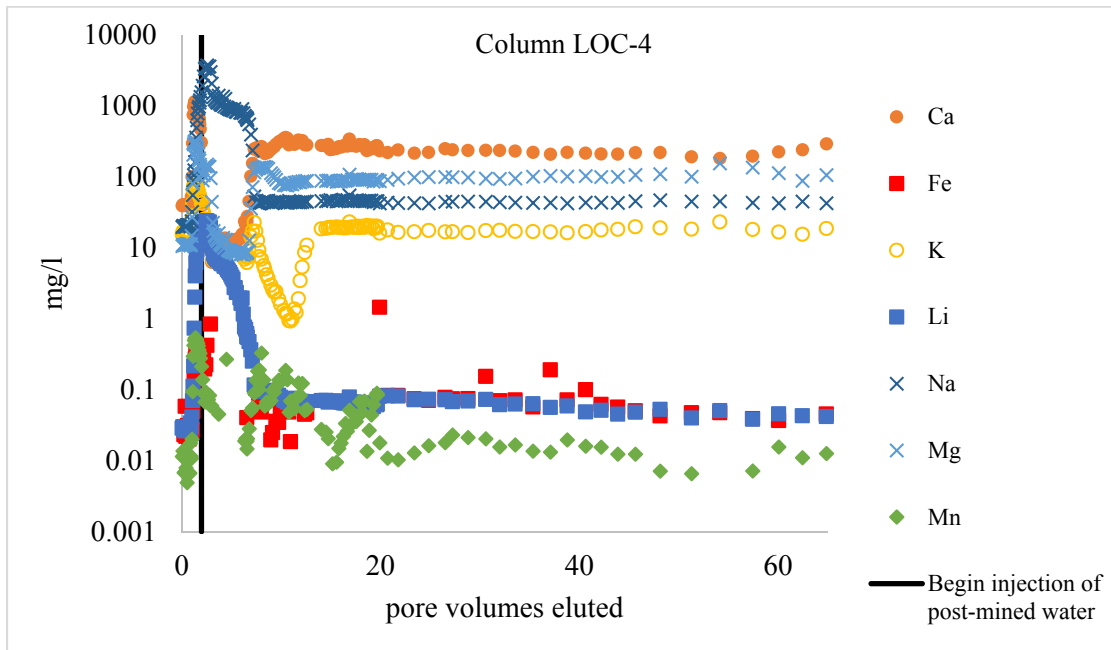


Figure 2.25. Cations in Column LOC-4 eluent plotted against pore volumes eluted.

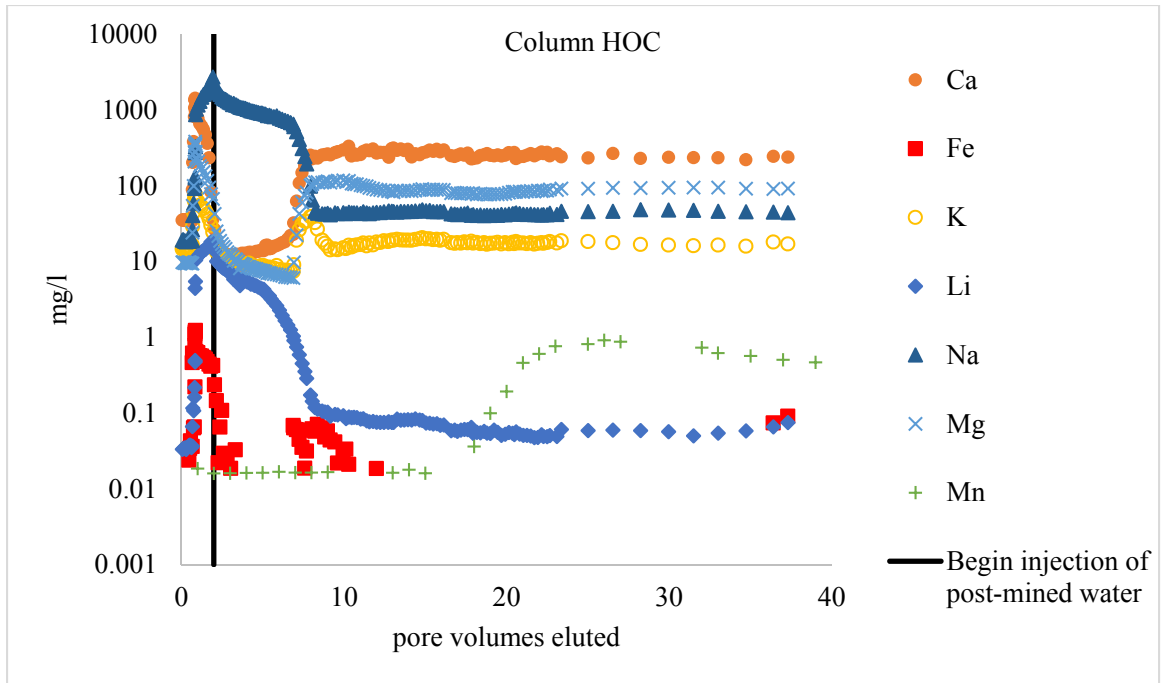


Figure 2.26. Cations in Column HOC eluent plotted against pore volumes eluted.

### **III. PUSH-PULL FIELD TESTS TO EVALUATE SODIUM DITHIONITE AS A GROUNDWATER RESTORATION OPTION FOLLOWING URANIUM IN-SITU RECOVERY MINING**

#### 3.1 Rationale

The goal of this field study is to evaluate the use of sodium dithionite as a groundwater restoration technique following uranium in-situ recovery. ~0.05 M sodium dithionite solutions were injected into two post-mined wells at the Smith Ranch Highland uranium in-situ recovery site. After a 60 hour reaction period, the wells were pumped until concentrations of uranium returned to their pre-test concentrations.

#### 3.2 Methods

##### *Test site*

The push-pull tests were conducted at the Smith Ranch-Highland (SRH) ISR site located near Douglas, Wyoming. The push-pull tests were conducted in Mining Unit 15, which was mined but not restored prior to the push-pull tests. Dithionite solutions were injected into wells 15P-308 and 15P-315, whose location relative to the site is shown in Figure 3.1. The well screens for 15P-308 and 15P-315 range from 449 feet bgs to 467 feet bgs (elevation of 4942.8 to 4924.8 feet) and 452 feet bgs to 470 feet bgs (elevation of 4944.1 to 4926.1 feet). The elevations for 15P-308 and 15P-315 are 5391.8 and 5396.1 feet, respectively. When the wells were drilled, the depth to water in well 15P-308 was measured as 15 feet bgs (elevation of 5376.8 feet), and the depth to water in 15P-315 was measured as 45 feet bgs (elevation of 5351.8 feet). Concentrations of selected constituents in these wells prior to the test is shown in Table 3.1.

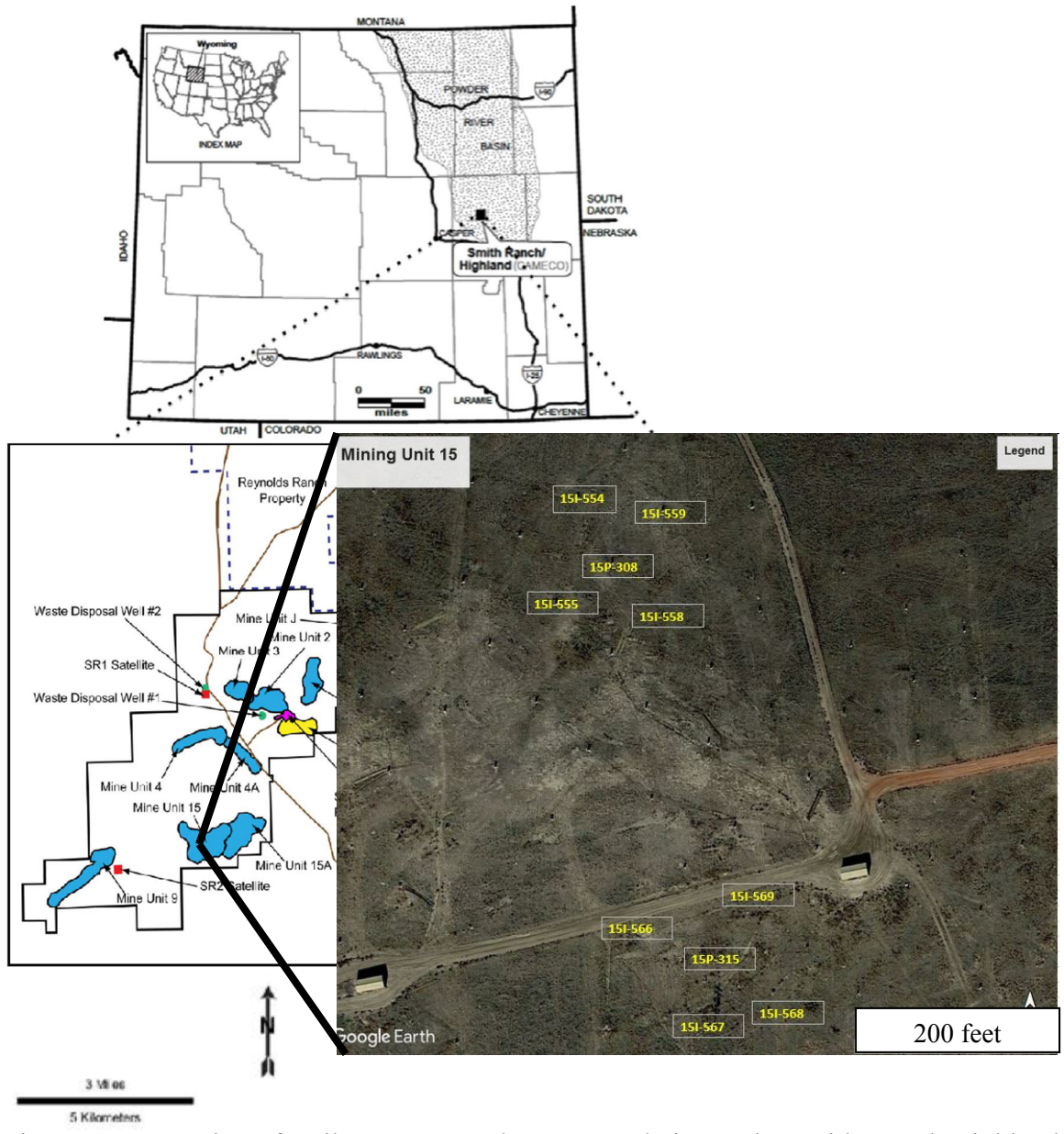


Figure 3.1. Location of wells 15P-308 and 15P-315 relative to the Smith-Ranch Highland uranium in-situ recovery mine.

<b>Constituent</b>	<b>15P-308</b>	<b>15P-315</b>
Alkalinity (mg/l) (total as HCO <sub>3</sub> )	599	644
Cl <sup>-</sup> (mg/l)	81	81
SO <sub>4</sub> <sup>2-</sup> (mg/l)	735	742
Ca <sup>2+</sup> (mg/l)	365	404
Mg <sup>2+</sup> (mg/l)	80	76
Na <sup>+</sup> (mg/l)	40	38
pH	6.39	6.41
Fe <sup>2+</sup> (mg/l)	0.93	0.37
U(VI) (mg/l)	11.3	15.4

Table 3.1. Concentrations of selected constituents in wells 15P-308 and 15P-315 before the push-pull tests. Data provided by Cameco.

*Injection and Pump-back*

5,000 gallons of a ~0.05 M sodium dithionite solution buffered with ~0.06 M sodium sulfite was injected into wells 15P-308 and 15P-315. The first four 1,000 gallon batches contained 73 pounds of sodium dithionite and 66.7 pounds of sodium sulfite, and the fifth 1,000 gallon batch was half-strength, and contained 36.5 pounds of dithionite and 33.3 pounds of sodium sulfite. The total masses were 328.5 pounds of dithionite and 300 pounds of sodium sulfite injected into each well.

Sodium sulfite was added to the dithionite solution to act as a buffer, because dithionite is unstable in solution and degrades faster at a lower pH (Rinker et al., 1960; Wayman & Lem, 1970). Sodium sulfite was determined to be a suitable buffer for use at the Smith Ranch-Highland site. Other buffers, such as bicarbonate are not suitable for use at SRH because the high calcium concentrations in the water could result in calcite precipitation which could plug the wells. Also, adding bicarbonate could promote the formation of calcium or magnesium ternary uranyl complexes (Dong & Brooks, 2006).



0.0026 M NaBr was also included in the injection solutions to serve as a tracer for the injection solution.

Five 1,000 gallon batches (with the fifth batch at half-strength) of the injection solutions were mixed in potable water collected from a shallow water well at SRH. The water was not degassed to remove oxygen prior to the addition of the dithionite. A pipe connected the mixing tank to Header House 15-16, a central location that controls the plumbing for a portion of Mining Unit 15. This allowed the injection solution to be injected directly into the wells. The production pumps from both wells had been pulled prior to injection and replaced with 1" ID polyethylene tubing that extended from the surface to the top of the screened intervals so that the injection solution could be injected with minimal exposure to oxygen. Each 1,000 gallon batch took around 30 minutes to inject. Following the 5,000 gallons of dithionite solution, 1,000 gallons of clean "chase" water was injected to ensure the dithionite solution was pushed out of the wells and into the formation. After the injections, the production pumps were reinstalled in the two wells to allow recovery of the solution. Sampling ports in the Header House 15-16 allowed samples to be collected easily during pumping.

Pumping began approximately 60 hours after each injection ended. Pumping rates averaged 4.8 gallons per minute (gpm) in well 15P-315, and 4.6 gpm in well 15P-308. Water pumped from 15P-308 and 15P-315 was directed into injection wells 15I-579, 15I-580, 15I-591, and 15I-592. These injection wells are the farthest away from 15P-308 and 15P-315 among all the injection wells plumbed into Header House 15-16, so directing re-injection into them would have minimal impact on the test. Pump-back was nearly continuous for approximately two months (interrupted only by occasional power outages).

Samples were collected at least once a day during pumping and analyzed for anions, cations, and trace metals. Several samples from each well were analyzed for uranium isotope ratios to look for evidence of uranium reduction.

### 3.3 Results and Discussion

#### *Reductive capacity*

Table 3.2 shows that the alkalinity and calcium concentrations were similar between the post-mined waters used in the column experiments discussed in Section II, and in wells 15P-308 and 15P-315 before the push-pull tests. Due to the formation of calcium-uranyl-carbonate complexes ( $\text{Ca}_2\text{UO}_2(\text{CO}_3)_3^0$  and  $\text{CaUO}_2(\text{CO}_3)_3^{2-}$ ), alkalinity and calcium concentrations are considered to be the most important groundwater chemistry parameters that influence uranium solubility and mobility (Dong & Brooks, 2006; Saunders et al., 2016). Because the calcium and alkalinity concentrations were similar, the retardation factor of 1.33 that was calculated for the column experiments was applied to the chloride breakthrough curves in wells 15P-308 and 15P-315 to account for a delay in breakthrough that would occur in the absence of dithionite. Sulfate in all post-mined waters was also included in Table 3.2 because as discussed in Section II, sulfate has the potential to consume reductive capacity imparted by the dithionite.

	<b>15P-308</b>	<b>15P-315</b>	<b>MP-423</b>	<b>15P-314</b>
Ca <sup>2+</sup> (mg/l)	365	404	409	383
U(VI) (mg/l)	11.3	15.4	3.8	26.1
SO <sub>4</sub> <sup>2-</sup> (mg/l)	735	742	647	609
Alkalinity (mg/l as HCO <sub>3</sub> <sup>-</sup> )	599	644	747	794

Table 3.2. Alkalinity, calcium, uranium, and sulfate in the post-mined waters used in the column experiments and in wells 15P-308 and 15P-315 before the push-pull tests.

Figure 3.2 shows the chloride (with imposed retardation factor of 1.33) and uranium breakthrough curves plotted relative to their pre-test concentrations for wells 15P-308 and 15P-315. Uranium stayed below its pre-test values for 40 injection volumes in 15P-308, and back 30 injection volumes in 15P-315.

Using Equation 3.1, taken from Istok et al. (1997), the volume of the aquifer ( $v_t$ ) penetrated by the dithionite solution plus chase water is estimated to be  $26.5 m^3$ . In the equation below,  $v_i$  is equal to the volume injected,  $v_w$  is equal to the volume of water in the well casing,  $v_s$  is the volume of the sand pack,  $\phi$  is the aquifer porosity, and  $\phi_s$  is the sand pack porosity.

$$v_t = \frac{v_i - v_w}{\phi} - \frac{v_s}{\phi_s} \text{ (Equation 3.1).}$$

Figure 3.2 shows that after 30 injection volumes were pumped from well 15P-315, uranium begins exceeding its pre-test concentration. This is likely because the pre-test value of 15.4 mg/l of uranium in well 15P-315 before the test may not represent the concentration of uranium in the ore zone. After recovering about 650,000 liters of water,

the concentration of uranium could be different farther out into the ore zone relative to the initial concentration that would have been measured closer to the well.

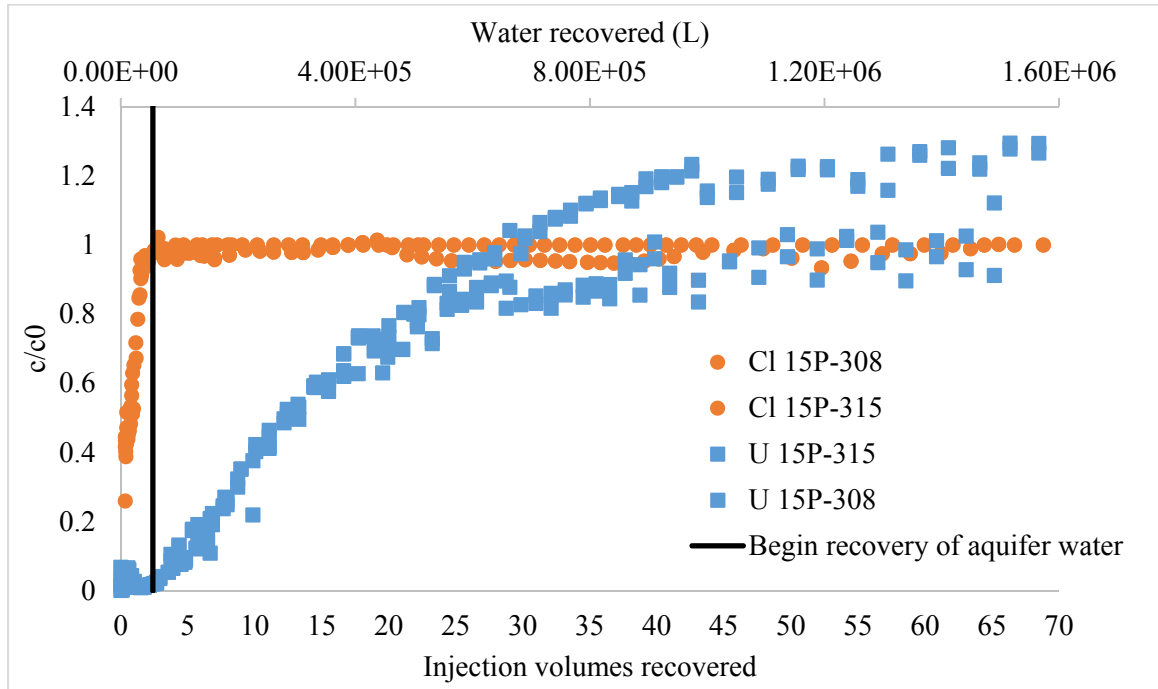


Figure 3.2. Chloride and uranium breakthrough curves for wells 15P-308 and 15P-315 relative to pre-test concentrations. The retardation factor of 1.33 calculated in the column experiments discussed in Section II was applied to the chloride breakthrough curves to account for any delay in uranium breakthrough that would occur in the absence of dithionite.

As in the column experiments discussed in Section II, the volume of water treated by the dithionite injection was calculated for wells 15P-308 and 15P-315. The area between the chloride and uranium breakthrough curves was integrated to calculate the volume of water recovered between the two curves. Table 3.3 shows the moles of dithionite injected, the liters of water recovered between chloride and uranium breakthrough, the ratio of liters of water recovered between chloride and uranium breakthrough relative to moles of dithionite injected, the moles of uranium reduced, and the ratio of moles of uranium reduced relative to dithionite injected in wells 15P-308 and

15P-315 as a result of the dithionite injection. As in the column experiments, the ratios of water recovered between chloride and uranium breakthrough relative to moles of dithionite injected (322 in 15P-308 and 335 in 15P-315 respectively) agree more closely than the moles of uranium reduced relative to moles of dithionite injected ( $2.0E-02$  in 15P-308 and  $1.3E-02$  in 15P-315). This further supports the idea that there are additional electron acceptors in the water besides U(VI) that are likely consuming the reduction capacity (and likely to a greater degree than U(VI)).

Well	Moles of dithionite injected	Liters of water recovered between chloride and uranium breakthrough	Ratio of liters of water recovered between chloride and uranium breakthrough relative to moles of dithionite injected	Moles uranium reduced	Moles uranium reduced to moles dithionite injected
15P-308	862	322,126	322	17	$2.0E-02$
15P-315	862	289,039	335	11	$1.3E-02$

Table 3.3. Moles of dithionite injected, liters of water recovered between chloride and uranium breakthrough, the ratio of liters of water recovered between chloride and uranium breakthrough relative to moles of dithionite injected, the moles of uranium reduced, and the moles of uranium reduced relative to dithionite injected in wells 15P-308 and 15P-315.

### *Iron*

Figure 3.3 shows concentrations of iron in wells 15P-308 and 15P-315 during pump-back. Pre-test concentrations of iron were 0.93 mg/l in 15P-308 and 0.37 mg/l in 15P-315. After the dithionite injection, concentrations spiked as high as 91.5 mg/l in 15P-308 and 88.9 mg/l in 15P-315. 14.7 kg of iron were recovered from well 15P-308 and 14.6 kg were recovered from well 15P-315. The large amounts of iron recovered from the wells are likely Fe(III) in the sediments that was reduced to Fe(II) by the dithionite (Amonette et al., 1994).

The large amounts of iron recovered from wells 15P-308 and 15P-315 agree with the idea that mobilized reduced species are recovered during the withdrawal phase of a dithionite push-pull test (Pacific Northwest National Laboratory, 1996). A push-pull test was conducted at the Hanford 100-H area in Washington, in which dithionite was deployed to create an in-situ redox zone to reduce chromium and other soluble contaminants in the groundwater. They hypothesized that during the injection phase, dithionite was pushed out of the well and into the aquifer to react with structural Fe(III). During the drift phase, dithionite reduced structural Fe(III) to Fe(II). During the withdrawal phase, unreacted dithionite products, buffers, and mobilized components including mobilized reduced species, such as iron were pumped back (Pacific Northwest National Laboratory, 1996). The Hanford 100-H push-pull test reported a contaminant plume treatment capacity of 51 to 85 pore volumes was calculated (7 to 12 years), assuming 1 mg/l chromium and 9 mg/l dissolved oxygen flowing through the dithionite treated area.

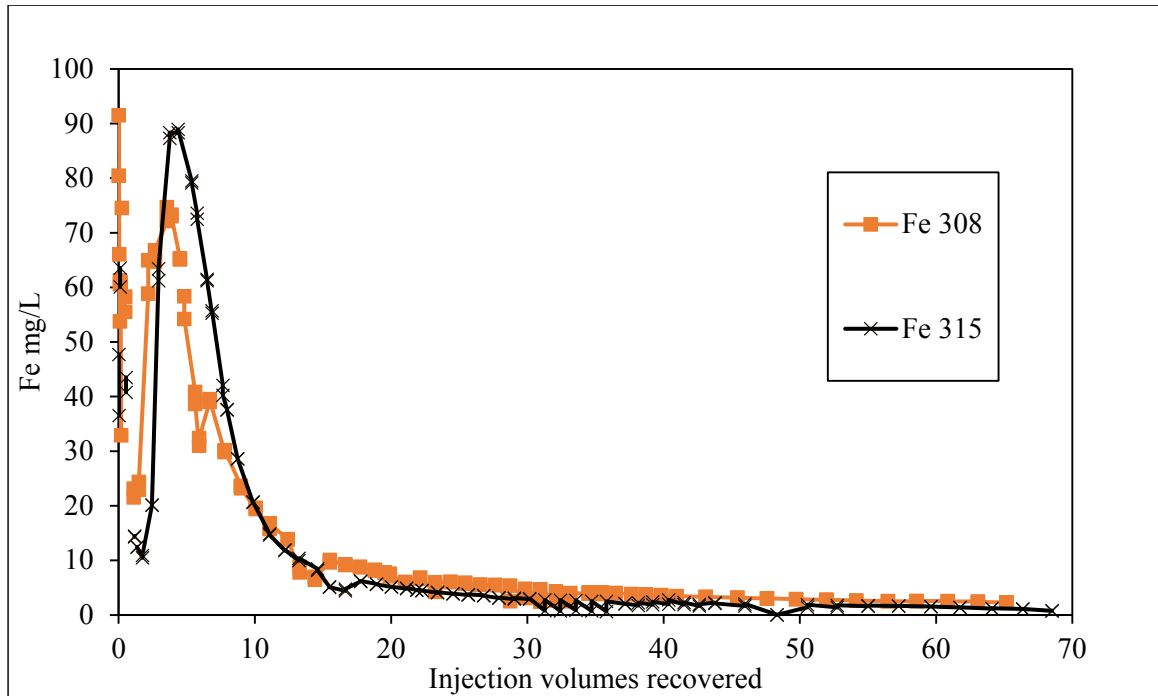


Figure 3.3. Concentrations of iron in wells 15P-308 and 15P-315 during pump-back.

#### *Uranium Reduction*

To look for evidence of reduction of U(VI) to U(IV), uranium isotopes were measured from each well on select days during pump-back. Because  $^{238}\text{U}$  tends to be reduced more readily than  $^{235}\text{U}$ , a decrease in the ratio of  $^{238}\text{U}/^{235}\text{U}$  can provide evidence of reduction of U(VI) to U(IV) (Bopp et al., 2009; Murphy et al., 2014; Weyer et al., 2008). Figure 3.4 shows the ratios of  $^{238}\text{U}/^{235}\text{U}$  in wells 15P-308 and 15P-315 relative to a baseline ratio obtained from nearby well 15P-311. On the dates sampled, the ratios in 15P-308 and 15P-315 are lower than the baseline from 15P-311, suggesting U(VI) was reduced to U(IV) after the dithionite injection. The breakthrough curves for uranium are also shown on this figure, and they show that uranium breakthrough in each well coincides with the rebound of the ratio of  $^{238}\text{U}/^{235}\text{U}$ .

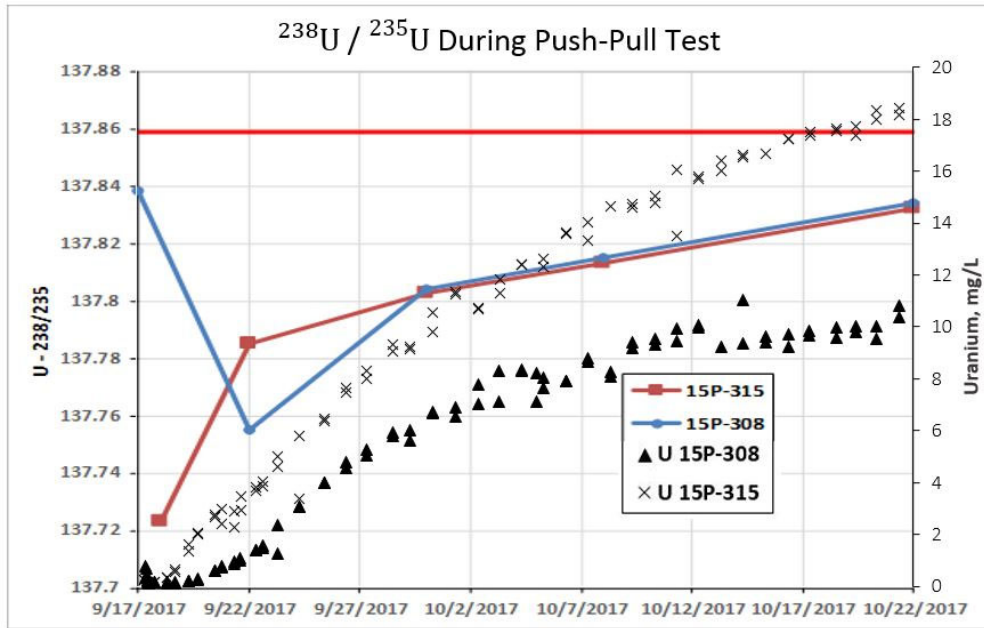


Figure 3.4. Ratios of  $^{238}\text{U}/^{235}\text{U}$  in wells 15P-308 and 15P-315 on select days during pump-back.

### 3.5 Conclusions

As in the column experiments, the moles of dithionite injected into wells 15P-308 and 15P-315 treated a given volume of water despite differing concentrations of uranium in the post-mined waters. This is a strong indication that there are additional electron acceptors in the water besides U(VI) that are likely consuming reduction capacity (and likely to a greater degree than U(VI)). Thus, the volume of water that can be effectively treated by a dithionite deployment will depend on the concentration (in equivalents/liter) of electron acceptors that the water contains.

The decrease in ratios of  $^{238}\text{U}/^{235}\text{U}$  during pump-back show that injecting dithionite into wells 15P-308 and 15P-315 reduced U(VI) to U(IV). Even though concentrations of uranium returned to their pre-test concentrations during the test, the accelerated pump-back rates used in the test exhausted the reductive capacity imparted by the dithionite on a much faster scale than would happen with natural groundwater flow rates.



#### **IV. EFFECTS OF SODIUM DITHIONITE ON POST-MINED SEDIMENTS WITH HIGH ORGANIC CARBON: SEDIMENT REDUCTION BATCH EXPERIMENT**

##### **4.1 Rationale**

The results of the high organic carbon content column experiment (discussed in Section II) showed that sodium dithionite did not impart a reductive capacity to post-mined sediments with high organic carbon content and uranium, and liberated uranium from the sediments. To further investigate these results, a sediment reduction batch experiment was conducted to compare the responses of post-mined sediments with varying amounts of uranium and organic carbon to treatment with sodium dithionite. We hypothesized that the sediments with low organic carbon content and low uranium would have a reduction capacity imparted to them after treatment with sodium dithionite, while the sediments with high organic carbon and uranium content would not have a reduction capacity imparted to them after treatment with sodium dithionite.

##### **4.2 Methods**

Sediments with low organic and high organic carbon content from post-mined core MOW 4-6 were treated with 0.1 M sodium dithionite to test this hypothesis. Sediments #4 (769 feet bgs) and #8 (779 feet bgs) both have high organic carbon content (>1 % organic carbon content). The sediments were assigned numeric identifiers in a previous report for convenience (LANL, 2012). Sediment #4 is the same sediment that was used in the high organic carbon content column experiment discussed in Section II.

Sediments #2 (766 feet bgs), #11 (780 feet bgs), #12 (782 feet bgs) and #14 (785 feet bgs) have low organic carbon (< 1 % organic carbon) and uranium content. Sediment #12 is the same sediment that was used in the low organic carbon content column experiments discussed in Section II. Table 4.1 shows the percentage of organic carbon

content and mg/g of uranium in the sediments used in this experiment. Figure 4.1 shows all sections of the MOW 4-6 core used in this experiment.

Sediment ID	Organic carbon content (%)	Uranium (mg/g)
2	0.93	0.11
4	7.73	2.10
8	48.42	24.84
11	0.4	0.04
12	0.38	0.005
14	0.49	0.003

Table 4.1. Organic carbon and uranium content for the sediments used in this experiment. Rows in white have low organic carbon content, and rows in gray have high organic carbon content (>1%).

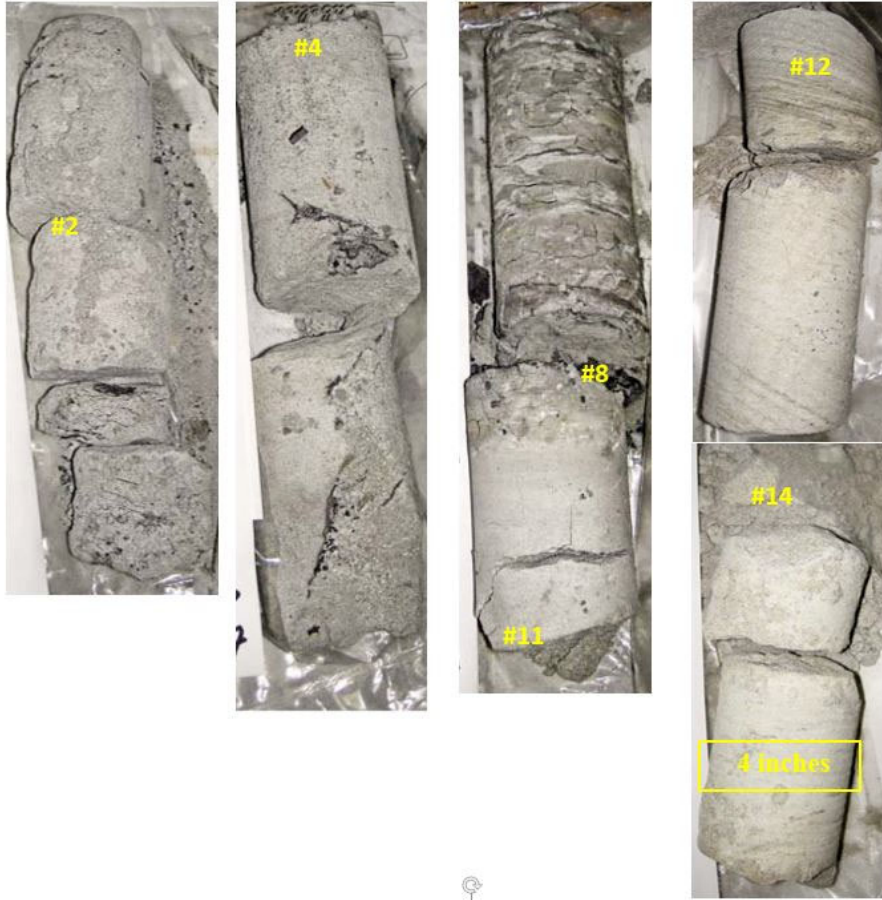


Figure 4.1. Sections of MOW 4-6 core used in sediment reduction batch experiment. Yellow numbers represent sections of the core used in this experiment.

Five gram aliquots (done in duplicate) of each sediment were exposed to a 0.1 M sodium dithionite solution buffered with 0.1 M sodium sulfite for 7 days. The 0.1 M dithionite/sulfite solutions were made in water from well M-402, whose concentration of selected constituents is listed in Table 4.2. The M-402 water was degassed before the addition of the dithionite and sulfite in an attempt to slow the degradation of dithionite, which degrades faster in the presence of oxygen (Rinker et al., 1960; Wayman & Lem, 1970).

20 ml of the dithionite/sulfite solution were added to each sediment. A control reactor in duplicate containing only dithionite solutions were included in the experiment. After 7 days, the solutions were decanted and the sediments were washed with DI water to remove any remaining sodium dithionite/sodium sulfite. The sodium dithionite solutions were analyzed for anions, cations, and trace metals.

Immediately after the dithionite solution was decanted, water from well MP-423 collected in October 2014 was added to the sediments. This was done to compare the reductive capacities of the sediments after being treated with sodium dithionite. If concentrations of uranium in the MP-423 water decreased significantly on days 1 and 7 after exposure to the dithionite-treated sediments, the sediments had a reductive capacity imparted on them by the dithionite. Concentration of selected constituents of the MP-423 water is shown in Table 4.2. The MP-423 water used in this experiment has a higher uranium concentration than the MP-423 water used in the column experiments discussed in Section II. The MP-423 water used in this experiment was collected in October 2014, after mining but before the well was treated with reverse osmosis. The MP-423 water used

in the column experiments was collected in April 2017, after the well was treated with reverse osmosis, which lowered the uranium concentration.

<b>Constituent</b>	<b>M-402</b>	<b>MP-423 (Oct 2014)</b>
Ca <sup>2+</sup> (mg/l)	51.1	405
Na <sup>+</sup> (mg/l)	18.9	43.9
Mg <sup>2+</sup> (mg/l)	13.0	110
K <sup>+</sup> (mg/l)	5.94	19.5
Fe <sup>2+</sup> (mg/l)	0	0
U(VI) (mg/l)	0.03	34
Cl <sup>-</sup> (mg/l)	4.20	129
SO <sub>4</sub> <sup>2-</sup> (mg/l)	75.6	838
pH	8.20	7.23
Alkalinity (mg/l as HCO <sub>3</sub> <sup>-</sup> )	199	598

Table 4.2. Concentrations of selected constituents of M-402 and MP-423 waters.

#### 4.3 Results and Discussion

Table 4.3 shows the pH and concentrations of selected constituents of the dithionite solutions after being exposed to the post-mined sediments for 7 days. In the dithionite solutions exposed to sediment 8 (the sediment with the highest uranium and organic carbon), the concentrations of sodium are significantly lower (4,646 mg/l in 8A and 4,446 mg/l in 8B) than in the dithionite solutions exposed to the other sediments (average of 8,158 mg/l). Sediments with higher organic carbon content have a higher cation exchange

capacity (Haghiri, 1974). The decreased sodium in the dithionite solutions exposed to sediment 8 relative to the other sediments could be due to the increased cation exchange capacity, which allowed the sediments to take up more sodium from the dithionite solution.

Sulfate is also lower in the dithionite solutions exposed to sediment 8 (5,912 mg/l in 8A and 5,202 mg/l in 8B) than in the dithionite solutions exposed to the other sediments (averaging 18,642.07 mg/l). Sulfate is a direct degradation product of dithionite (LANL, 2018). The lower sulfate concentrations in the dithionite solutions exposed to the sediments with the highest organic carbon supports the hypothesis from the HOC column experiment discussed in Section II, that sediments with higher uranium and organic carbon content appear to result in a different set of degradation reactions for dithionite which suppress the reduction of U(VI) to U(IV).

The uranium is highest in the dithionite solutions exposed to the post-mined sediments with the highest organic carbon (45 mg/l in 8A and 20 mg/l in 8B). The uranium in all other dithionite solutions was less than 1 mg/l. This agrees with the results of the high organic carbon column experiment discussed in Section II, in which dithionite liberated uranium from sediments with high organic carbon.

Sample ID	pH	Ca <sup>2+</sup> (mg/l)	Fe <sup>2+</sup> (mg/l)	Mg <sup>2+</sup> (mg/l)	Na <sup>+</sup> (mg/l)	SO <sub>4</sub> <sup>2-</sup> (mg/l)	U(VI) (mg/l)
2A-2	6.54	28	4.9	32	7686	14083	0.1
2B-2	6.65	39	5.6	32	8085	14288	0.2
4A-2	6.60	27	6.6	27	8070	20019	0.1
4B-2	6.54	39	8.2	28	8156	20849	0.2
8A-2	6.08	69	8.6	27	4646	5912	45
8B-2	6.03	70	8.3	25	4446	5202	20
11A-2	6.58	45	12.7	26	7960	17553	0.2
11B-2	6.63	23	10.0	24	7620	18890	0.1
12A-2	6.60	26	19.1	22	8371	40855	0.0
12B-2	6.61	51	15.2	21	7882	20953	0.0
14A-2	6.68	32	19.3	24	7923	13786	0.1
14B-2	6.58	21	15.2	24	7569	13519	0.1
Control A-2- M402	6.50	28	0.5	15	9254	14514	0.0
Control B-2- M402	6.54	33	0.5	15	9324	14395	0.0

Table 4.3. pH and concentrations of selected constituents in dithionite solutions exposed to post-mined sediments.

Figure 4.2 shows photographs of each reactor containing the dithionite solutions after 7 days. There is a gray precipitate on the surface of all the sediments, except on sediment 8, the sediment with the highest organic carbon content. The gray precipitate on the surface of all other sediments could have been elemental sulfur.

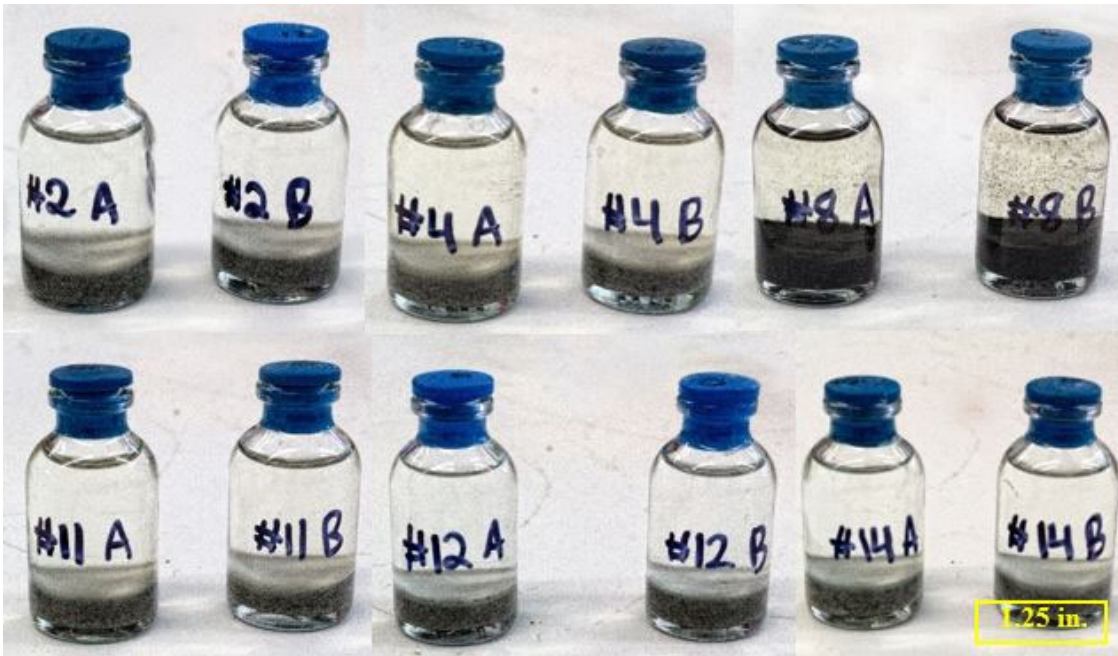


Figure 4.2. Dithionite solutions exposed to sediments after 7 days. Gray precipitate is visible on the surface of the sediments except in reactors #8A and #8B.

After the dithionite solutions were decanted, post mined water from well MP-423 was added to the dithionite treated sediments to compare reduction capacities imparted by the dithionite. Figure 4.3 and Table 4.4 show the concentrations of uranium in the MP-423 water on days 1 and 7 after being exposed to the sediments that had been treated with sodium dithionite. The baseline concentration of uranium in the MP-423 water was 34 mg/l. After 1 day, the MP-423 water that had been exposed to sediments 8A and 8B (the most organic/uranium rich sediments) increased to 36 and 41 mg/l. In the MP-423 water



exposed to all the other sediments (2, 4, 11, 12, and 14) that had been treated with sodium dithionite, there were significant reductions in uranium concentrations after 1 day.

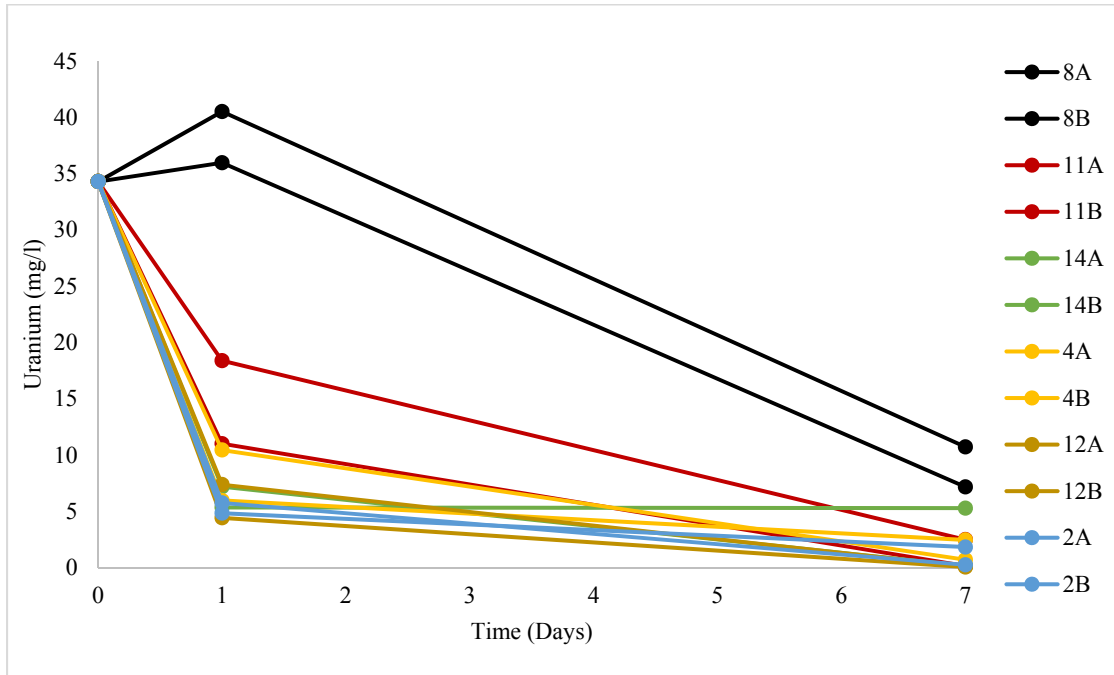


Figure 4.3. Concentrations of uranium in MP-423 water on days 1 and 7 after being exposed to dithionite treated sediments.

<b>Sample ID</b>	<b>Day 1 - U(VI) (mg/l)</b>	<b>Day 7 - U(VI) (mg/l)</b>
2A-MP-423	5.75	0.26
2B-MP-423	4.84	1.83
4A-MP-423	10.45	0.71
4B-MP-423	5.97	2.47
8A-MP-423	35.97	7.17
8B-MP-423	40.52	10.73
11A-MP-423	18.39	2.49
11B-MP-423	11.01	0.15
12A-MP-423	4.43	0.05
12B-MP-423	7.38	0.11
14A-MP-423	7.19	0.16
14B-MP-423	5.35	5.29
Control A-MP-423	34.68	34.87
Control B-MP-423	33.95	34.37

Table 4.4. Uranium concentrations (mg/l) in MP-423 water on days 1 and 7 after being exposed to sediments treated with sodium dithionite.

The increased concentrations of uranium in the MP-423 water after one day of being exposed to dithionite treated sediments 8A and 8B support the hypothesis that sodium dithionite does not impart a reductive capacity to post-mined sediments with high organic carbon. The increase in uranium in the MP-423 water may be uranium that was displaced from the sediments. The dithionite solutions exposed to sediments 8A and 8B contained less sodium, so the sediments could have taken up more sodium from the dithionite which displaced uranium from the sediments.

The concentration of uranium decreased in the MP-423 water exposed to sediments 8A and 8B after treatment with sodium dithionite after 7 days. Uranium can cation exchange with, be reduced by, or sorb onto organic carbon (or a combination of these three mechanisms) (Zielinski et al., 1988). The decrease in uranium in MP-423 water exposed to sediments 8A and 8B after 7 days was likely due to uranium sorption onto the sediments.

Reduction is unlikely based on the uranium liberated by the dithionite from the sediments, the decreased sulfate in the dithionite solution after 7 days, and the lack of gray precipitate in the dithionite solutions exposed to sediments 8A and 8B.

The sediments with the next highest uranium and organic carbon was sediment #4. Sediment #4 was the same sediment used in the high organic carbon column experiment discussed in Section II. In the column experiment, Sediment #4 had no reduction capacity with respect to U(VI) imparted to it after treatment with sodium dithionite, and uranium was liberated from the sediments. In contrast to the column experiment, there was a reductive capacity imparted to sediment #4 in the batch experiment after treatment with sodium dithionite. Table 4.5 shows the moles of dithionite per gram of organic carbon in the column experiment and in the sediment reduction batch experiment. In the sediment reduction batch experiment, there were 16 times as many moles of dithionite per gram of organic carbon than in the column experiment. Perhaps the dithionite was able to impart a reductive capacity to sediment 4 in the batch experiment when it was not able to in the column experiment because there was a higher amount of dithionite per gram of organic carbon.

Sediment	Organic carbon in sediment (%)	Sediment used in experiment (g)	Organic carbon in experiment (g)	Dithionite introduced (moles)	Moles of dithionite per g organic carbon
4 (column experiment)	7.73	209.6	16.20	0.0056	3.5E-04
4 (batch experiment)	7.73	5	0.39	0.002	5.2E-03
8 (batch experiment)	48.42	3	1.45	0.002	1.4E-03

Table 4.5. Ratios of moles of dithionite per gram of organic carbon for the high organic carbon column experiment and sediment reduction batch experiment, and sediment 8 in the sediment reduction batch experiment.

#### 4.4 Conclusions

The hypothesis that sodium dithionite does not impart a reductive capacity to sediments with high organic carbon content was supported by Sediment 8, but not Sediment 4. Concentrations of uranium were highest in the dithionite solutions and post-mined waters exposed to sediments 8A and 8B. The fact that a gray precipitate did not form on the surface of sediments 8A and 8B, and that much less aqueous sulfate was generated after dithionite contact with these sediments suggests that dithionite reacts differently when exposed to sediments with high organic carbon content. The experimental observations collectively suggest that high organic carbon content in sediments may suppress the formation of dithionite reaction products that impart reductive capacity.

Sediment 4, the sediment with the next highest uranium and organic carbon content did have a reductive capacity imparted to it after treatment with sodium dithionite. This contrasts to the high organic carbon content column experiment, in which the sediments liberated uranium and there was no reductive capacity imparted to them after treatment with dithionite. The difference in behavior may be attributed to the higher ratio of dithionite to organic carbon content in the batch experiment than in the column experiment. Conducting additional batch and column experiments with different ratios of dithionite to organic carbon content could provide insight to if exceeding a certain ratio of dithionite to organic carbon content results in a reductive capacity being imparted.

The hypothesis that sediments with low uranium and organic carbon content have a reduction capacity imparted to them after treatment with sodium dithionite was supported by the experiment. The sediments with low uranium and organic carbon content (2, 11, 12, and 14) did have a reductive capacity imparted to them after treatment with dithionite.

## V. CONCLUSIONS

*The volume of water that will be treated by a dithionite field deployment will depend on the concentration in equivalents per liter of electron acceptors that the water contains.*

It is reasonable to expect, for similar sediments, that every mole of dithionite deployed should impart a reduction capacity to the sediments that is capable of reducing a given number of equivalents of aqueous electron acceptors (e.g.,  $O_2$ ,  $NO_3^-$ , U(VI)) as they flow through the dithionite-treated zone. Thus, the volume of water that can be effectively treated by a dithionite deployment (the metric that mining companies most care about) will depend on the concentration (in equivalents/liter) of electron acceptors that the water contains.

Table 5.1 shows the moles of dithionite injected, the liters of water recovered between the chloride and uranium breakthrough, the ratios of liters of water recovered between chloride and uranium breakthrough relative to moles of dithionite injected, the moles of uranium reduced, and the ratio of moles of uranium reduced relative to moles of dithionite injected for the low organic carbon content column experiments and for the push-pull field tests. The ratios of liters of water recovered between chloride and uranium breakthrough relative to the moles of dithionite injected (179, 238, 321, 322, and 335 in Columns LOC-2, LOC-3, LOC-4, well 15P-308, and 15P-315) were in closer agreement than the moles of uranium reduced relative to the moles of dithionite injected ( $2.2E-02$ ,  $2.2E-02$ ,  $5.3E-03$ ,  $2.02E-02$ , and  $1.3E-02$  in Columns LOC-2, LOC-3, LOC-4, well 15P-308, and 15P-315). This implies that there are additional electron acceptors in the water besides U(VI) that are consuming the reductive capacity (and likely to a greater degree

than U(VI)). Sulfate seems to be the most likely electron acceptor in post-mined waters at SRH.

Column Experiment or Well	Moles of dithionite injected	Liters of water recovered between chloride and uranium breakthrough	Liters of water recovered between chloride and uranium breakthrough relative to moles of dithionite injected	Moles of uranium reduced	Moles of uranium reduced per mole of dithionite injected
LOC-2	0.0048	0.09	179	1.06E-05	2.2E-02
LOC-3	0.001	0.24	238	2.30E-05	2.2E-02
LOC-4	0.0056	1.80	321	2.96E-05	5.3E-03
15P-308	862	322,126	322	17	2.02E-02
15P-315	862	289,039	335	11	1.3E-02

Table 5.1. Moles of dithionite injected, liters of water recovered between chloride and uranium breakthrough, the ratio of liters of water recovered between chloride and uranium breakthrough relative to the moles of dithionite injected, moles of uranium reduced, and moles of uranium reduced relative to moles of dithionite injected in the LOC column experiments and push-pull field tests.

The fact that there was somewhat more water treated per mole of dithionite in the push-pull tests than in the low organic carbon content column experiments can likely be attributed to the presence of dissolved oxygen as an additional electron acceptor in the lab experiments that was not present in the field tests. However, the fact that similar volumes of water were treated in the two push-pull tests despite nearly a factor of two difference in U(VI) concentrations in the waters suggests that another aqueous species besides U(VI) was likely accepting electrons from the dithionite-treated sediments. Given the absence of O<sub>2</sub> and the negligible concentrations of NO<sub>3</sub><sup>-</sup> and dissolved Fe(III) in the resident ore zone water, the most logical electron acceptor is SO<sub>4</sub><sup>2-</sup> which was highly abundant in the ore zone water. The confounding influence of the large amounts of dithionite injected and the fact

that  $\text{SO}_4^{2-}$  is a prominent dithionite degradation product (which remained elevated well above background concentrations throughout the push-pull tests) made it impossible to estimate how much inflowing  $\text{SO}_4^{2-}$  might have been reduced in the field (or lab) tests. However, even if only a small amount of the inflowing  $\text{SO}_4^{2-}$  was reduced, it could have easily exceeded the equivalents of U(VI) reduced, thus resulting in a similar volume of water treated despite significantly different U(VI) concentrations in the waters. The background concentrations of  $\text{SO}_4^{2-}$  in both push-pull tests were  $\sim 15$  meq/L (assuming only 2 eq/mole  $\text{SO}_4^{2-}$ , which assumes reduction of  $\text{SO}_4^{2-}$  only to  $\text{SO}_3^{2-}$ , the most oxidized of many potential reduction products of  $\text{SO}_4^{2-}$ ), whereas the background concentrations of U(VI) were 0.2-0.3 meq/L, so it is easy to see how a small fraction of  $\text{SO}_4^{2-}$  reduced could have consumed most of the reduction capacity in the dithionite-treated zone and thus rendered the amount of U(VI) in the water rather insignificant in terms of equivalents of electron acceptors.

Another major difference between the column experiments and the field tests was the amount of iron that was liberated. 14.6 kg and 14.7 kg of iron were recovered from wells 15P-308 and 15P-315, and concentrations of iron went up to nearly 100 mg/l during pump-back in both wells. In the column experiments, minimal iron was measured in the column eluent. In the push-pull field test, after the dithionite injection and reaction period, the flow was reversed for pump-back, allowing iron that was reduced during the dithionite injection to easily be pumped back (Pacific Northwest National Laboratory, 1996). There was no flow reversal in the column experiments, meaning that iron reduced from the dithionite injection would have had to travel through the entire column before being eluted. Iron was leached

from the sediments of Columns LOC-2 and LOC-3. If Columns LOC-2 and LOC-3 were run for longer, this iron likely would have eluted out of the column.

*High organic carbon and uranium content in post-mined sediments appear to interfere with the degradation of dithionite.*

Post-mined sediments with high organic carbon and uranium content used in the HOC column experiment (Sediment 4 or 769 feet bgs of the MOW 4-6 core) and in the sediment reduction batch experiment (Sediment 8A and 8B) liberated uranium after treatment with dithionite. The sediments with high organic carbon content and uranium appear less permeable, and unaffected by leaching fluids during ISR (WoldeGabriel et al., 2014). The reduced state of the sediments, higher uranium content, and higher organic carbon content must suppress the formation of dithionite's degradation products necessary to impart reductive capacity. This was supported by the absence of a precipitate on the surface of sediments 8A and 8B after treatment with dithionite (when all low organic carbon content and uranium sediments had a gray precipitate), and significantly lower sulfate concentrations in the dithionite solution after reacting with the sediments for 7 days (relative to sulfate concentrations in all other dithionite solutions that had reacted with the sediments).

However, sediment 4, which had no reductive capacity imparted to it during the HOC column experiment, did have a reductive capacity imparted to it in the sediment reduction batch experiment. The difference in behavior may be explained by the ratio of moles of dithionite to grams of organic carbon. There was 16 times as many moles of dithionite per gram of organic carbon in the batch experiment versus the column experiment. Conducting additional batch or column experiments varying the ratio of dithionite to organic carbon



could help provide insight as to if exceeding a certain ratio of dithionite to organic carbon allows a reduction capacity to be imparted to sediments with high organic carbon.

*The results of the column experiments, batch experiments, and push-pull field tests suggest that dithionite is effective in reducing U(VI) in post-mined waters after treatment with sodium dithionite, as long as the sediments have low uranium and organic content.*

More research is needed to assess whether dithionite should be deployed as a groundwater restoration option following uranium ISR.

## **LIST OF APPENDICES**

Appendix A – Aqueous Batch Experiment

Appendix B - X-ray photoelectron spectroscopy

Appendix C – Speciation of Uranium Liberated from Sediments in Dithionite Solution

Appendix D - Fluvial Deposition in the Paleocene Fort Union Formation at the Smith Ranch-Highland Site in Wyoming

## **Appendix A - Aqueous Batch Experiment**

### **A.1 Rationale**

An aqueous batch experiment (water only), was conducted to test the hypothesis that sodium dithionite reduces uranium (VI) directly in post-mined untreated water. The literature suggests the reductive capacity imparted by sodium dithionite comes from reducing ferrous iron in the sediments (Amonette et al., 1994). If dithionite reduces uranium in the aqueous phase when no sediments are present, that suggests there is another mechanism for dithionite to reduce uranium that does not rely on reducing ferrous iron. The ability of sodium sulfide to reduce uranium was also tested in this experiment as a comparison to sodium dithionite, because it is currently used at the Smith Ranch-Highland site for post-mining groundwater restoration.

### **A.2 Methods**

The water used in this experiment was collected from well MP-423 in October 2014. It was collected after mining and before restoration was conducted. The concentration of selected constituents in the MP-423 water is shown in Table A.1.

There were a total of nine reactors with 20 ml of solution each for this experiment. One reactor was a blank of the MP-423 water. Four of the reactors contained 0.0025 M, 0.0055 M, 0.012 M, and 0.025 M concentrations of dithionite, and the remaining four reactors contained the same concentrations of sodium sulfide. Before the dithionite and sulfide were added, concentrations of  $\text{HCO}_3^-$  equal to the dithionite or sulfide were added to the 8 reactors as a buffer to help stabilize the sodium dithionite. While the sodium sulfide did not need to be buffered,  $\text{HCO}_3^-$  was added anyway so a fair comparison could be made with the sodium dithionite.

Immediately upon addition of the sodium dithionite and sodium sulfide, a white precipitate was observed. This precipitate was probably calcite due to the high calcium concentration in the water and the elevated pH from the  $\text{HCO}_3^-$  buffer. The solutions were analyzed for uranium using inductively coupled plasma mass spectrometry (ICP-MS) after twenty four hours.

Constituent	MP-423 (Oct 2014)
$\text{Ca}^{2+}$ (mg/l)	405
$\text{Na}^+$ (mg/l)	43.9
$\text{Mg}^{2+}$ (mg/l)	110
$\text{K}^+$ (mg/l)	19.5
$\text{Fe}^{2+}$ (mg/l)	0.00
U(VI) (mg/l)	38.2
$\text{Cl}^-$ (mg/l)	129
$\text{SO}_4^{2-}$ (mg/l)	838
pH	7.23
Alkalinity (mg/l as $\text{HCO}_3^-$ )	598

Table A.1. Concentration of selected constituents in MP-423 water used in aqueous batch experiment.

### A.3 Results

Table A.2 shows the concentrations of uranium in MP-423 water after being exposed to sodium dithionite or sodium sulfide for 24 hours. Concentrations of uranium in the MP-423 water exposed to the 0.0055 M, 0.012 M, and 0.025 M sodium dithionite decreased from 38.2 mg/l to 0.09 mg/l, 0.34 mg/l, and 0.53 mg/l, respectively. When the MP-423 water exposed to the 0.0025 M dithionite was analyzed, the result was reported as

“re-run,” suggesting the sample needed to be reanalyzed, perhaps due to bad spike recovery or a dilution issue. The sample was disposed of before the sample was reanalyzed, so there is no result for that dithionite concentration.

There were very minor changes in the concentration of uranium in the MP-423 water exposed to sodium sulfide. Concentrations of uranium in the MP-423 water exposed to the 0.0025 M, 0.0055 M, 0.012 M, and 0.025 M sodium sulfide decreased from 38.22 mg/l to 37.29 mg/l, 36.15 mg/l, 32.90 mg/l, and 2.41 mg/l respectively. The analytical result for the MP-423 water exposed to the 0.025 M sodium sulfide solution is questionable. It seems unlikely that the 0.025 M sodium sulfide would have initiated so much uranium reduction, when almost no reduction was seen for the other aliquots of MP-423 water exposed to the sodium sulfide. One possibility is that the MP-423 water exposed to the 0.025 M sodium sulfide was mixed up with the sample exposed to the 0.0025 M sodium dithionite (which had no result reported) during analysis. The sample was disposed of before it could be reanalyzed.

<b>Solution</b>	<b>Uranium (mg/l) in MP-423 after 24 hours</b>
0.0025 M sodium dithionite	-
0.0055 M sodium dithionite	0.093
0.012 M sodium dithionite	0.344
0.025 M sodium dithionite	0.530
0.0025 M sodium sulfide	37.29
0.0055 M sodium sulfide	36.154
0.012 M sodium sulfide	32.89
0.025 M sodium sulfide	2.41
MP-423 water	38.22

Table A.2. Uranium concentrations of post-mined untreated MP-423 water after being exposed to sodium dithionite or sodium sulfide for 24 hours.

#### A.4 Conclusions

This experiment is significant for three reasons. First, it shows that dithionite can reduce uranium in the absence of sediments, even when alkalinity and calcium concentrations are both high (which tends to stabilize U(VI) against reduction). This suggests there is another mechanism for dithionite to reduce uranium that does not rely upon reducing ferrous iron in sediments. Second, it shows that sodium sulfide is not effective in reducing uranium in unrestored ground waters that have both high alkalinity and calcium concentrations. If it is to be considered as a treatment option for groundwater restoration following uranium ISR mining at the Smith Ranch-Highland, the water should be treated with reverse osmosis to lower alkalinity and calcium concentrations before injecting sodium sulfide. Third, it showed that  $\text{HCO}_3^-$  should not be used as a buffer for dithionite at the Smith Ranch-Highland. The high calcium concentrations in the water combined with the elevated pH from the  $\text{HCO}_3^-$  results in calcite precipitation, which could plug the injection wells. Also, adding bicarbonate could promote the formation of calcium ternary uranyl complexes. After this experiment, sodium sulfite was used to buffer dithionite solutions in all laboratory and field experiments.

## **Appendix B -X-ray photoelectron spectroscopy**

### **B.1 Rationale**

X-ray photoelectron spectroscopy (XPS) was used to look for evidence of uranium reduction on post-mined sediments after they were treated with sodium dithionite and exposed to uranium.

### **B.2 Methods**

Post-mined sediments from the 769 feet bgs section of the MOW 4-6 core were exposed to 0.1 M sodium dithionite buffered with 0.1 M sodium sulfite for 1 week. After one week, the dithionite solutions were decanted and the sediments were washed with DI water to remove any excess dithionite remaining on the sediments. Then, post-mined water from well MP-423 collected in October 2014 containing 38 ppm uranium was added to the sediments for 7 days. These sediments were scanned using XPS to look for U(IV) on the sediments that would have been reduced out of the MP-423 water.

### **B.3 Results**

No uranium was detected on the sediments.

### **B.4 Conclusions**

Uranium was not detected because it was below the detection limit of XPS.

## **Appendix C - Speciation of Uranium Liberated from Sediments in Dithionite Solution**

### **C.1 Rationale**

C18 cartridges and anion exchange resins were used to gain insights into the speciation of uranium in dithionite solutions after contact with various sediments from SRH. The first hypothesis was that uranium may be associated with hydrophobic organic matter. If that was the case, C18 cartridges would retain hydrophobic organic matter and associated uranium. The second hypothesis was that uranium may have an anionic association, with an overall negative charge. If that was the case, uranium and anions would be retained by anion exchange resins.

### **C.2 Methods**

These experiments were conducted using the dithionite solutions exposed to the post-mined sediments in the sediment reduction batch experiment discussed in Section IV. Sample splits of the 0.1 M sodium dithionite solutions that were exposed to sediments from the MOW 4-6 core with varying levels of organic carbon and uranium were passed through C18 cartridges and anion exchange resins. Sample splits were analyzed for uranium using ICP-MS.

### **C.3 Results**

Figure C.1 and Table C.1 show the concentrations of uranium in the dithionite solutions exposed to post-mined sediments that were passed through C18 cartridges, and that were not passed through C18 cartridges. Concentrations of uranium are very similar between the sample splits that were passed through the C18 cartridge, and the sample splits that were not passed through the C18 cartridge. The biggest difference between sample splits was 62 % for solution exposed to sediment 4B, while several sample splits had no difference in uranium concentration.



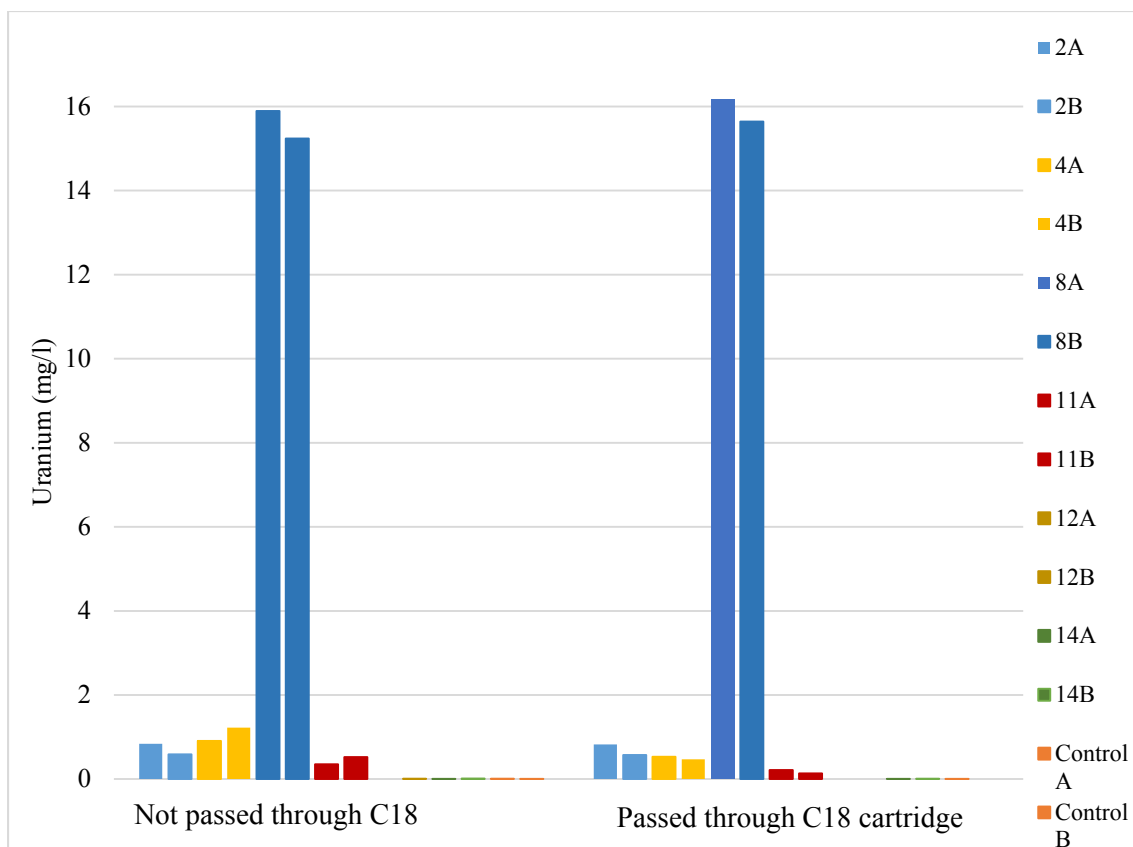


Figure C.1. Concentrations of uranium in sodium dithionite solutions exposed to sediments from the MOW 4-6 core of the sample splits that were passed through C18 cartridges, and that were not passed through C18 cartridges.

Sample ID	U(VI) (mg/l) Not passed through C18 cartridge	U(VI) (mg/l) Passed through C18 cartridge	pH
2A-2	0.84	0.82	6.61
2B-2	0.59	0.57	6.50
4A-2	0.91	0.53	6.31
4B-2	1.23	0.47	6.35
8A-2	15.89	16.17	6.32
8B-2	15.24	15.64	6.31
11A-2	0.35	0.21	6.49
11B-2	0.52	0.14	6.29
12A-2	<0.004	<0.004	6.35
12B-2	0.01	<0.004	6.48
14A-2	0.01	0.01	6.32
14B-2	0.01	0.01	6.38
Control A-2-M402	0.01	0.01	6.30
Control B-2- M402	0.01	<0.004	6.38

Table C.1. Concentrations of uranium in sodium dithionite solutions in the 3 sample splits, passed through the C18 cartridge, and not passed through the C18 cartridge.

Figures C.2, C.3, and Table C.2 shows concentrations of uranium in sodium dithionite solutions that were exposed to sediments from the MOW 4-6 core that were passed through anion exchange resins, and that were not passed through anion exchange resins. Concentrations of uranium are lower in the sample splits that were passed through the anion exchange resins.



Figure C.2. Concentrations of uranium in dithionite solutions passed through anion exchange resins, and solutions not passed through anion exchange resins. Dithionite solution exposed to sediment 8A and 8B are shown in Figure C.3.

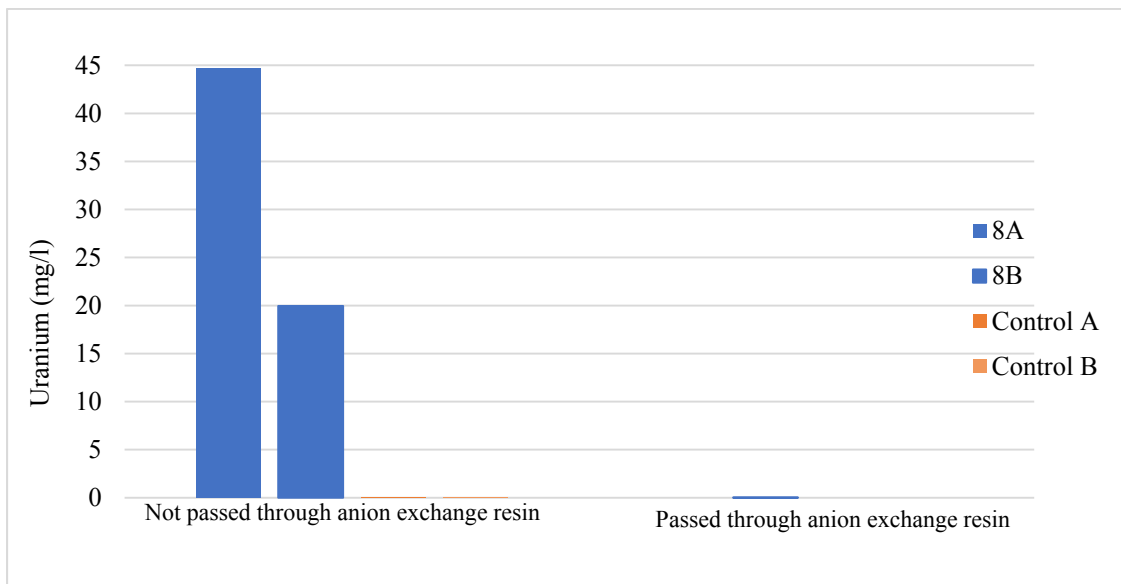


Figure C.3. Concentrations of uranium in dithionite solution passed through anion exchange resins, and not passed through anion exchange resins for dithionite solutions exposed to sediments 8A and 8B.

Sample ID (Dithionite solutions exposed to sediments)	U( VI) (mg/l) Not passed through anion exchange resin	U(VI) (mg/l) Passed through anion exchange resin
2A-2	0.11	n.a.
2B-2	0.16	<0.002
4A-2	0.10	<0.002
4B-2	0.15	<0.002
8A-2	44.69	<0.002
8B-2	19.97	0.023
11A-2	0.19	<0.001
11B-2	0.05	0.009
12A-2	0.00	0.007
12B-2	0.02	<0.001
14A-2	0.12	0.010
14B-2	0.11	0.01
Control A-2-M402	0.01	<0.002
Control B-2- M402	0.00	<0.002

Table C.4. Concentrations of uranium in dithionite solutions passed through anion exchange resins, and solutions not passed through anion exchange resins. Sample 2A-2 was spilled, so there was not enough solution to pass through the anion exchange resin for analysis.

#### C.4 Discussion

Uranium has an anionic association in dithionite solution and does not appear to be associated with hydrophobic organic matter in dithionite solution. The results of the high organic carbon column experiment discussed in Section II, and the sediment reduction batch experiment discussed in Section IV revealed that dithionite liberates uranium from organic carbon, and that dithionite does not seem to impart a reductive capacity with respect to uranium to sediments with high organic carbon. Therefore, the fact that dithionite has an anionic association in dithionite solution suggests that uranium liberated from organic carbon in the sediments could have formed  $\text{CaUO}_2(\text{CO}_3)_3^{2-}$  complexes in the dithionite solution, explaining the anionic association. The M-402 water that was used to make the dithionite solutions contained 51 mg/l calcium and has an alkalinity as 198 mg/l as  $\text{HCO}_3^-$ , which could have been high enough for calcium uranyl ternary complexes to form.

## **Appendix D- Fluvial Deposition in the Paleocene Fort Union Formation at the Smith Ranch-Highland Site in Wyoming**

### **D.1 Rationale**

This section contains information on the fluvial deposition of the Paleocene Fort Union Formation at the Smith Ranch-Highland site. Well logs and core taken from SRH were studied, and observations were related to the literature to improve understanding of the site's geology.

### **D.2 Background**

The Smith Ranch-Highland site is in the southern Powder River Basin, a structural basin that covers northeast Wyoming and southern Montana (Dahl & Hagmaier, 1976; Ayers, 1986). The Powder River Basin is bounded by the Laramie Mountains to the south, the Black Hills to the northeast, the Casper Arch and Bighorn Mountains to the west, and the Miles City Arch to the north (Ayers, 1986). The Powder River Basin formed during the Late Cretaceous during the Laramide orogeny (Ayers, 1986). The Paleocene Fort Union formation is one of the geologic units that formed in the Powder River Basin as a result of sediments eroding from the surrounding mountains (Ethridge et al 1981; Flores et al 1981; Ayers, 1986).

The Fort Union is a heterogeneous mixture of sandstones, clay, siltstone, coal, and carbonaceous shale (Ethridge et al 1981). The Fort Union at SRH hosts epigenetic uranium ore as roll-front deposits (Dahl & Hagmaier, 1976, Ethridge, Jackson & Youngberg, 1981; Ayers, 1986). The uranium originated in granitic rocks along the southern margin of the basin and in tuffaceous debris in the formation (Dahl & Hagmaier, 1976; WoldeGabriel et al 2014). It traveled through permeable sandstone under oxidizing conditions until it was deposited at a reduction-oxidation boundary as a roll-front deposit (Ayers, 1986, Woldegabriel et al 2014). The uranium deposits lie in the Tongue River Member of the

Fort Union Formation at varying depths of 61 – 366 meters below the ground surface (Brown et al., 2016). Uranium roll-front deposits are in sandstone, but carbonaceous shale and coal of the Fort Union are also uranium-rich, as organic carbon has an affinity for uranium (Hatcher et al., 1986).

Ethridge et al. (1981) hypothesized that the Fort Union was deposited by a northward flowing intermountain basinal fluvial system with a trunk stream along the basinal axis. Figure D.2 shows this potential depositional model. In Figure D.2, the Smith Ranch-Highland site is just south of Bear Creek Mine. According to Ethridge et al. (1981), in the southern portion of the basin, bed-load to mixed load channel deposits consist of medium-to-coarse grained sandstones with lenses of sandy conglomerate. Individual channel deposits have sharp basal contacts, and have fining upward patterns overlain by mudstones, siltstones, and coals. Further north, deposits are finer-grained and have fining-upward sequences associated with point bar deposits of a meandering stream. These meandering channel deposits are interbedded with crevasse splay and overbank deposits.

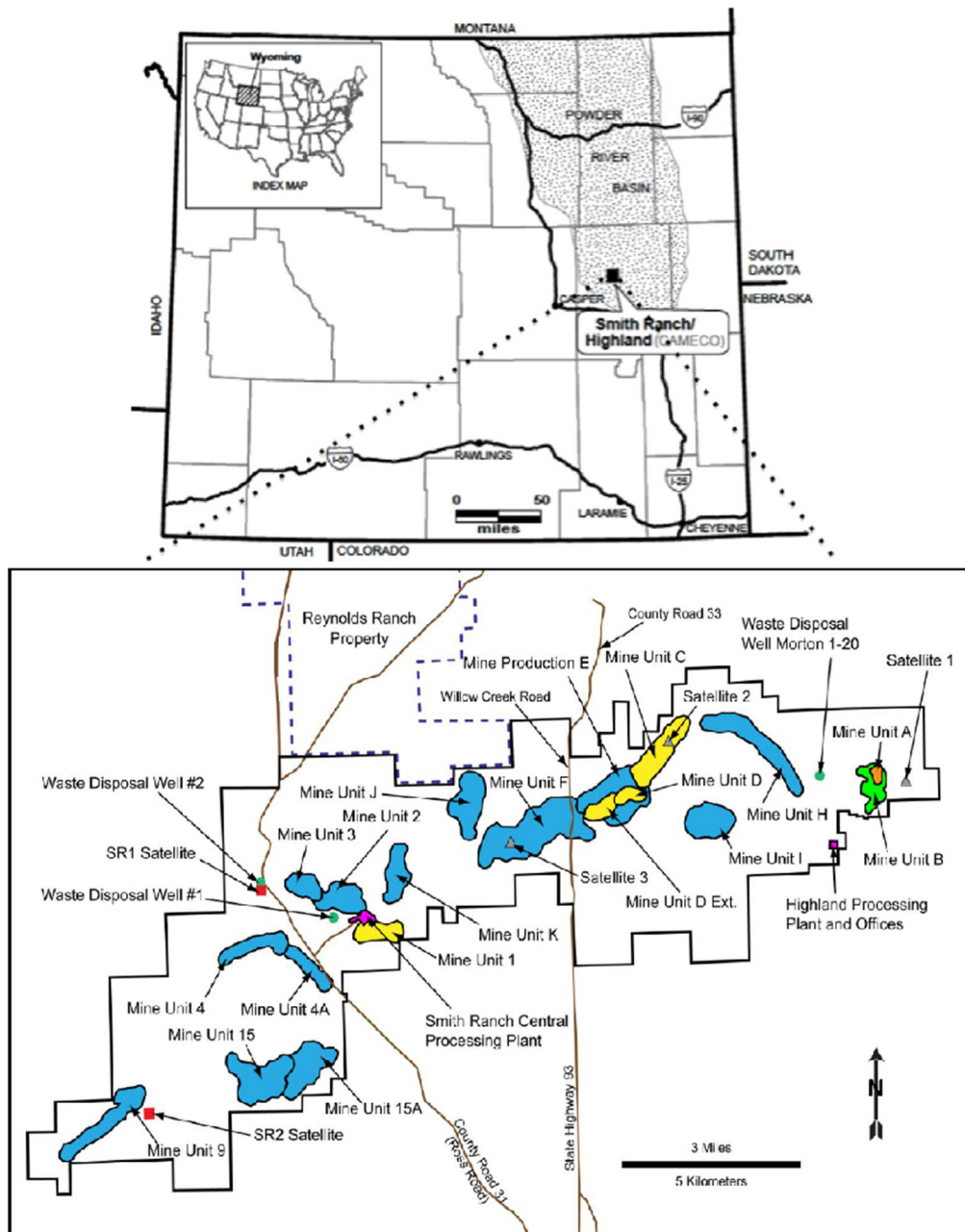


Figure D.1. Modified from WoldeGabriel et al., 2014. Map of the Smith Ranch-Highland site shown in relation to its location in the Powder River Basin.



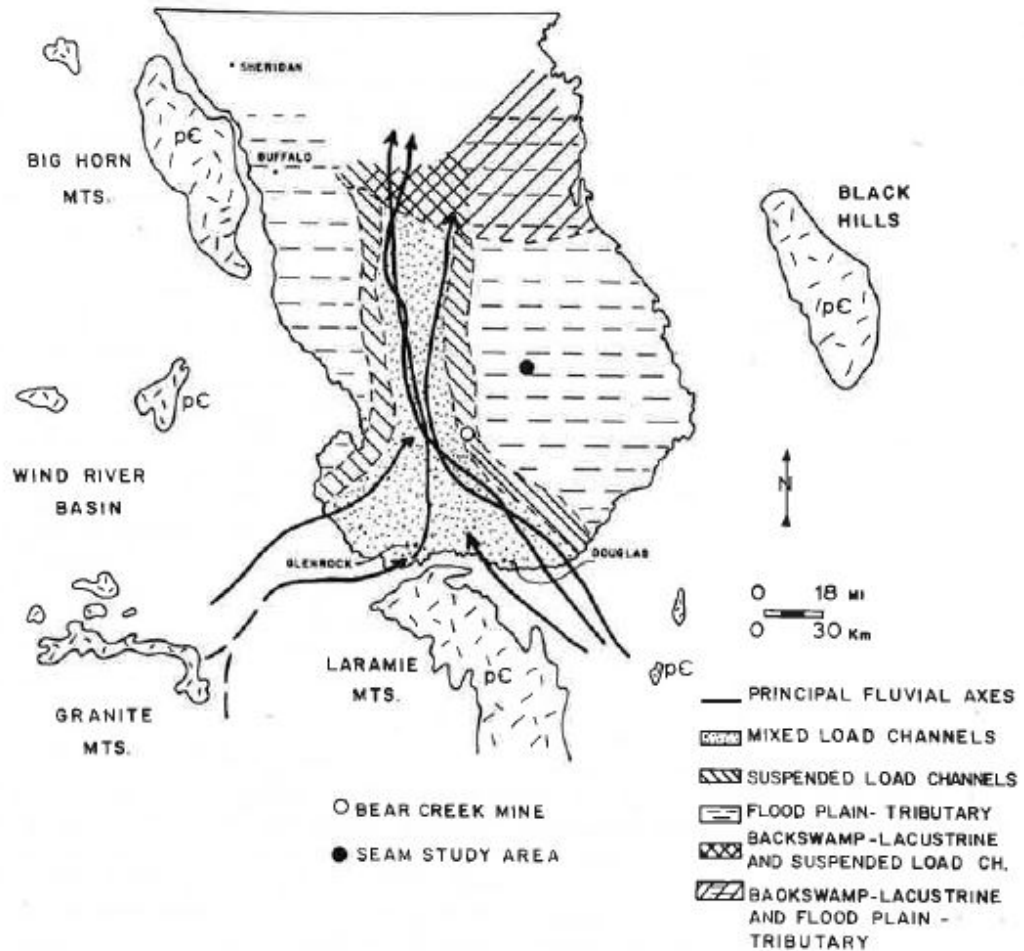


Figure D.2. Taken from Ethridge et al. 1981. Inferred depositional system and subsystems upper part of Fort Union, southern Powder River Basin. The Smith Ranch-Highland is just south of Bear Creek Mine.

Because the Fort Union was deposited when the Powder River Basin was an active sedimentary basin, Weissmann et al.'s (2010) sedimentary basin model, in which a distributive fluvial system (DFS) transports sediment through basins is another depositional model for the Fort Union. A DFS is a pattern of channel and floodplain deposits that radiate outward from an apex that is located where the river enters the sedimentary basin (Weissmann et al., 2010). As distance from the apex increases, channel size decreases, abundance of floodplain fines increases, avulsions are common, and preservation of organic matter is possible (Weissmann et al., 2013). Using a DFS model,

fan apices in the Laramie Mountains south of SRH could have transported sediment northward into the basin. This is consistent with groundwater flow in the area, which is generally southwest to northeast and has not changed since the early Paleocene (Dahl & Hagmaier, 1976). SRH is about 30 miles north of the Laramie Mountains, so it may have been a distal area on the DFS.

### D.3 Core

The MOW 4-6 core, which was used in all the laboratory experiments for this thesis was collected from Mining Unit 4 in 2007. Figure D.3 shows the core with relevant features indicated. The core consisted of uranium-rich carbonaceous shale underlain by sandstone with trough cross-bedding. The 766 feet bgs to about 780 feet bgs section lacks any obvious bed forms, contain carbonaceous shale, a coal seam, and appears to be finer grained. All these features are consistent with deposition in a floodplain environment. Below 780 feet bgs, trough cross bedding and planar laminations are visible. This is indicative of deposition in a lower flow regime. The preservation of organic matter and evidence for a lower flow regime are consistent with the idea that the MOW 4-6 core could have been deposited in the distal area of a DFS, where preservation of channel and floodplain deposits is likely. Figure D.8 shows these photographs in relation to the well log. Only the bottom portion of the well log is shown because the instrument did not appear to take measurements above this depth.

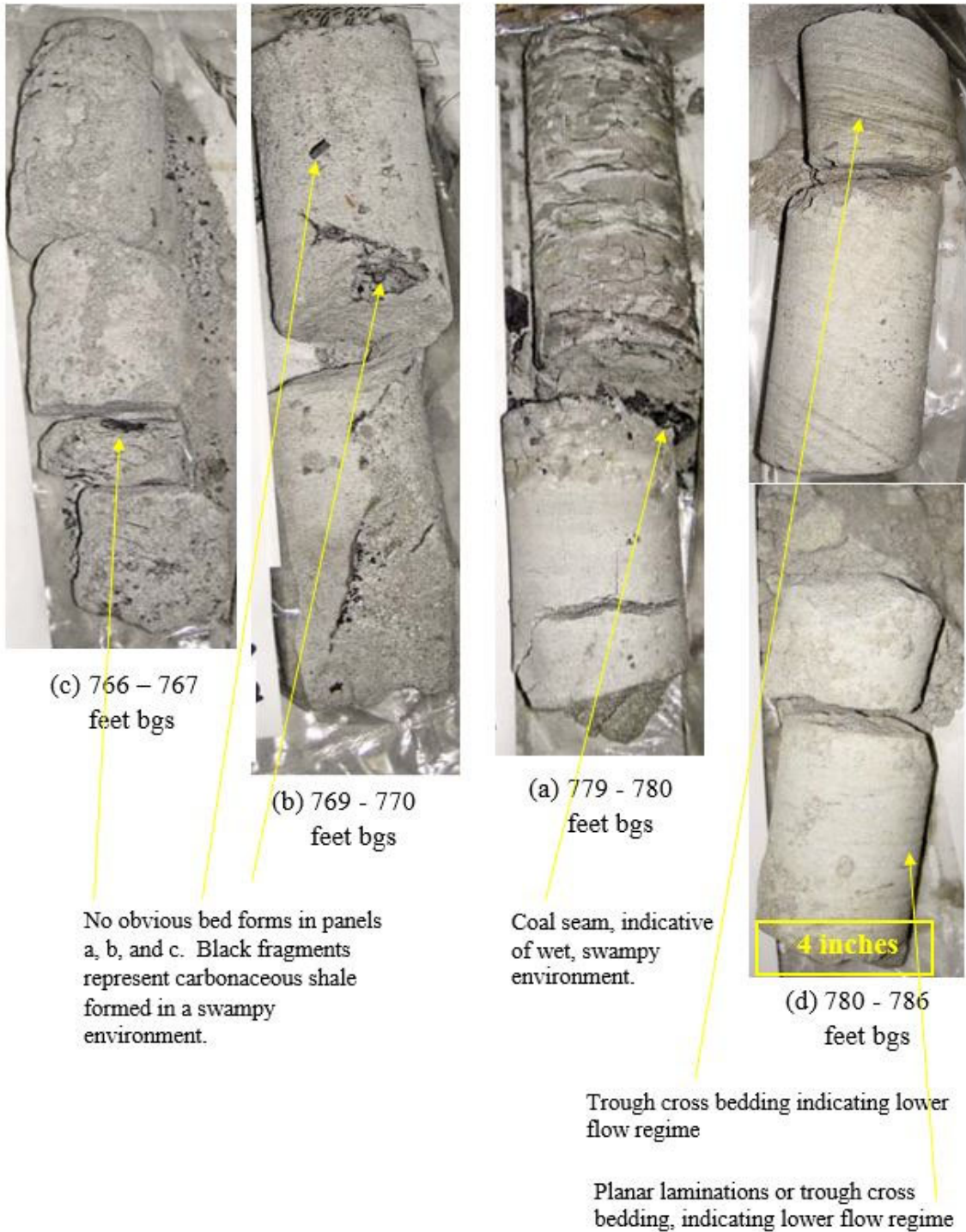


Figure D.3. MOW 4-6 core.

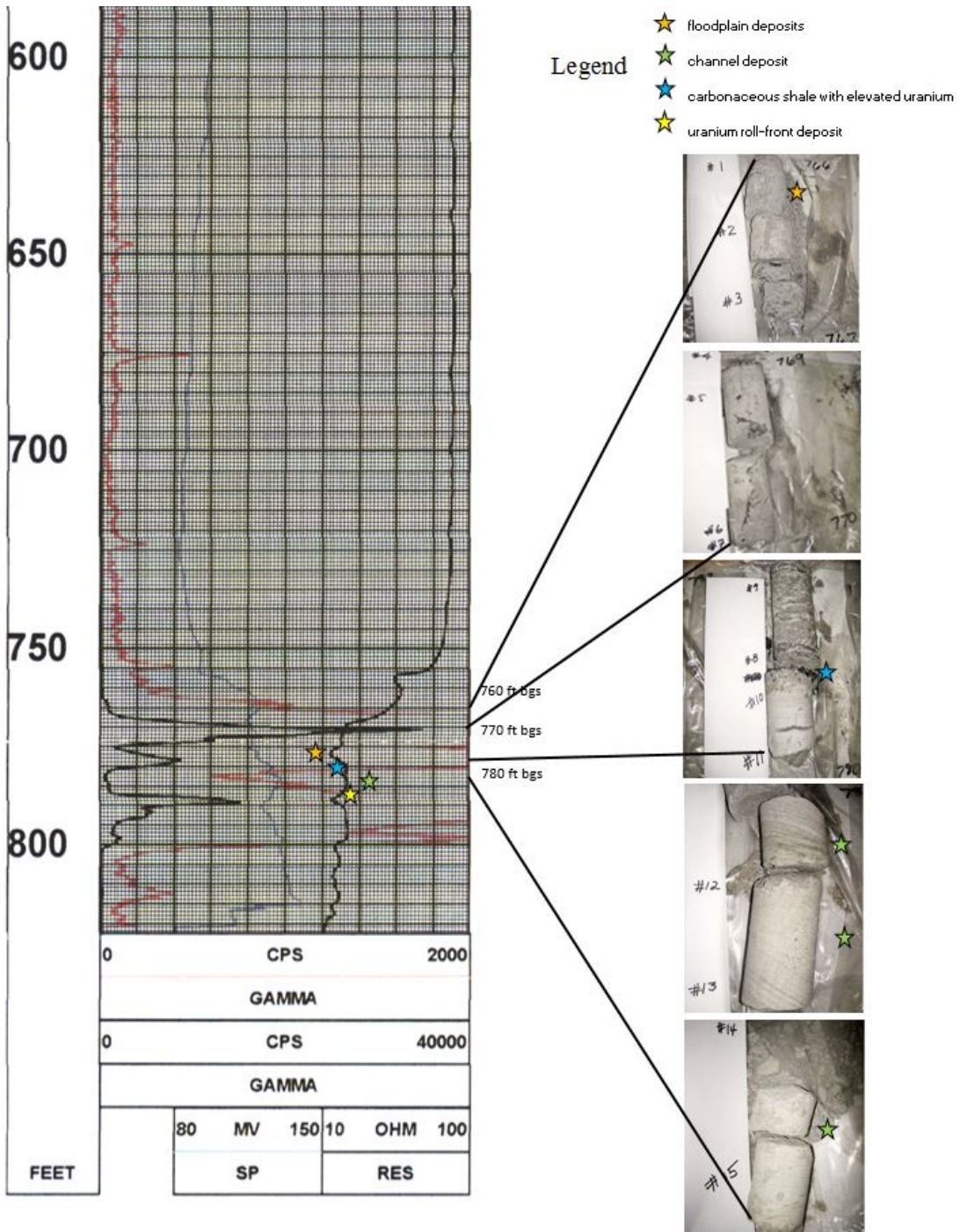


Figure D.4. Well log showing resistivity (black lines), and gamma counts (red and blue lines) for MOW 4-6 core. Photos of MOW 4-6 core are shown with corresponding depth in the well log.

#### D.4. Well logs

Well logs were obtained for 10 wells from Mining Unit 15, the location of the two push-pull field tests whose results are discussed in Section III. Mining Unit 15 can be seen in Figure D.1, about 2 miles south of Mining Unit 4. Figure D.5 shows the wells 15P-308 and 15P-315 are part of five spot patterns, with a production well in the center of four injection wells. Injection wells are about 100 feet apart, and injection and production wells are about 75 feet apart. Screen depths, shown in Table D.1, range from 440 to 478 feet bgs. The wells were correlated to one another to look for similarities or differences in fluvial deposition. To correlate the wells, the top left injector well was correlated to the next well following a clockwise pattern. The top left injection well in each pattern was also correlated to the production well in the center, and both production wells were correlated to each other.

Well logs (Figures D.6 through D.16) show resistivity (black lines) and gamma counts (red and blue lines). The blue line shows gamma counts at an order of magnitude greater than red, so trends can be observed for higher counts. Resistivity is a measure of how strongly the formation opposes the electric current being sent through it. Sandstones have higher resistivity than finer grained rocks. Shales and clays which hold more water in their pore space have lower resistivities. Elevated gamma counts paired with a higher resistivity likely represent sandstone roll front deposits. Elevated gamma counts paired with a lower resistivity likely represent uranium-rich carbonaceous shale.







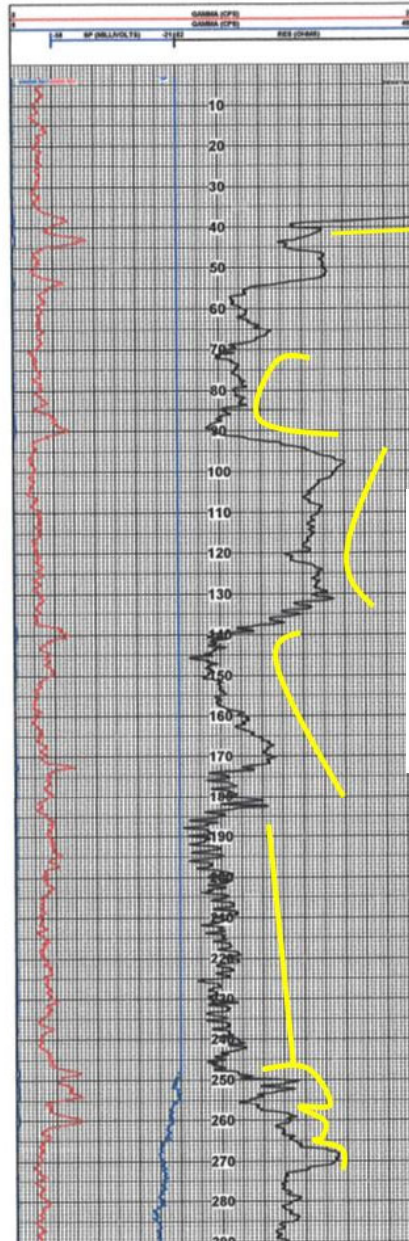
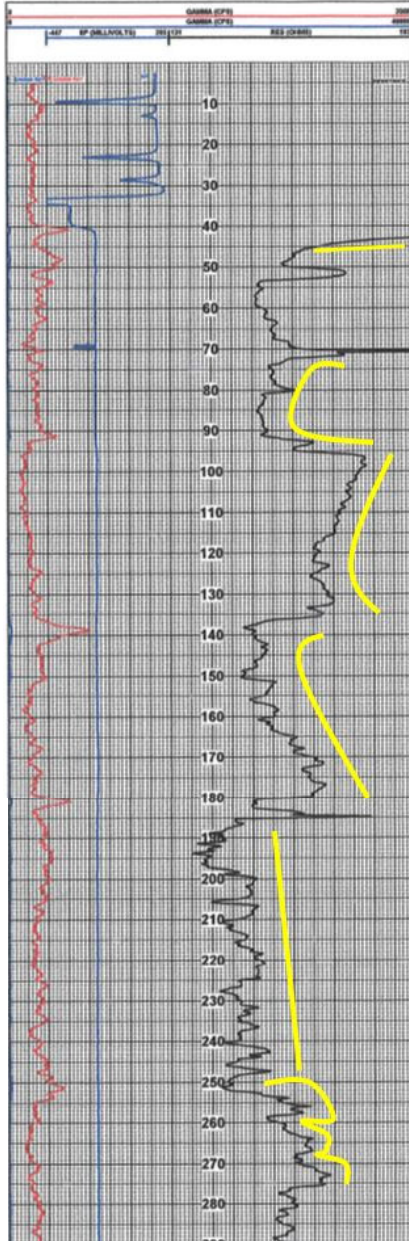
Figure D.5. Wells that were correlated in Mining Unit 15.

Well ID	Depth (feet below ground surface)	
	Top of screen	Bottom of screen
15P-308	449	467
15I-554	441	459
15I-555	453	472
15I-558	458	477
15I-559	440	457
15P-315	452	470
15I-566	454	471
15I-567	450	464
15I-568	447	472
15I-569	459	478

Table D.1. Well screen intervals for wells in Mining Unit 15.

		3574-11-151-554	
		POWER RESOURCES, INC.	
		31.20	12.50
Company:	POWER RESOURCES, INC.		
Well:	3574-11-151-554	Coordinates:	Distance: 4.45 Admth: 185.81
Location/Field:	SR/SP-MU-SW	North:	85134
County:	CORWISSE	East:	305395
State:	WYO		
Section:	11	Log Meas. From:	OL Elevation:
Township:	35N	Dist. Meas. From:	OL 5396.3
Range:	76E		
Date:	MON MAR 19 16:52:44 2007	Logging Unit:	LU-12
Depth Order:	520	Field Office:	SMITH RANCH
Log Bottom:	520.2	Recorded By:	PARKETT
Log Top:	2.4		
SP Case:	3.25	SP Case From:	MUJ
Magnetic Dev:	14	SP Correction:	
Probe Number:	2025-4		
4-Factor:	5.240E-08	Driller:	WILD/POTTER 15-16
Deadline:	179E-08	Remarks:	

		3574-11-151-559	
		POWER RESOURCES, INC.	
		31.10	13.40
Company:	POWER RESOURCES, INC.		
Well:	3574-11-151-559	Coordinates:	Distance: 7.5 Admth: 119.6
Location/Field:	SR/SP-MU-SW	North:	85125
County:	CORWISSE	East:	305494
State:	WYO		
Section:	11	Log Meas. From:	OL Elevation:
Township:	35N	Dist. Meas. From:	OL 5383.2
Range:	76E		
Date:	TUE MAR 20 09:48:24 2007	Logging Unit:	LU-14
Depth Order:	500	Field Office:	SMITH RANCH
Log Bottom:	500.1	Recorded By:	G GREENWALD
Log Top:	2.4		
SP Case:	7.05	SP Case From:	MUJ
Magnetic Dev:	14	SP Correction:	
Probe Number:	2025-08		
4-Factor:	6.000E-08	Driller:	WILD/P. POTTER 15-16
Deadline:	8.000E-09	Remarks:	









Legend	
	well screens
	floodplain deposits
	channel deposit
	carbonaceous shale with elevated uranium
	uranium roll-front deposit
	similar resistivity trends

Figure D.6.a. Well 151-554 to 151-559 (0 - 280 feet bgs). At about 430 feet bgs, both wells show a resistivity spike of about the same length, suggesting it may be a channel that flowed through both wells.



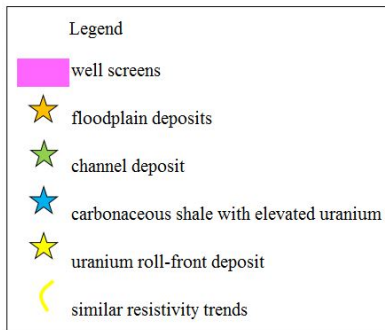
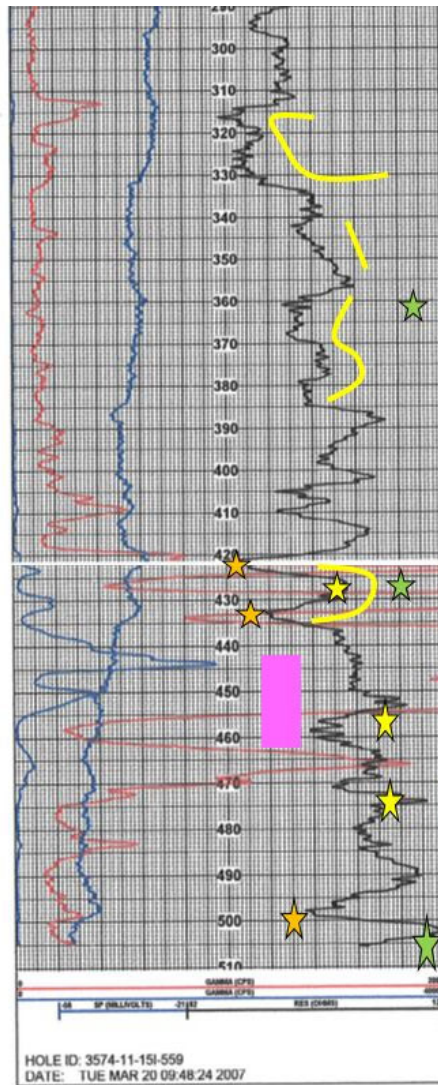
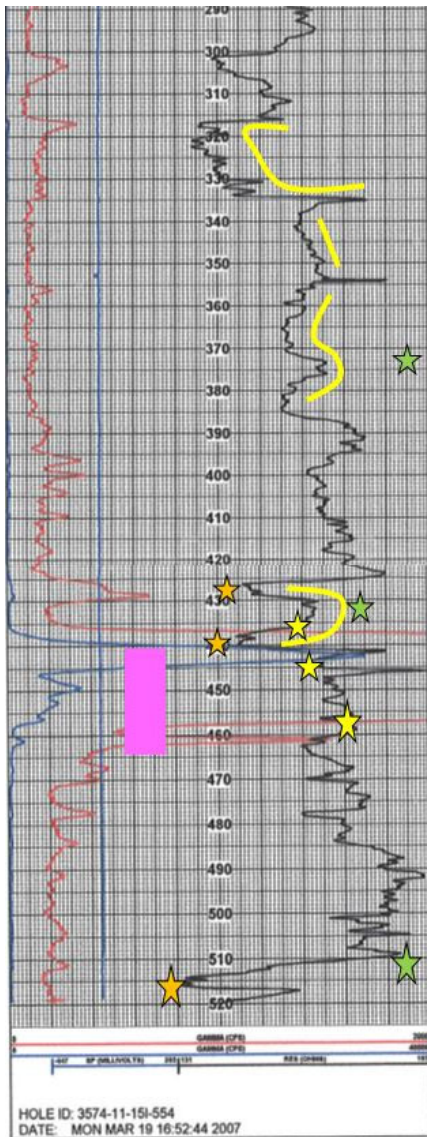
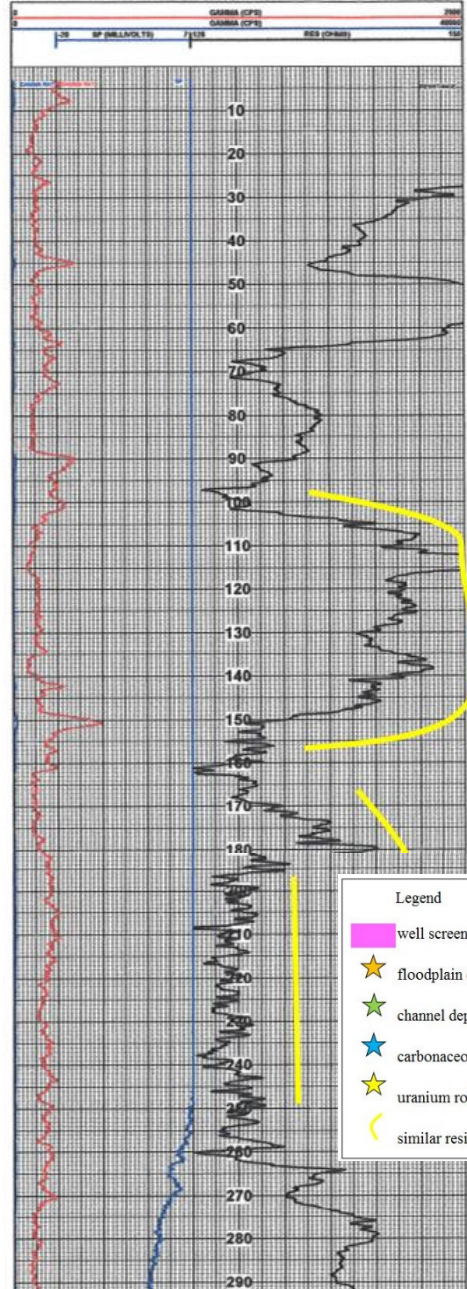
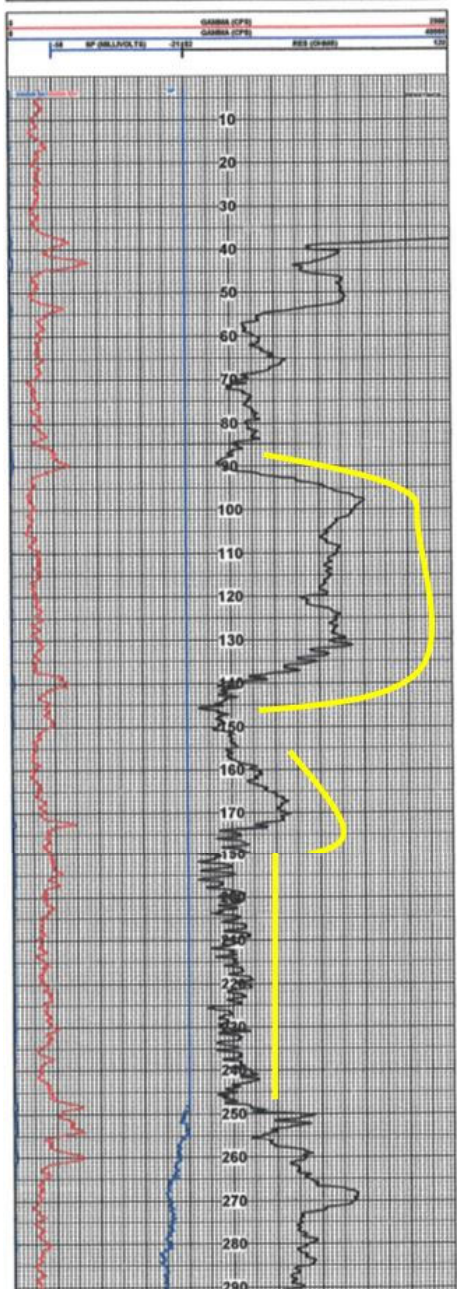


Figure D.6.b. Well 151-554 to 151-559 (280 - 520 feet bgs). At about 430 feet bgs, both wells show a resistivity spike of about the same length, suggesting it may be a channel that flowed through both wells.



	3574-11-151-559		
	POWER RESOURCES, INC.		
	31.10	13.40	
Company:	POWER RESOURCES, INC.		
Well:	3574-11-151-559	Coordinate:	Distance: 7.9
Location/Field:	SR HUP/W/K	North:	Admitt: 119.8
County:	CONVERSE	East:	355494
State:	WYO		
Section:	11	Log Meas. From:	GL Elevation:
Township:	34	DI Meas. From:	GL 8383.2
Range:	35		
Date:	TUE MAR 20 09 48 24 2007	Logging Unit:	LU-14
Depth/Drill:	500	Field Office:	SMITH RANCH
Log Bitrate:	506.1	Recorded By:	G GREENWALD
Log Top:	2.4		
Bit Size:	7 / 8	Core Hole Size:	MUJ
Magnetic Dec:	14	SP Correction:	
K-Factor:	0000548		
Drilltime:	0000109	Drill:	WLD/B POTTER
		Remarks:	15-16

	3574-11-151-558		
	POWER RESOURCES, INC.		
	30.10	13.30	
Company:	POWER RESOURCES, INC.		
Well:	3574-11-151-558	Coordinate:	Distance: 4.0
Location/Field:	SR HUP/W/K	North:	Admitt: 127.8
County:	CONVERSE	East:	355477
State:	WYO		
Section:	11	Log Meas. From:	GL Elevation:
Township:	35N	DI Meas. From:	GL 5393.8
Range:	74W		
Date:	WED APR 04 17 11 10 2007	Logging Unit:	LU-14
Depth/Drill:	520	Field Office:	SMITH RANCH
Log Bitrate:	522.1	Recorded By:	G GREENWALD
Log Top:	2.4		
Bit Size:	7 / 8	Core Hole Size:	MUJ
Magnetic Dec:	14	SP Correction:	
K-Factor:	0000548		
Drilltime:	0000109	Drill:	WLD/B POTTER
		Remarks:	15-16



- Legend
- █ well screens
  - ★ floodplain deposits
  - ★ channel deposit
  - ★ carbonaceous shale with elevated uranium
  - ★ uranium roll-front deposit
  - ~ similar resistivity trends

Figure D.7.a. (0 - 290 feet bgs). Well 151-559 to 151-558.

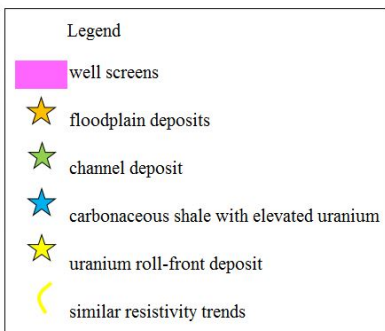
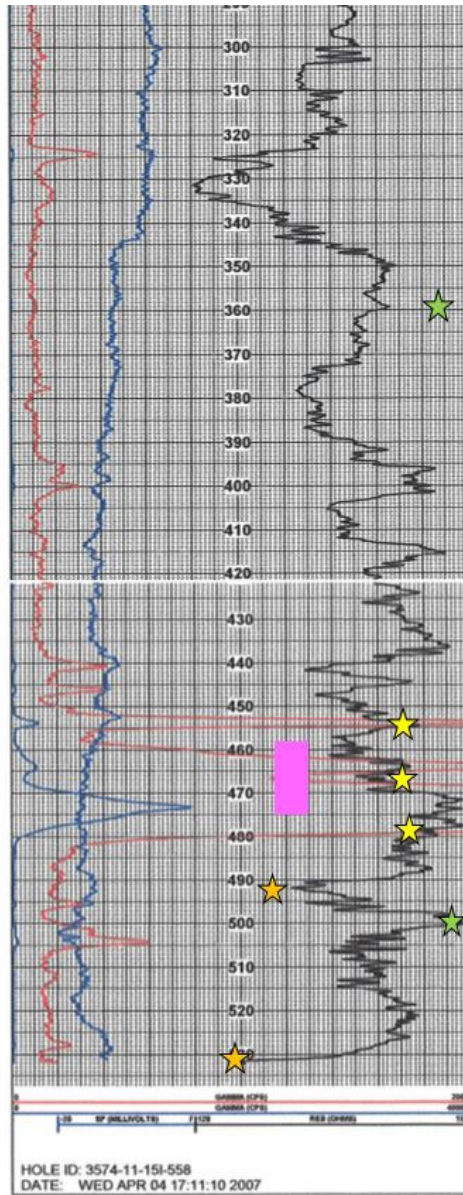
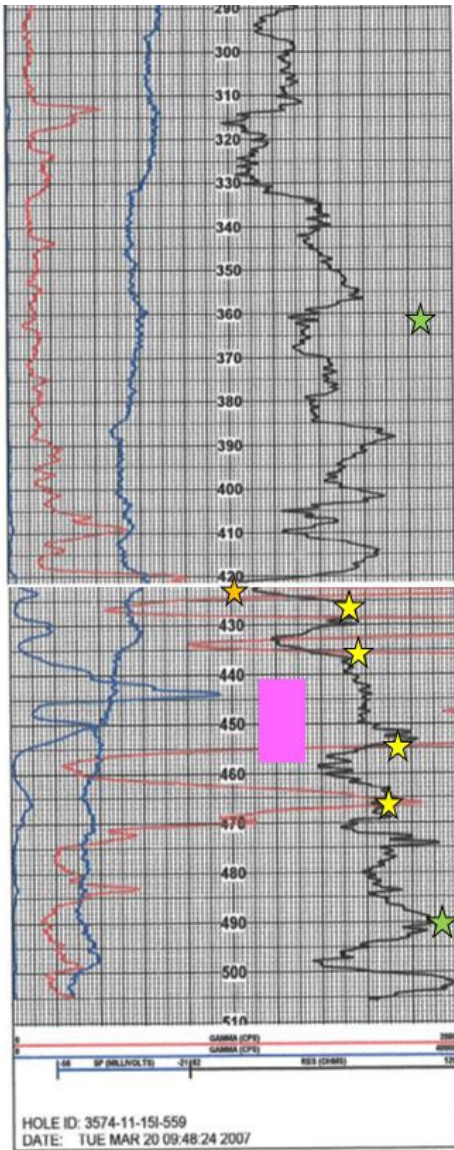


Figure D.7.b. (290 - 530 feet bgs). Well 15I-559 to 15I-558.



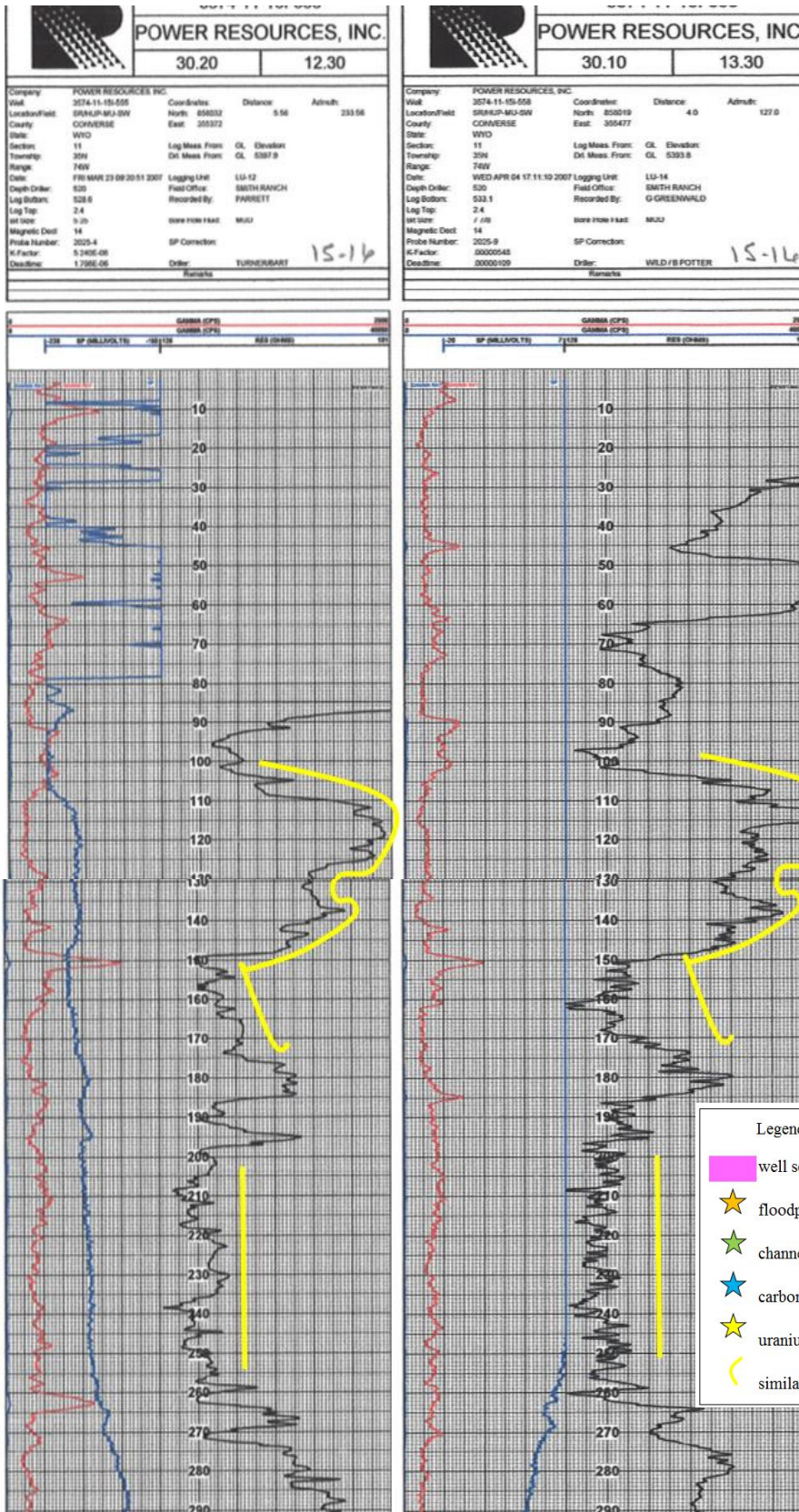


Figure D.8.a. (0 - 290 feet bgs). Well 15I-558 to 15I-555.

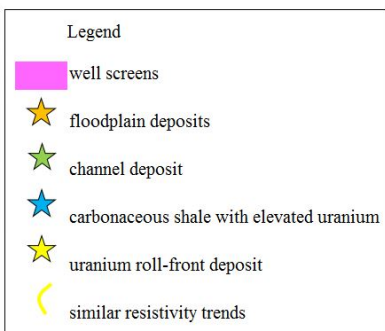
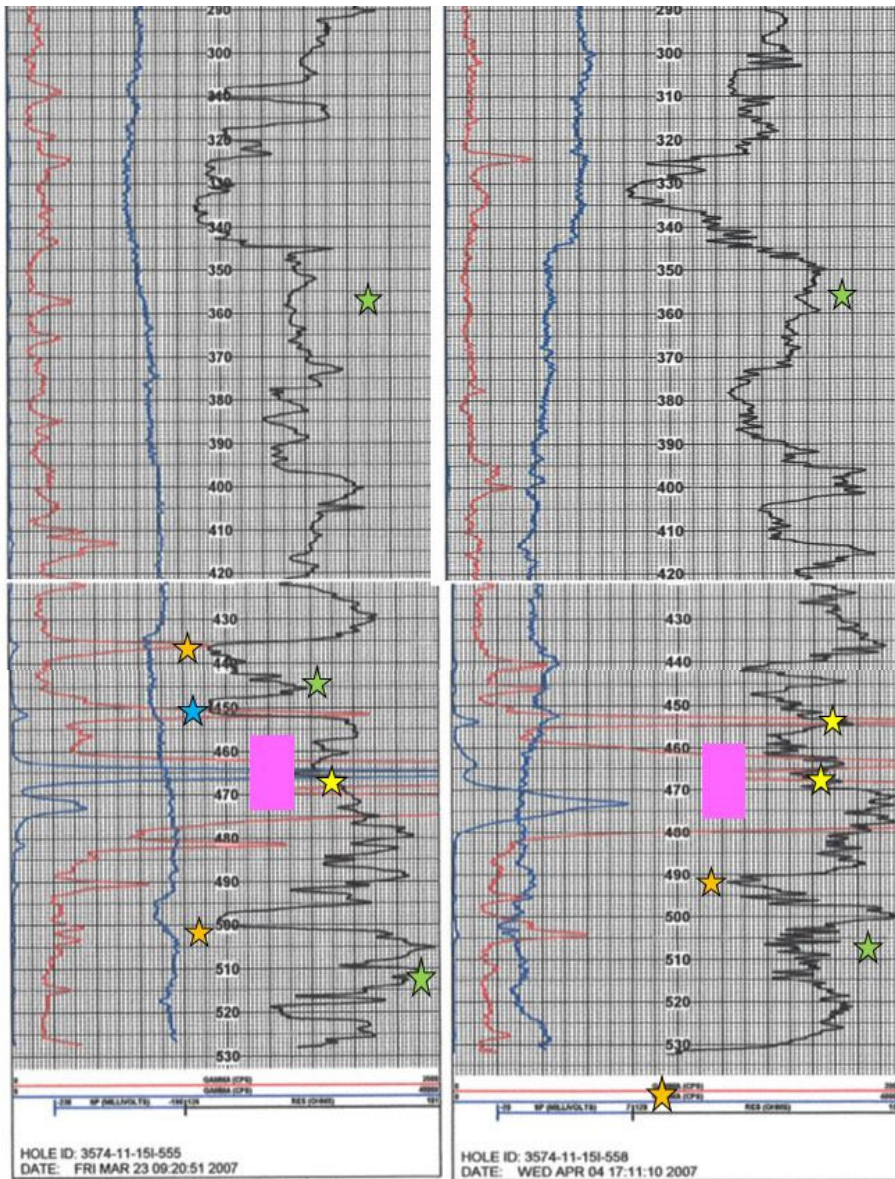

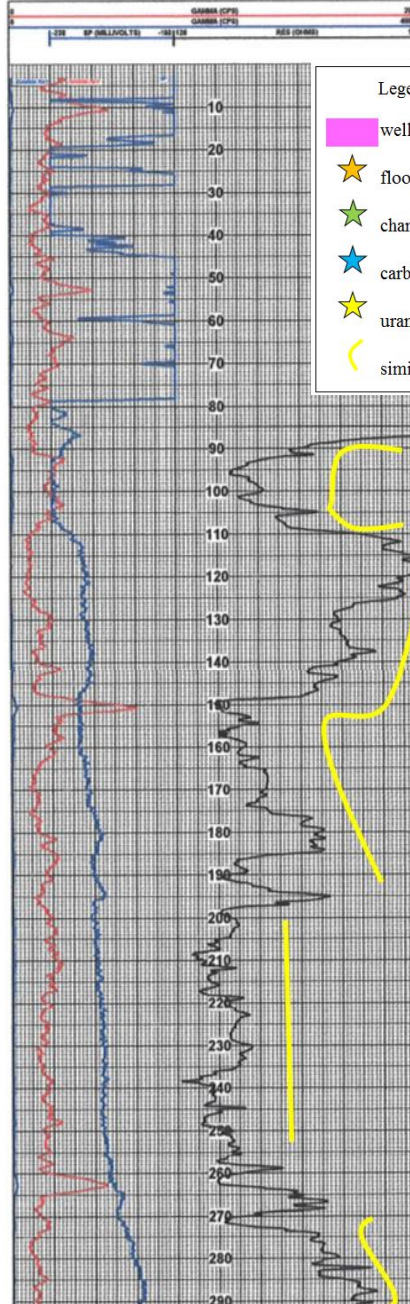
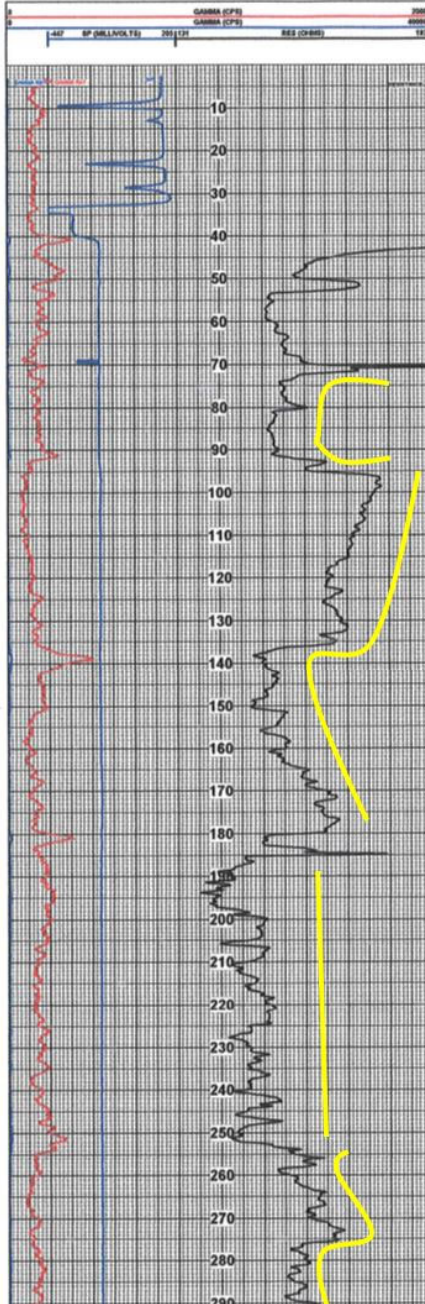


Figure D.8.b. (290- 530 feet bgs). Well 151-558 to 151-555.



		3574-11-151-554	
		POWER RESOURCES, INC.	
		31.20	12.50
Company	POWER RESOURCES, INC.		
Well	3574-11-151-554	Coordinates	Distance Admuth
Location/Field	SRH/JR-MU-DW	North: 856134 East: 355395	4.45 185.81
County	CORNWELLSE		
State	WYO		
Section	11	Log Mass. Front	GL Elevation
Township	20N	DI Mass. Front	GL 5336.3
Range	76W		
Date	MON MAR 19 16:52:44 2007	Logging Unit	LU-12
Depth Order	520	Field Office	SMITH RANCH
Log Bottom	520.2	Recorded By	FARRETT
Log Top	2.4		
Bit Size	5.25	Bore Hole Name	MUJ
Magnetic Decl	14	SP Correction	
Probe Number	2025-4		
K-Factor	5.240E-05		
Decline	1.795E-05	Driller	WILDPOTTER 15-16
Remarks			

		3574-11-151-555	
		POWER RESOURCES, INC.	
		30.20	12.30
Company	POWER RESOURCES, INC.		
Well	3574-11-151-555	Coordinates	Distance Admuth
Location/Field	SRH/JR-MU-DW	North: 856032 East: 355372	5.56 233.56
County	CORNWELLSE		
State	WYO		
Section	11	Log Mass. Front	GL Elevation
Township	20N	DI Mass. Front	GL 5337.9
Range	76W		
Date	FRI MAR 23 09:20:51 2007	Logging Unit	LU-12
Depth Order	520	Field Office	SMITH RANCH
Log Bottom	520.6	Recorded By	FARRETT
Log Top	2.4		
Bit Size	5.25	Bore Hole Name	MUJ
Magnetic Decl	14	SP Correction	
Probe Number	2025-4		
K-Factor	5.240E-05		
Decline	1.795E-05	Driller	TURNERBAET 15-16
Remarks			



- Legend
- well screens
  - floodplain deposits
  - channel deposit
  - carbonaceous shale with elevated uranium
  - uranium roll-front deposit
  - similar resistivity trends

Figure D.9.a. Well 151-555 to 151-554 (0 - 280 feet bgs).

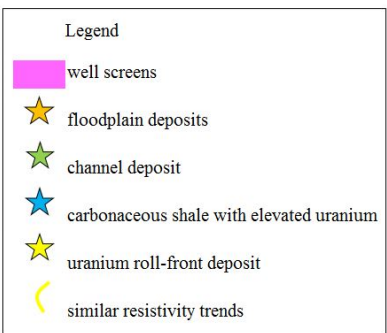
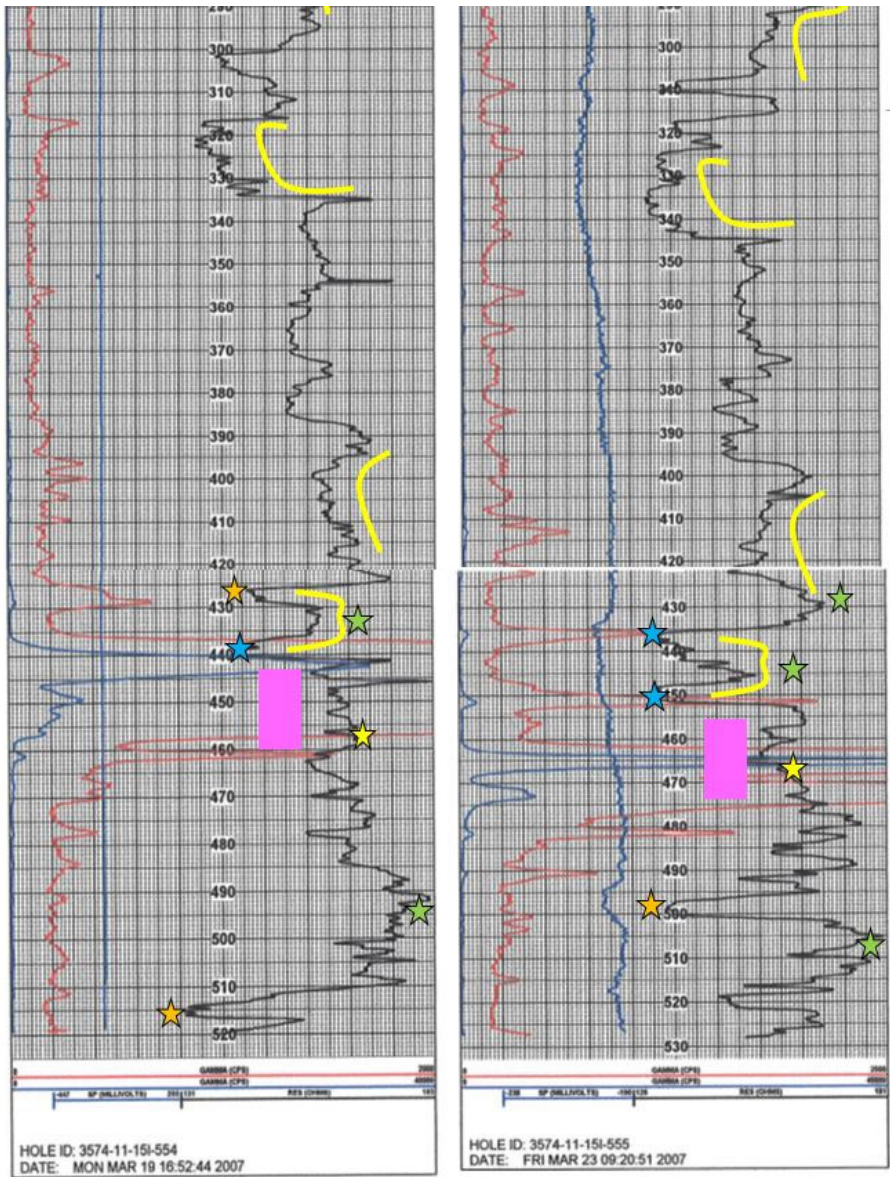


Figure D.9.b. Well 15I-555 to 15I-554 (290 - 530 feet bgs). Matching features at ~390 - 430 feet bgs, could be a channel deposit with upward fining then coarsening. Another matching channel deposit from 430 - 450 feet bgs.



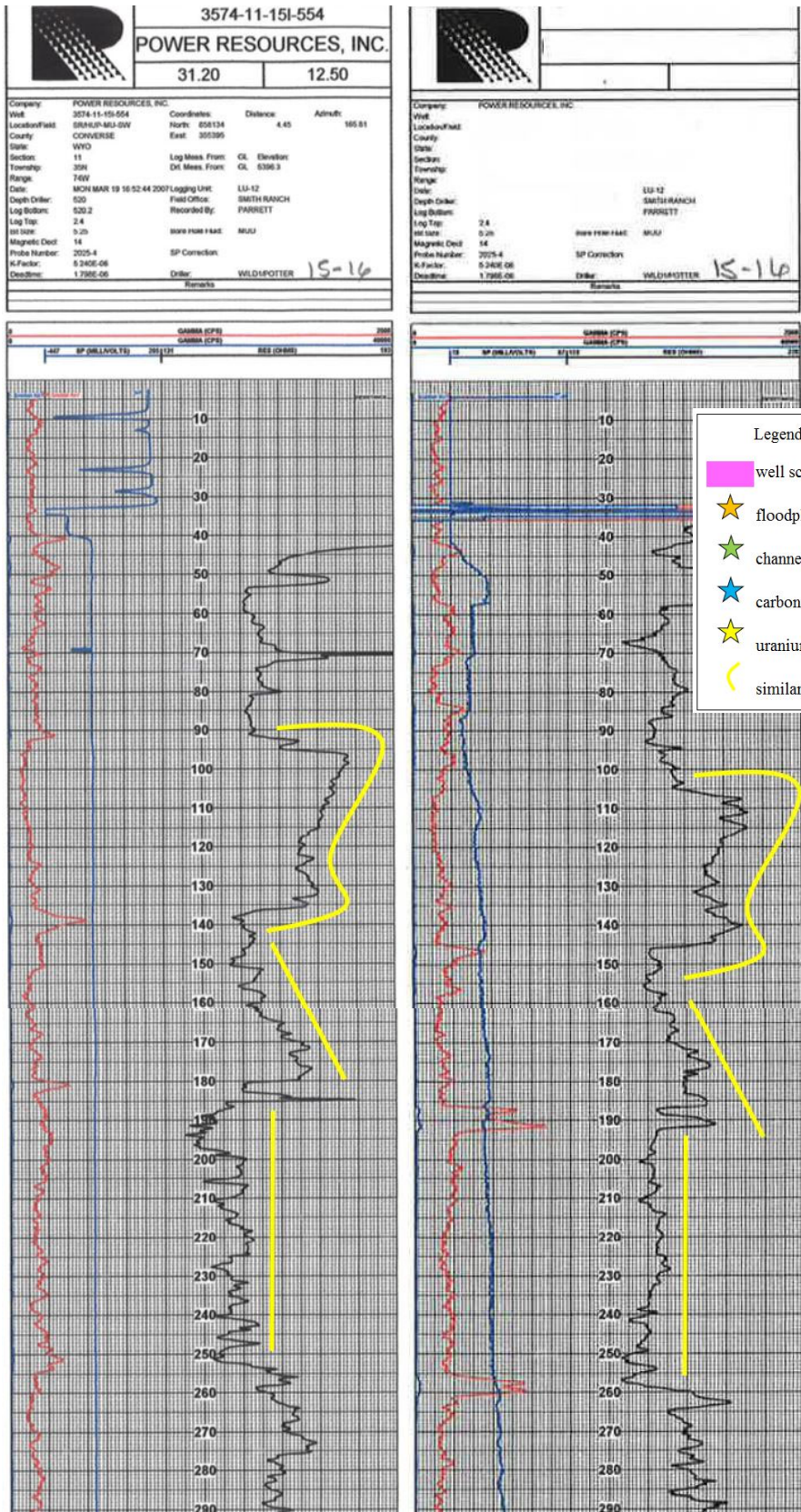


Figure D.10.a. Well 151-554 to 15P-308 (0 - 280 feet bgs).

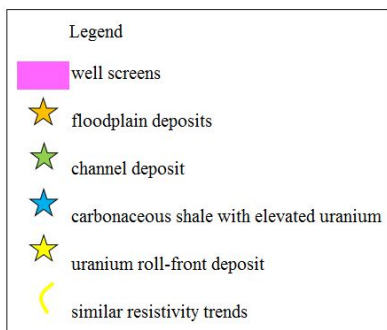
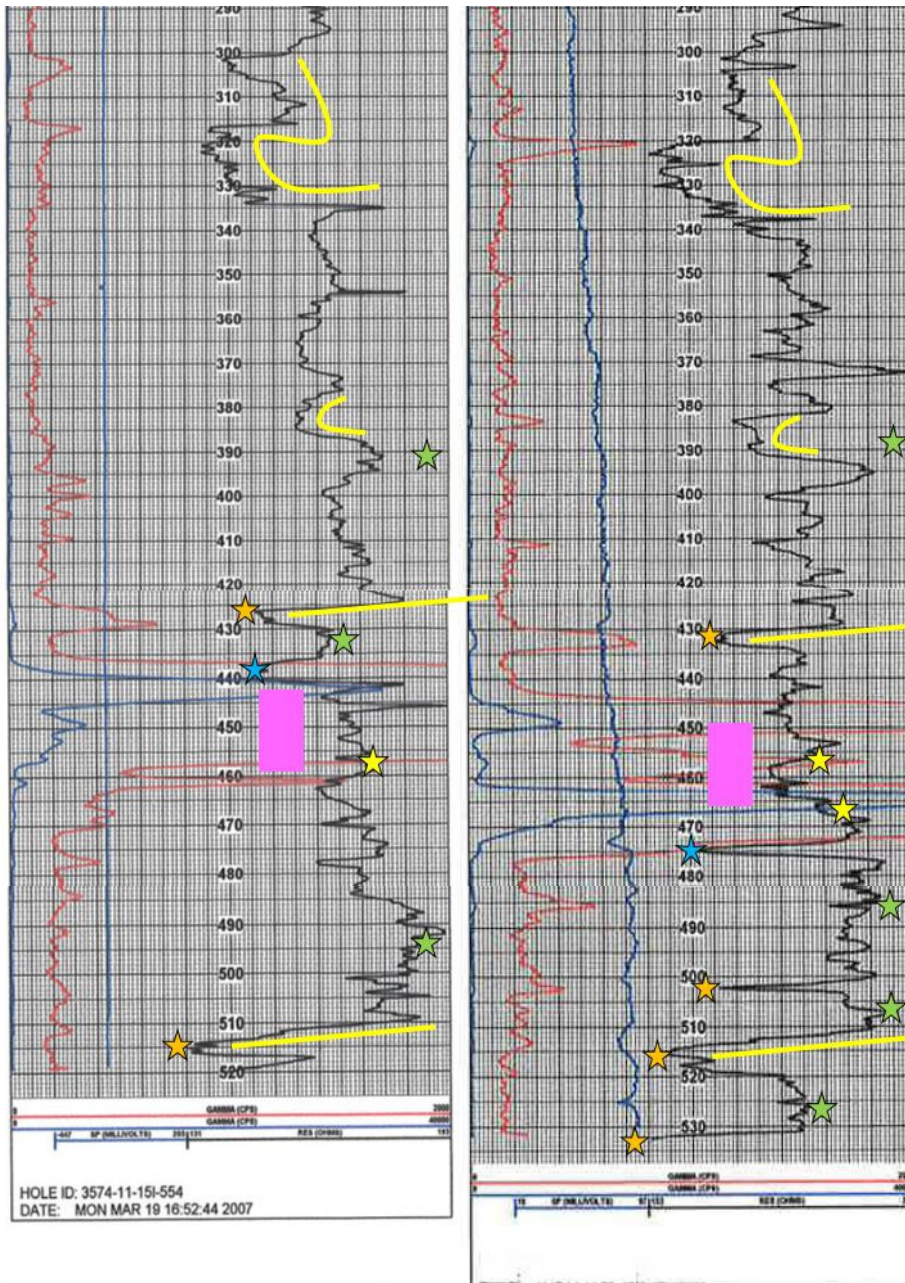


Figure D.10.b. Well 151-554 to 15P-308 (290 - 530 feet bgs). In both wells, sharp contacts to finer grained deposited at 510 feet bgs and 430 feet bgs. At about 380 feet bgs, similar upward coarsening to upward fining is observed.



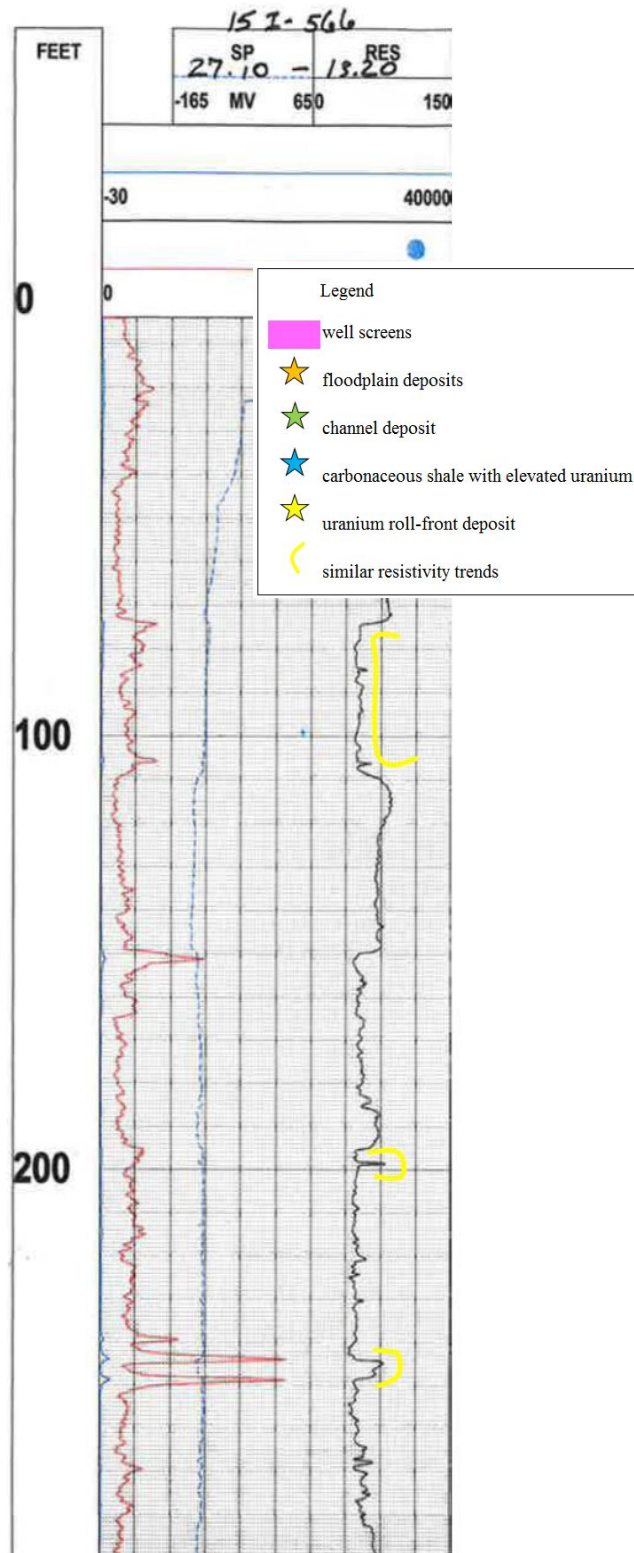
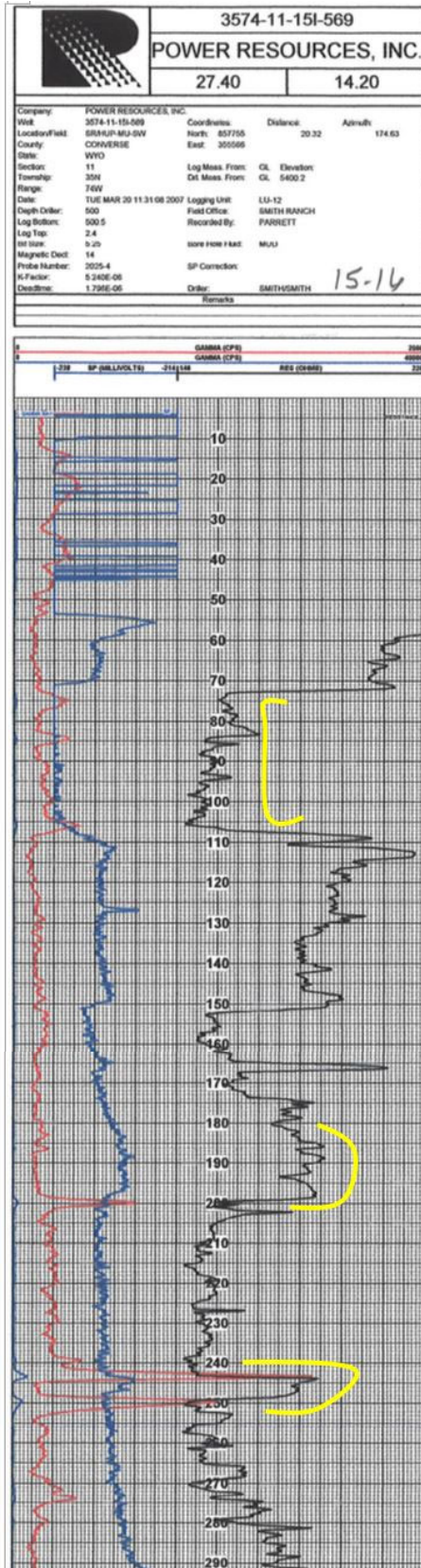
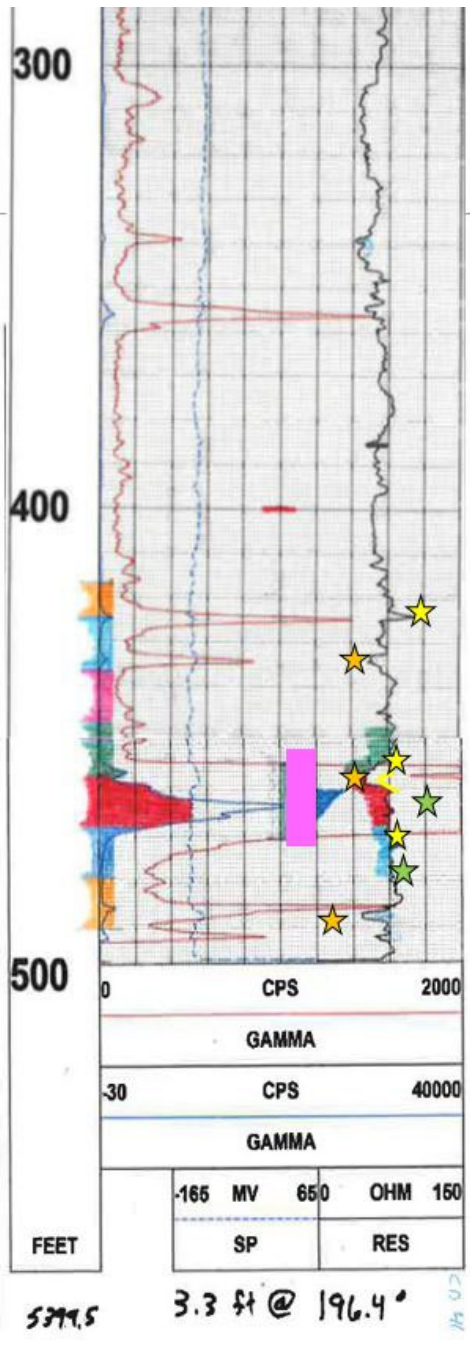
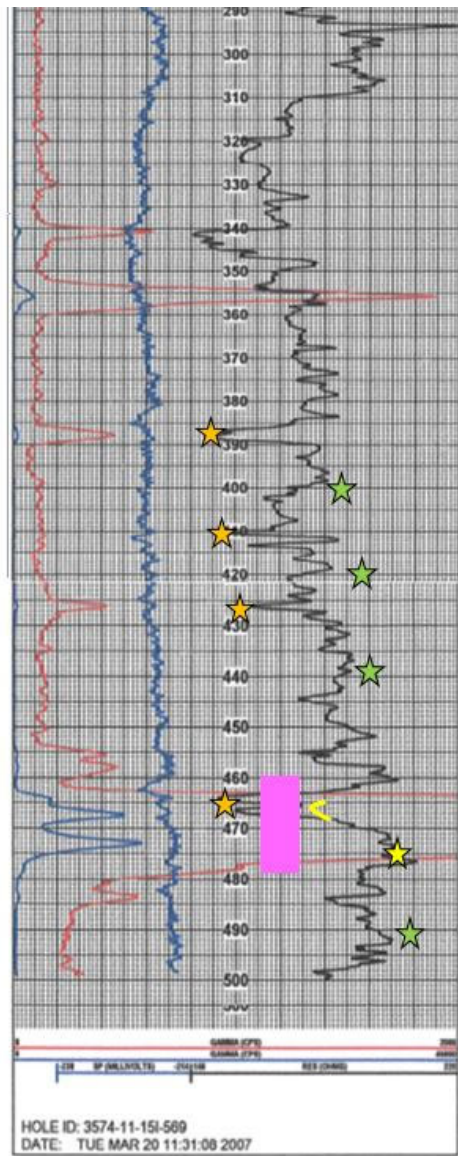



Figure D.11.a. Well 151-566 - 151-569 (0 - 290 feet bgs).




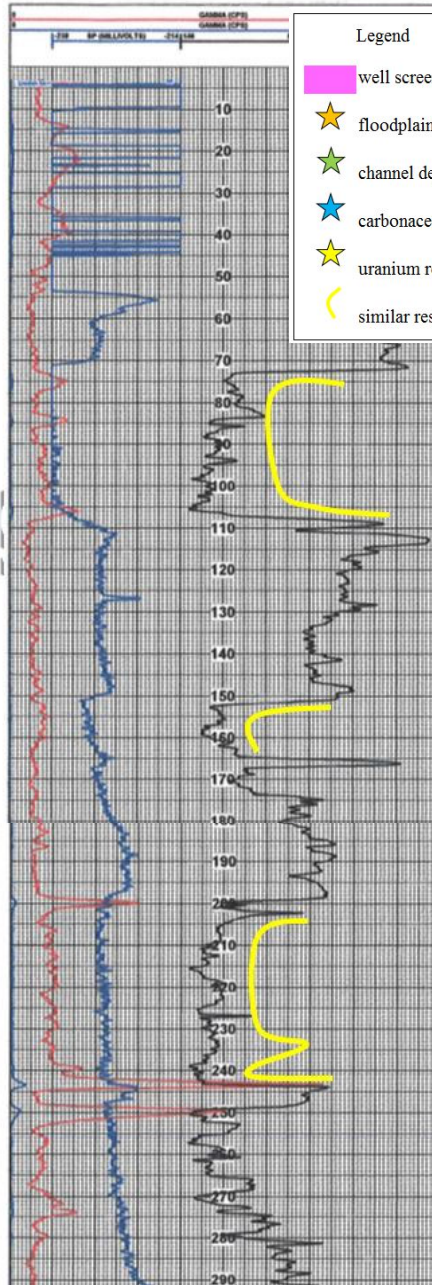
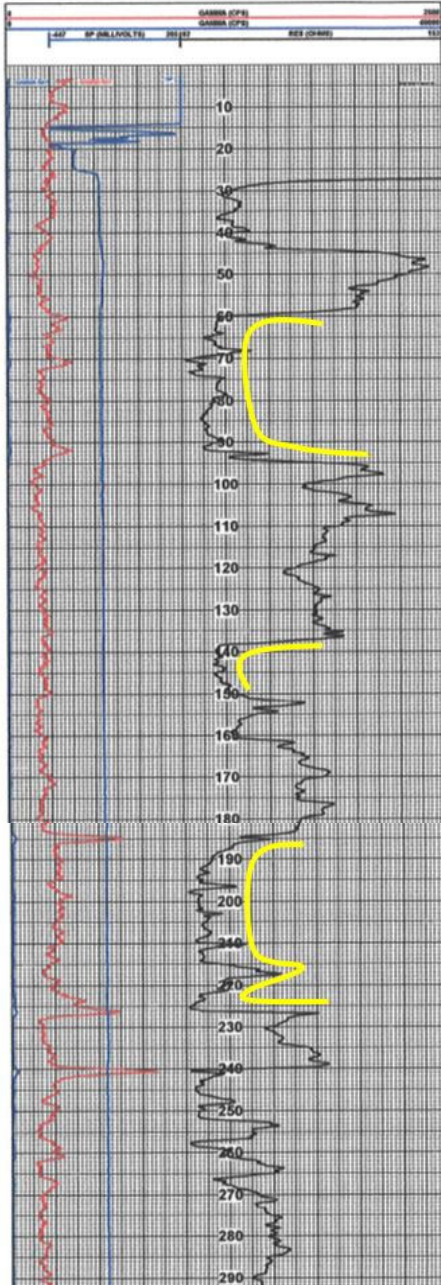
- Legend
- well screens
  - floodplain deposits
  - channel deposit
  - carbonaceous shale with elevated uranium
  - uranium roll-front deposit
  - similar resistivity trends

Figure D.11.b. Well 151-566 to 151-569 (290 - 510 feet bgs).



	3574-11-151-568		
	POWER RESOURCES, INC.		
	26.40	14.30	
Company:	POWER RESOURCES, INC.		
Well:	3574-11-151-568	Coordinates:	Distance: 6.91
Location/Pack:	BRHUP-MU-SW	North:	857646
County:	CONVERSE	East:	366577
State:	WYO	Admth:	154.68
Section:	11	Log Mass. From:	OL Elevation
Township:	35N	Dr. Mass. From:	OL 5288.1
Range:	76W		
Date:	FRI MAR 18 12:27:06 2007	Logging Unit:	LU-12
Depth Order:	500	Field Office:	SMITH RANCH
Log Bottom:	500.8	Recorded By:	PARRETT
Log Top:	2.4	Wire Size:	MUJ
Bit Size:	5.25	SP Correction:	
Magnetic Dev:	14	Driller:	SMITHSMITH
Probe Number:	2025-4		15-16
K-Factor:	5.245E-06		
Deadline:	1.795E-06		
Remarks:			

	3574-11-151-569		
	POWER RESOURCES, INC.		
	27.40	14.20	
Company:	POWER RESOURCES, INC.		
Well:	3574-11-151-569	Coordinates:	Distance: 20.32
Location/Pack:	BRHUP-MU-SW	North:	857756
County:	CONVERSE	East:	365599
State:	WYO	Admth:	174.83
Section:	11	Log Mass. From:	OL Elevation
Township:	35N	Dr. Mass. From:	OL 5430.2
Range:	76W		
Date:	TUE MAR 20 11:31:08 2007	Logging Unit:	LU-12
Depth Order:	500	Field Office:	SMITH RANCH
Log Bottom:	502.5	Recorded By:	PARRETT
Log Top:	2.4	Wire Size:	MUJ
Bit Size:	5.25	SP Correction:	
Magnetic Dev:	14	Driller:	SMITHSMITH
Probe Number:	2025-4		15-16
K-Factor:	5.245E-06		
Deadline:	1.795E-06		
Remarks:			



Legend

- well screens
- floodplain deposits
- channel deposit
- carbonaceous shale with elevated uranium
- uranium roll-front deposit
- similar resistivity trends

Figure D.12.a. Well 151-569 to 151-568 (0 - 290 feet bgs).

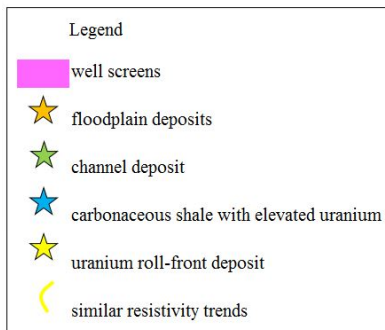
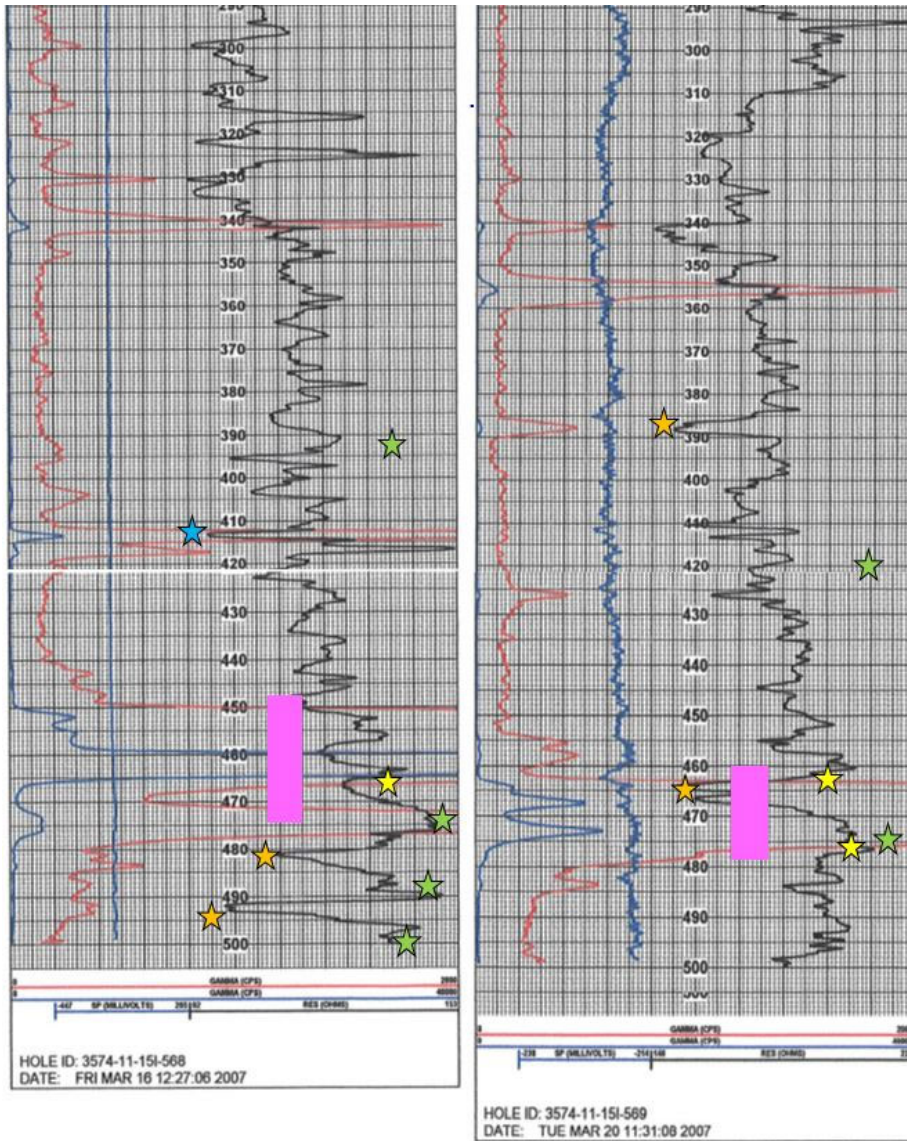


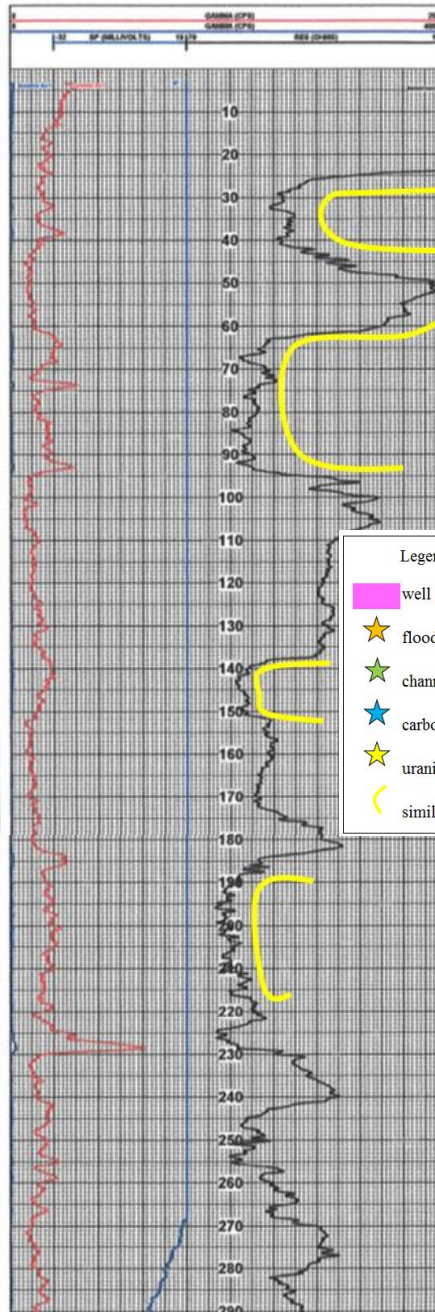
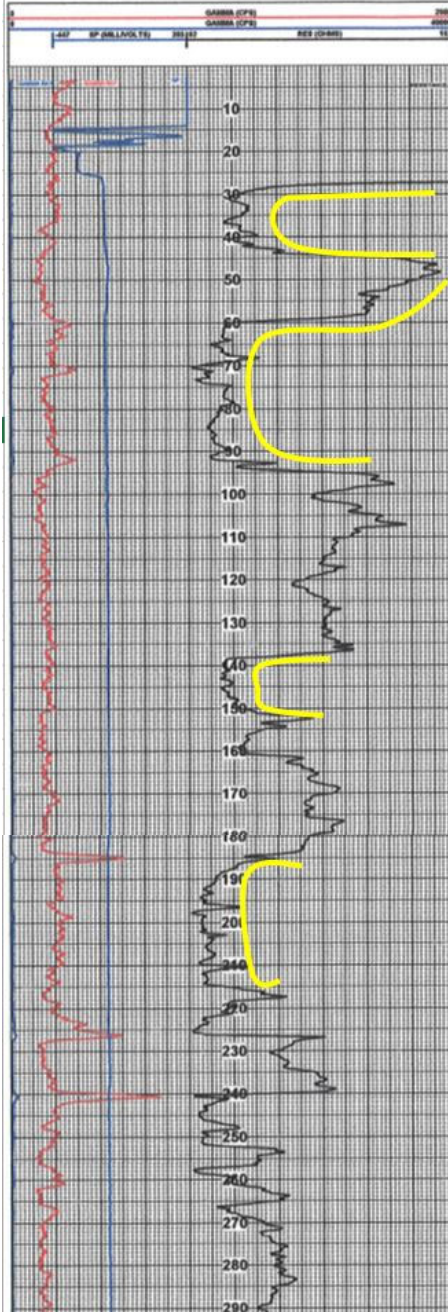


Figure D.12.b. Well 151-569 - 151-568 (290 - 500 feet bgs).



		3574-11-151-568	
		POWER RESOURCES, INC.	
		26.40	14.30
Company:	POWER RESOURCES, INC.		
Well:	3574-11-151-568	Coordinates:	Distance: 6.91 Admth: 194.58
Location/Field:	SRHUP-MU-SW	North:	857645
County:	CONVERSE	East:	305577
State:	WYO	Log Meas. From:	GL Elevation
Section:	11	Dist Meas. From:	GL 5388.1
Township:	35N	Logging Unit:	LU-12
Range:	76W	First Office:	SMITH RANCH
Date:	FRI MAR 16 12:27:06 2007	Recorded By:	PARRETT
Depth Order:	500	SP Correction:	
Log Bottom:	500.8	Order:	SMITH/SMITH
Log Top:	2.4	Remarks:	15-16
Log Size:	3.25		
Magnetic Dev:	14		
Probe Number:	3025-4		
K-Factor:	0.2406-06		
Deadline:	1.7395-06		

		3574-11-151-567	
		POWER RESOURCES, INC.	
		26.30	13.40
Company:	POWER RESOURCES, INC.		
Well:	3574-11-151-567	Coordinates:	Distance: 7.64 Admth: 267.07
Location/Field:	SRHUP-MU-SW	North:	857642
County:	CONVERSE	East:	305454
State:	WYO	Log Meas. From:	GL Elevation
Section:	11	Dist Meas. From:	GL 5381.9
Township:	35N	Logging Unit:	LU-14
Range:	76W	First Office:	SMITH RANCH
Date:	FRI MAR 16 08:09:08 2007	Recorded By:	PARRETT
Depth Order:	500	SP Correction:	
Log Bottom:	498.4	Order:	SMITH/SMITH
Log Top:	2.4	Remarks:	15-14
Log Size:	3.25		
Magnetic Dev:	14		
Probe Number:	3025-9		
K-Factor:	0.0005548		
Deadline:	0.0000100		



- Legend
- █ well screens
  - ★ floodplain deposits
  - ★ channel deposit
  - ★ carbonaceous shale with elevated uranium
  - ★ uranium roll-front deposit
  - { similar resistivity trends

Figure D.13.a. Well 151-568 to 151-567 (0 - 290 feet bgs).

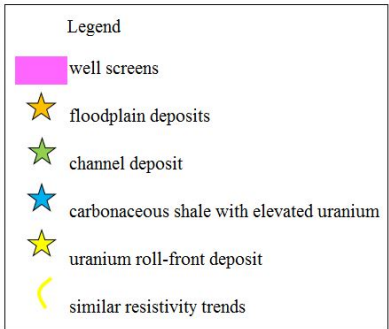
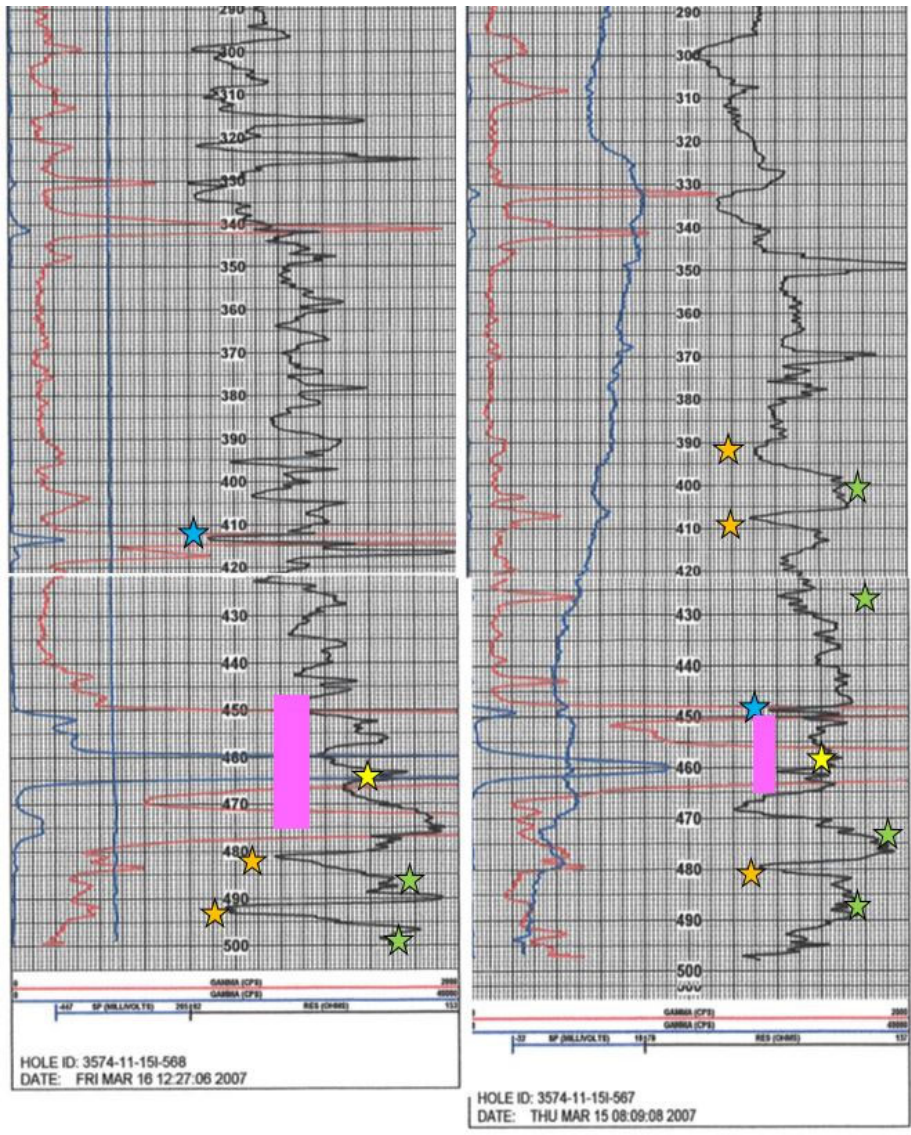

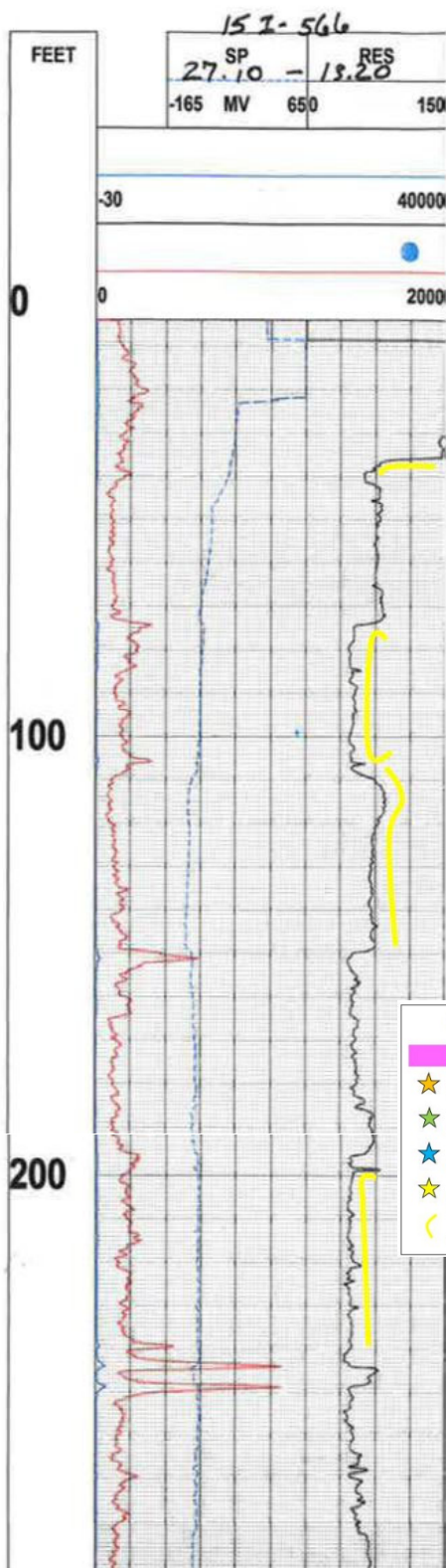
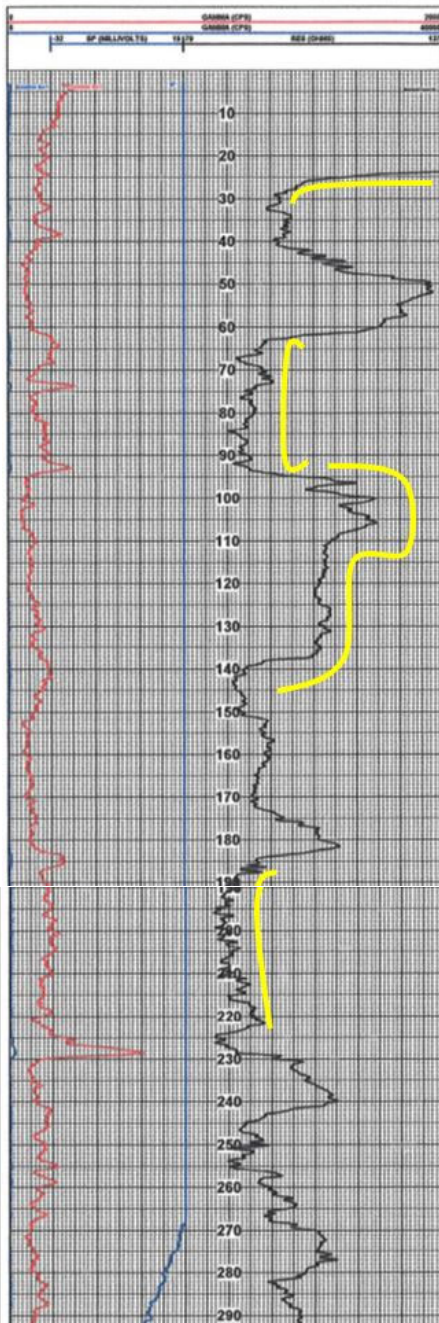


Figure D.13.b. Well 15I-568 to 15I-567 (290 - 500 feet bgs).



		3574-11-15I-567	
		POWER RESOURCES, INC.	
		26.30	13.40
Company: POWER RESOURCES, INC. Well: 3574-11-15I-567 Location/Well: BRADUP-MU-04V County: CONVERSE State: WY Section: 11 Township: 35N Range: 76W Date: THIS MAR 15 08 09 08 2007 Depth/Driller: 500 Log Bottom: 498.4 Log Top: 2.4 Well Type: 9.25 Magnetic Dev: 14 Probe Number: 2025-9 W-Factor: 0000568 Quality: 00000100 Coordinates: North: 857842 East: 205484 Distance: 7.64 Admits: 267 07 Log West. From: GL Elevator Dist West. From: GL 5381.9 Logging Unit: LU-14 Field Office: SMITH RANCH Recorded By: FARRETT SP Correction: 15-14 Driller: SMITH SMITH			
Remarks			



- Legend
- █ well screens
  - ★ floodplain deposits
  - ★ channel deposit
  - ★ carbonaceous shale with elevated uranium
  - ★ uranium roll-front deposit
  - ~ similar resistivity trends

Figure D.14.a. Well 15I-567 to 15I-566 (0 - 290 feet bgs).

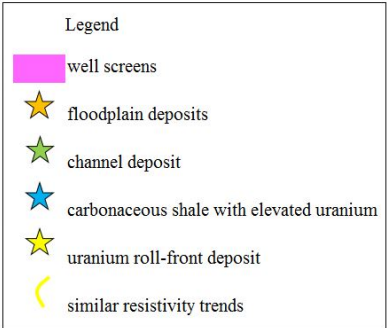
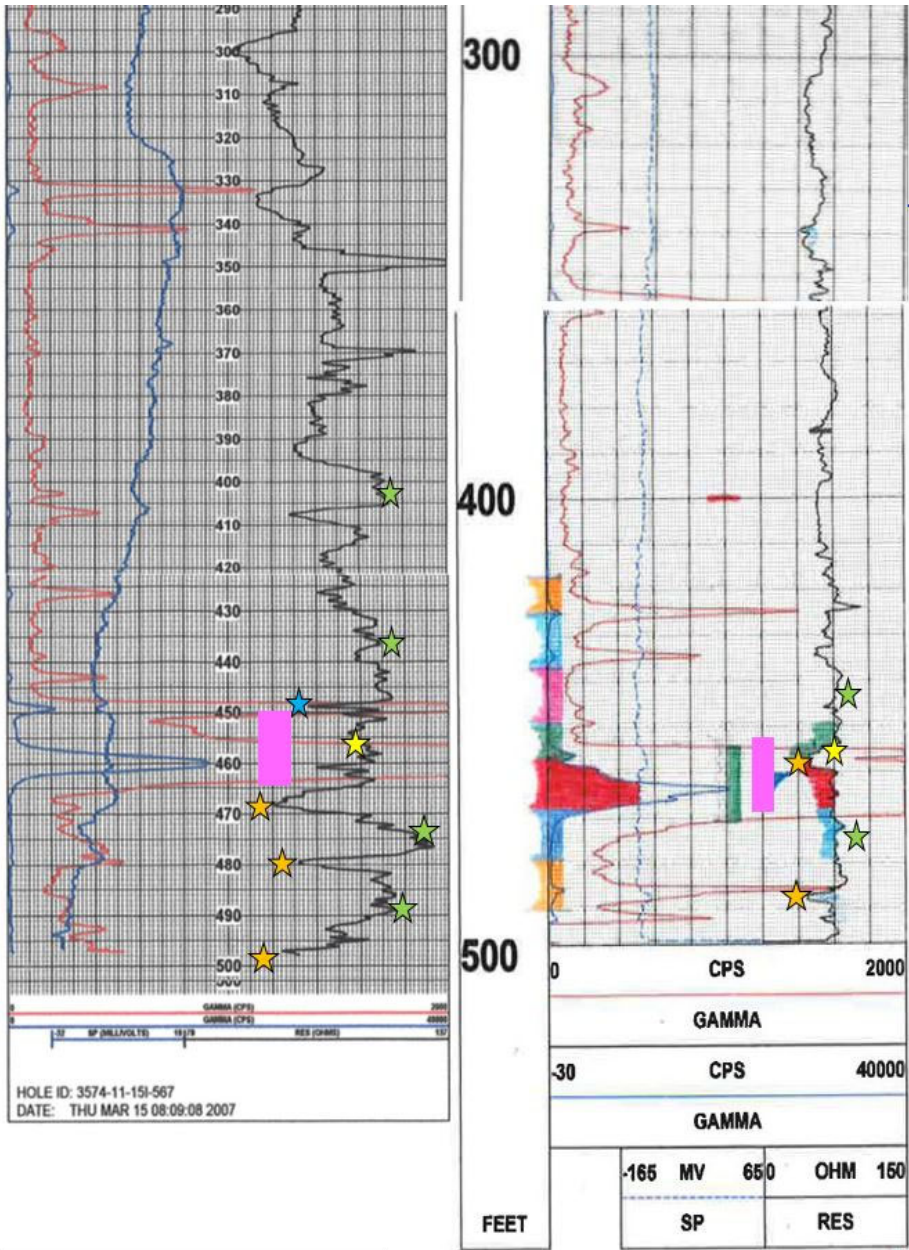


Figure D.14.b. Well 15I-567 to 15I-566 (290 - 500 feet bgs).



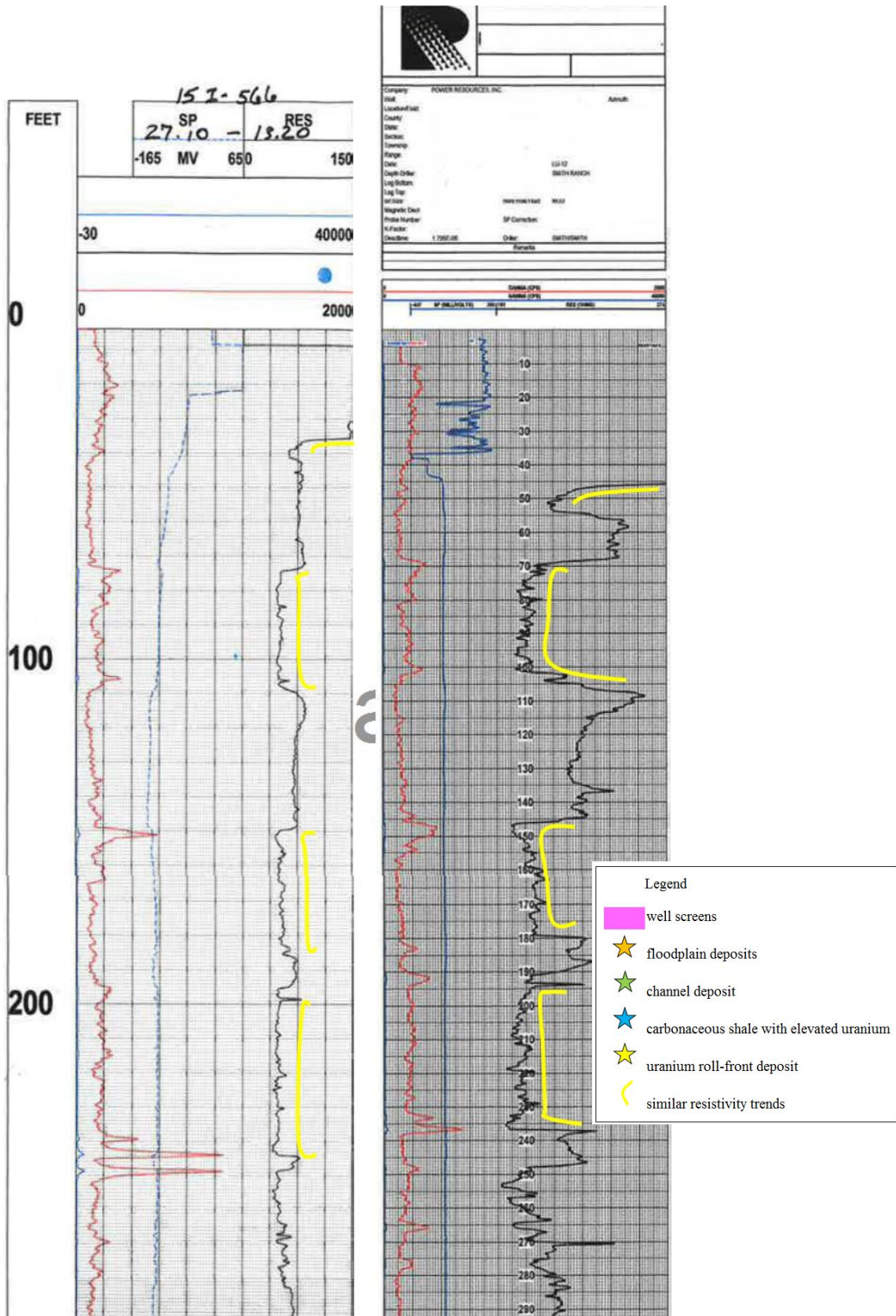


Figure D.15.a. Well 15I-566 to 15P-315 (0 - 290 feet bgs).

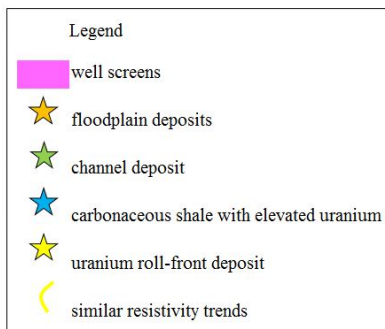
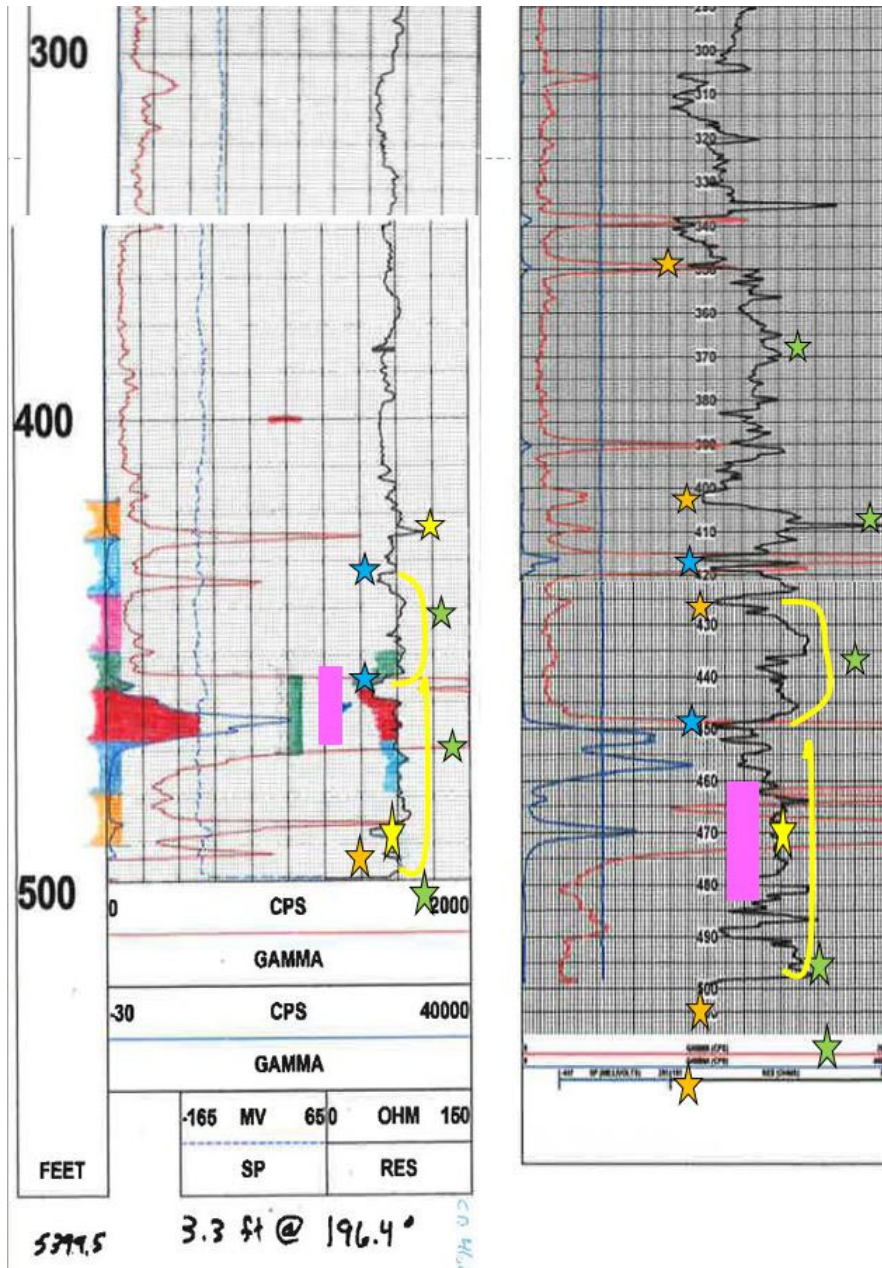


Figure D.15.b. Well 151-566 - 15P-315 (290 - 500 feet bgs). Two possible matching channel deposits, about 420 to 450 feet bgs, and 450 to 480 feet bgs.



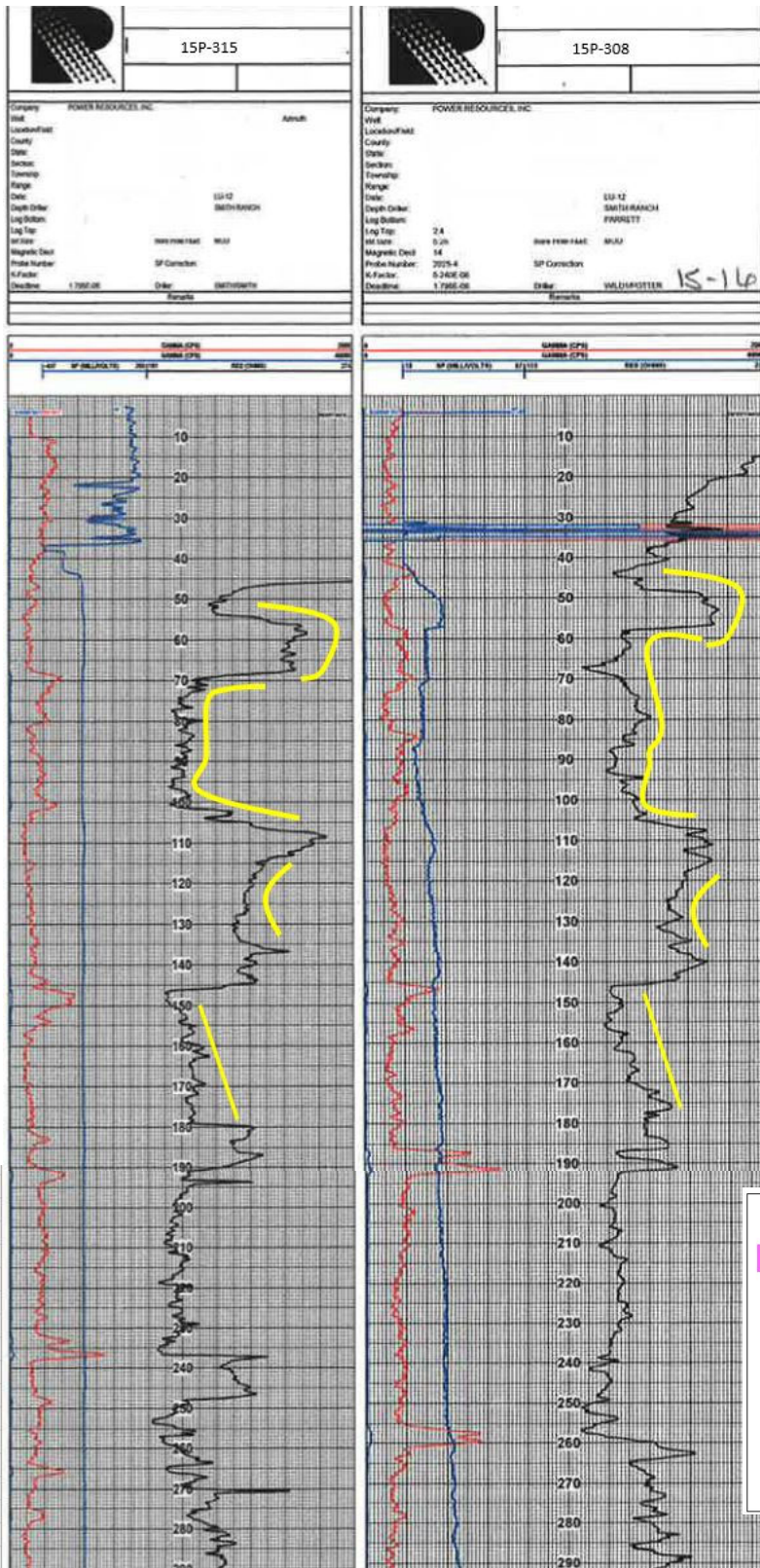


Figure D.16.a. Well 15P-308 to 15P-315 (0 - 290 feet bgs).

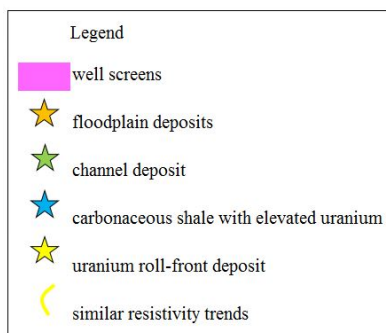
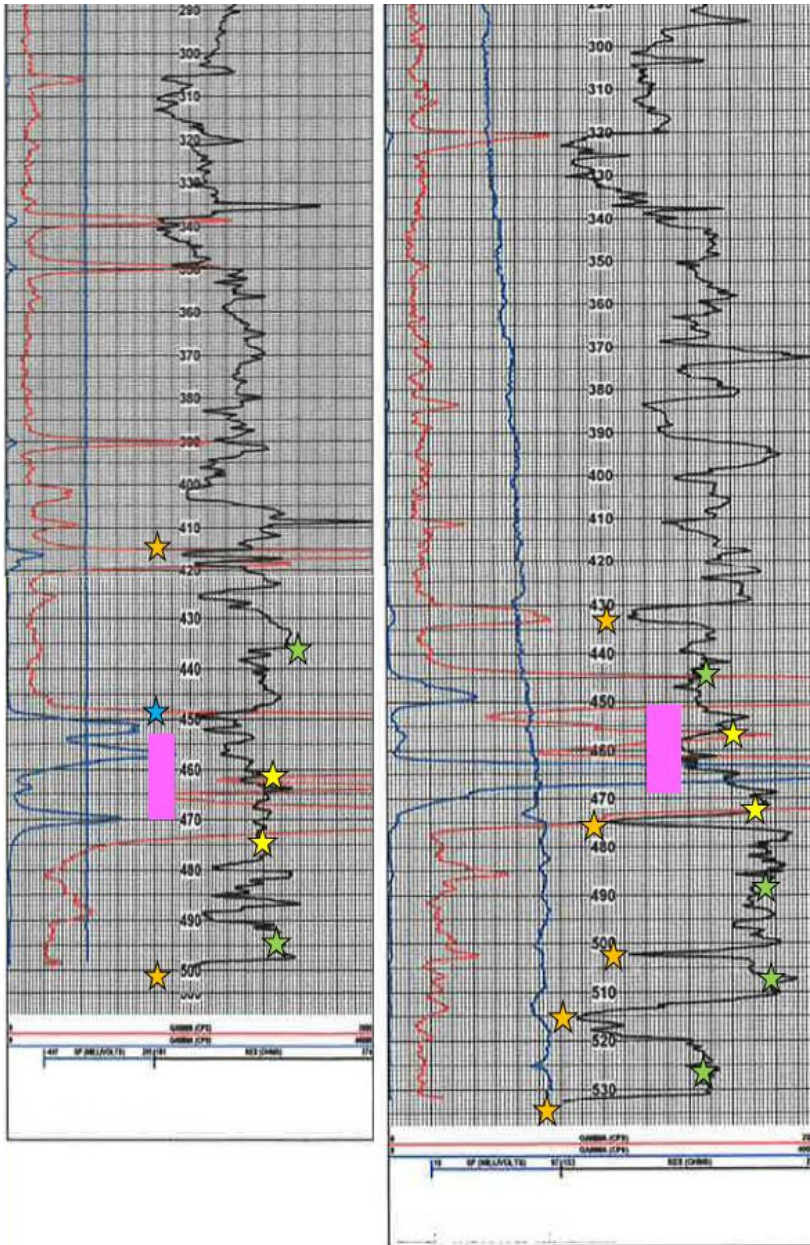


Figure D.16.b. Well 15P-308 to 15P-315 (290 - 530 feet bgs).

Overall, higher resistivities imply that sandstones dominate the well field, with finer-grained shales and clays also present. Injection wells, spaced by about 100 feet, and injection/producer wells, spaced by about 70 to 75 feet, did not correlate strongly to another in terms of resistivity. This is unsurprising because the sediments were deposited in a fluvial environment, so heterogeneity is expected.

The sharp edges to coarse packages and fining upward seen in the well logs are consistent with the model set forth by Ethridge et al. (1981), that the Fort Union was deposited by a northward axial fluvial system. Because the Powder River Basin was an active sedimentary basin at the time the Fort Union was deposited, a DFS model can be applied to the deposition of the Fort Union. If there was a fan apex in the Laramie Mountains to the south, the mix of sandstones with shales seen in the well logs suggest that SRH could fall within a distal location on a DFS. At a distal location on a DFS, channel size would decrease, and the abundance of fine grained floodplain deposits increase, with the preservation of organic matter possible.

## REFERENCES

- Amonette J.E., Szecsody J.E., Schaef H.T., Templeton J.C., Gorby, Y.A., & Fruchter J.S. (1994). Abiotic Reduction of Aquifer Materials by Dithionite: A Promising In-Situ Remediation Technology, presented at the Thirty-Third Symposium on Health & the Environment In Situ Remediation: Scientific Base for Current & Future Technologies, Richland Washington, November 7, 1994. Richland Washington: Pacific Northwest Laboratory.
- Anderson, R. T., Vrionis, H. A., Ortiz-Bernad, I., Resch, C. T., Long, P. E., Dayvault, R., ... & White, D. C. (2003). Stimulating the in situ activity of *Geobacter* species to remove uranium from the groundwater of a uranium-contaminated aquifer. *Applied and environmental microbiology*, 69(10), 5884-5891.
- Ayers, W.B. (1986). Lacustrine and Fluvial-Deltaic Depositional Systems, Fort Union Formation (Paleocene), Powder River Basin, Wyoming and Montana. *The American Association of Petroleum Geologists Bulletin*, 70(11), 1651-1673.
- Bopp, C. J., IV; Lundstrom, C. C., Johnson, T. M., and Glessner, J. J. G. 2009. Variations in  $^{238}\text{U}/^{235}\text{U}$  in uranium ore deposits: Isotopic signatures of the U reduction process? *Geology*, 37, 611–614.
- Borch, T., Roche, N., & Johnson, T. E. (2012). Determination of contaminant levels and remediation efficacy in groundwater at a former in situ recovery uranium mine. *Journal of Environmental Monitoring*, 14(7), 1814-1823.
- Cheng, C. J., Lin, T. H., Chen, C. P., Juang, K. W., & Lee, D. Y. (2009). The effectiveness of ferrous iron and sodium dithionite for decreasing resin-extractable Cr (VI) in Cr (VI)-spiked alkaline soils. *Journal of hazardous materials*, 164(2-3), 510-516.
- Brown, S.T., Basu A., Christensen, J.N., Reimus, P.W., Heikoop, J., Simmons, A., WoldeGabriel G., Maher, K., Weaver, K., Clay, J., & DePaolo, D.J. (2016) Isotopic Evidence for Reductive Immobilization of Uranium Across a Roll-Front Mineral Deposit. *Environmental Science and Technology*, 50 (12), 6189-9198.
- Dahl, A. R., & Hagmaier, J. L. (1976). Genesis and characteristics of the southern Powder River Basin uranium deposits, Wyoming.
- Dangelmayr, M. A., Reimus, P. W., Wasserman, N. L., Punsal, J. J., Johnson, R. H., Clay, J. T., & Stone, J. J. (2017). Laboratory column experiments and transport modeling to evaluate retardation of uranium in an aquifer downgradient of a uranium in-situ recovery site. *Applied geochemistry*, 80, 1-13.
- Davis, J. A., & Curtis, G. P. (2007). Consideration of geochemical issues in groundwater



restoration at uranium in-situ leach mining facilities. Division of Fuel Engineering, and Radiological Research, Office of Nuclear Regulatory Research, US Nuclear Regulatory Commission.

- Dong, W., & Brooks, S. C. (2006). Determination of the formation constants of ternary complexes of uranyl and carbonate with alkaline earth metals ( $Mg^{2+}$ ,  $Ca^{2+}$ ,  $Sr^{2+}$ , and  $Ba^{2+}$ ) using anion exchange method. *Environmental science & technology*, 40(15), 4689-4695.
- Dreesen, D. R., Williams, J. M., Marple, M. L., Gladney, E. S., & Perrin, D. R. (1982). Mobility and bioavailability of uranium mill tailings contaminants. *Environmental Science & Technology*, 16(10), 702-709.
- Elias, D. A., Krumholz, L. R., Wong, D., Long, P. E., & Suflita, J. M. (2003). Characterization of microbial activities and U reduction in a shallow aquifer contaminated by uranium mill tailings. *Microbial Ecology*, 46(1), 83-91.
- Ethridge, F. G., Jackson, T. J., & Youngberg, A. D. (1981). Floodbasin sequence of a fine-grained meander belt subsystem: the coal-bearing Lower Wasatch and Upper Fort Union Formations Southern Powder River Basin, Wyoming.
- Flores, R. M. (1981). Coal deposition in fluvial paleoenvironments of the paleocene tongue river member of the fort union formation, powder river area, powder river basin, wyoming and montana.
- Gallegos, T.J., Campbell, K.M., Zielinski, R.A., Reimus, P.W., Clay, J.N., Janot, N., Bargar, J.J., & Benzel, W.M. (2015) Persistent U(IV) and U(VI) following in-situ recovery (ISR) mining of a sandstone uranium deposit, Wyoming, USA. *Applied Geochemistry*, 63, 222-234.
- Haghiri, F. (1974). Plant Uptake of Cadmium as Influenced by Cation Exchange Capacity, Organic Matter, Zinc, and Soil Temperature 1. *Journal of Environmental Quality*, 3(2), 180-183.
- Hatcher, P.G., Spiker, E.C., Orem, W.H., Romankiw, L.A., & Szeverenyi, N.M. (1986). Organic Geochemical Studies of Uranium-Associated Organic Matter from the San Juan Basin: A New Approach Using Solid-State  $^{13}C$  Nuclear Magnetic Resonance. *American Association of Petroleum Geologists*, (22), 171-184.
- Idiz, E. F., Carlisle, D., & Kaplan, I. R. (1986). Interaction between organic matter and trace metals in a uranium rich bog, Kern County, California, USA. *Applied geochemistry*, 1(5), 573-590.
- Istok, J. D., Amonette, J. E., Cole, C. R., Fruchter, J. S., Humphrey, M. D., Szecsody, J.

- E., ... & Yabusaki, S. B. (1999). In situ redox manipulation by dithionite injection: Intermediate-scale laboratory experiments. *Groundwater*, 37(6), 884-889.
- Istok, J. D., Humphrey, M. D., Schroth, M. H., Hyman, M. R., & O'Reilly, K. T. (1997). Single-well, "push-pull" test for in situ determination of microbial activities. *Groundwater*, 35(4), 619-631.
- Lem, W. J., & Wayman, M. (1970). Decomposition of aqueous dithionite. Part I. Kinetics of decomposition of aqueous sodium dithionite. *Canadian Journal of Chemistry*, 48(5), 776-781.
- Li, Y., Cundy, A. B., Feng, J., Fu, H., Wang, X., & Liu, Y. (2017). Remediation of hexavalent chromium contamination in chromite ore processing residue by sodium dithionite and sodium phosphate addition and its mechanism. *Journal of environmental management*, 192, 100-106.
- Lister, M. W., & Garvie, R. C. (1959). Sodium dithionite, decomposition in aqueous solution and in the solid state. *Canadian Journal of Chemistry*, 37(9), 1567-1574.
- Los Alamos National Laboratory. (2012) UC Fee Project Final Report. Characterization of Aquifer, Rock, and Mineral Properties at a Uranium In Situ Recovery Site. Los Alamos, NM. Paul Reimus.
- Los Alamos National Laboratory. (2018) Chemical Remediation Bench-Scale Studies Report. Los Alamos, NM. Paul Reimus.
- Ludwig R.D., Su C., Lee T.R., Wilkin R.R., Acree S.D., Ross R.R., & Keeley A. (2007). In Situ Chemical Reduction of Cr (VI) in Groundwater Using a Combination of Ferrous Sulfate and Sodium Dithionite: A Field Investigation. *Environmental Science & Technology*, 41, 5299-5305.
- Murphy, M. J., Stirling, C. H., Kaltenbach, A., Turner, S. P., and Schaefer, B. F. 2014. Fractionation of  $^{238}\text{U}/^{235}\text{U}$  by reduction during low temperature uranium mineralisation processes, *Earth and Planetary Sci. Letters.*, 388, 306–317.
- Pacific Northwest National Laboratory. (1996) In Situ Redox Manipulation Field Injection Test Report – Hanford 100-H Area. Richland, WA. J.S. Fruchter, J.E. Amonette, C.R. Cole, Y.A. Gorby. M.D. Humphrey, J.D. Istok, F.A. Spane, J.E. Szecsody, S.S. Teel, V.R. Vermuel, M.D. Williams, S.B. Yabusaki.
- Ray, A. E., Bargar, J. R., Sivaswamy, V., Dohnalkova, A. C., Fujita, Y., Peyton, B. M., & Magnuson, T. S. (2011). Evidence for multiple modes of uranium immobilization by an anaerobic bacterium. *Geochimica et Cosmochimica Acta*, 75(10), 2684-2695.



- Rinker, R. G., Lynn, S., Mason, D. M., & Corcoran, W. H. (1965). Kinetics and mechanism of thermal decomposition of sodium dithionite in aqueous solution. *Industrial & Engineering Chemistry Fundamentals*, 4(3), 282-288.
- Saunders, J. A., Pivetz, B. E., Voorhies, N., & Wilkin, R. T. (2016). Potential aquifer vulnerability in regions down-gradient from uranium in situ recovery (ISR) sites. *Journal of Environmental Management*, 183, 67-83.
- Singh, G., Şengör, S. S., Bhalla, A., Kumar, S., De, J., Stewart, B., ... & Sani, R. K. (2014). Reoxidation of biogenic reduced uranium: a challenge toward bioremediation. *Critical Reviews in Environmental Science and Technology*, 44(4), 391-415.
- Wayman, M., & Lem, W. J. (1970). Decomposition of aqueous dithionite. Part II. A reaction mechanism for the decomposition of aqueous sodium dithionite. *Canadian Journal of Chemistry*, 48(5), 782-787.
- Weissmann, G. S., Hartley, A. J., Nichols, G. J., Scuderi, L. A., Olson, M., Buehler, H., & Banteah, R. (2010). Fluvial form in modern continental sedimentary basins: distributive fluvial systems. *Geology*, 38(1), 39-42.
- Weissmann, G. S., Hartley, A. J., Scuderi, L. A., Nichols, G. J., Owen, A., Wright, S., Felicia, A.L., Holland, F., & Anaya, F. M. L. (2015). Fluvial geomorphic elements in modern sedimentary basins and their potential preservation in the rock record: a review. *Geomorphology*, 250, 187-219.
- Weissmann, G. S., Hartley, A. J., Scuderi, L. A., Nichols, G. J., Davidson, S. K., Owen, A., Atchley, S.C., Bhattacharyya, P., Chakraborty, T., Ghosh, P., Nordt, L. C., Michel, L., & Tabor, N.J. (2013). Prograding distributive fluvial systems: geomorphic models and ancient examples. In *New Frontiers in Paleopedology and Terrestrial Paleoclimatology* (Vol. 104, pp. 131-147). SEPM, Special Publication 104.
- Weyer, S., Anbar, A. D., Gerdes, A., Gordon, G. W., Algeo, T. J., and Boyle, E. A. 2008. Natural fractionation of  $^{238}\text{U}/^{235}\text{U}$ , *Geochimica et Cosmochimica Acta*, 72, 345-359.
- WoldeGabriel, G., Boukhalfa, H., Ware, S. D., Cheshire, M., Reimus, P., Heikoop, J. & Simmons, A. (2014). Characterization of cores from an in-situ recovery mined uranium deposit in Wyoming: Implications for post-mining restoration. *Chemical Geology*, 390, 32-45.
- Zielinski, R. A., & Meier, A. L. (1988). The association of uranium with organic matter

in Holocene peat: an experimental leaching study. *Applied geochemistry*, 3(6), 631-643.